Modelling Bacterial Growth, Dispersal and Biodegradation

An experiment-based modelling study
of the spatiotemporal dynamics of bacterial colonies,
their responses to dispersal networks,
and their performance in degrading organic contaminants

Dissertation for the degree of Doctor of Natural Sciences (Dr. rer. nat.)
at the University of Osnabrück, Department of Mathematics/Computer Science
submitted by Thomas Banitz from Leipzig
Osnabrück 2010

Preface

For more than one hundred years now, human activities involved a perpetually increasing fabrication and usage of synthetic organic chemicals. This has lead to extensive environmental contamination with these chemicals all over the planet. Either released on purpose, for instance, as pesticides, or accidently, for instance, during extraction and consumption of fossil fuels, many organic chemicals cause a variety of problems, be it by directly threatening the health of organisms or by disturbing important ecosystem processes.

Recognising the dangerous consequences of this human-made contamination, scientists have developed several strategies for environmental remediation, that is, for removing contaminants from the environment. Additionally, the recognition of the need for sustainable development has lead to growing concern about the environmental footprint of remediation strategies. This includes the cleanup performance itself, but also the use of energy, water and other resources. Sustainable remediation approaches therefore aim at an optimal balance of effects and benefits for environment, economy and society.

One idea for sustainably reducing soil contamination is to take advantage of the natural potential of bacteria to degrade organic contaminants. However, this potential is often limited by environmental conditions that hinder the dispersal of bacteria and prohibit them from reaching the contaminants. A suggested solution is to deliberately grow networks of soil fungi that can be used by bacteria for quick dispersal, and thus enhance their degradation performance considerably. Indeed, microbiologists have shown in experiments that fungal networks are much less sensitive to environmental conditions and can drastically accelerate bacterial dispersal. However, before novel remediation approaches based on fungal networks can be put into practice, further research is needed to find the main factors and processes that govern the spatial and temporal interactions of bacteria and fungi, and understand how they affect degradation performance.

In experiments, one can address these research questions to some extent and observe the dynamics of microbiological systems under specific conditions. A powerful approach to reveal the mechanisms underlying the observed dynamics and to extrapolate to different conditions is provided by simulation models. In this doctoral thesis, laboratory experiments and simulation modelling are therefore combined to gain knowledge about microbiological systems consisting of organic contaminants, degrading bacteria and dispersal networks. The goal is to better understand and predict these systems' complex spatiotemporal dynamics under various environmental conditions, in order to advance the development of sustainable remediation strategies based on fungal networks.

Brief Contents

Contents

Chapter 1

Introduction

1.1 Biodegradation in soil

1.1.1 Soil pollution

Along with the rising level of industrialisation, the production and use of chemicals by humans has increased drastically since the beginning of the 19th century and lead to an ever-increasing presence of anthropogenic chemicals in virtually all natural soil environments (cf. Schwarzenbach et al. 2002). For instance, oil and fuel are spilled (Fig. 1.1a), synthetic organic chemicals are released to control unwanted organisms (Fig. 1.1b) or accompanying the daily use of certain products (e.g. solvents, dyes, varnishes, plastics and textiles; cf. Schwarzenbach et al. 2002), domestic wastes are leached (Fig. 1.1c) or industrial wastes are discharged directly to soils. Additionally, chemicals arrive in soils indirectly. For instance, contaminants emitted to the atmosphere diffuse and sediment in soils, or contaminated water percolates to subsurface layers.

Albeit not always visible, this pollution of soils represents a severe threat to both humans and the environment. Human health is primarily endangered through consumption of groundwater from contaminated soils, but also, for instance, through direct contact with contaminated soils or inhalation of vaporised soil contaminants. This

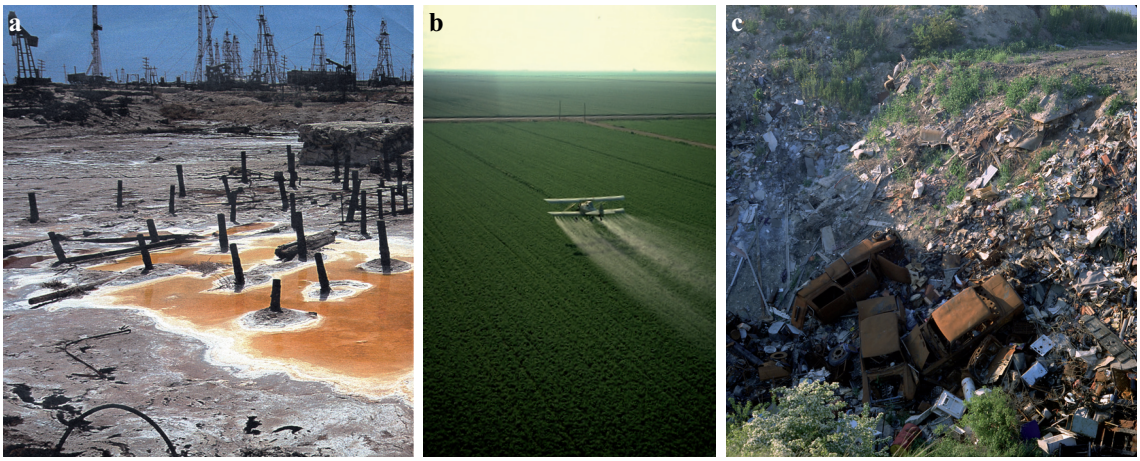

Figure 1.1 Oil mining, pesticide use and landfills are typical exemplary sources of soil contamination. **a** Petroleum wells near Baku, Azerbaijan (source: Stern magazine, Gruner + Jahr AG & Co KG). **b** Pesticide spraying in California, USA (source: United States Department of Agriculture) **c** Illegal landfill near Halle (Saale), Germany (source: Dr. Stefan Klotz, Helmholtz Centre for Environmental Research – UFZ).

may cause a variety of diseases and even have negative effects on human reproduction (Carlsen et al. 1992; Auger et al. 1995). Negative effects on the environment include alterations of food chains, potential extinction of species, losses of ecosystem function and stability or recreation facilities.

1.1.2 Soil remediation

In the light of these dangers, various strategies for cleaning up contaminated soils have been developed. Many standard methods are applied *ex situ* and based on *physicochemical* treatments (e.g. soil separation or chemical extraction). They require excavation of soils, which may be unfeasible for large sites and, most important, is usually related to high costs and energy usage (e.g. Tiehm et al. 2010). The advantage of *in situ* strategies is that they allow for treating contamination directly where it occurs. Examples include aeration or heating of soil to induce evaporation, or addition of chemicals to induce immobilisation or detoxification of contaminants (e.g. cf. Alvarez and Illman 2006). However, these strategies may also be restricted to smaller sites and they are often cost and energy-intensive, too. That is why more natural, biotechnological approaches have been developed.

Bioremediation covers spontaneous or managed biological processes in which environmental contamination is remedied or eliminated from the environment (cf. Alvarez and Illman 2006). It is therefore an example of a service provided by ecosystems that contributes to human welfare (cf. Costanza et al. 1997). For instance, *phytoremediation*, the usage of plants to remove or stabilise contaminants, became recognised in the past 10-15 years due to its cost-effectiveness and environment-friendliness (cf. Salt et al. 1998; Pilon-Smits 2005 for reviews). The same advantages apply to the utilisation of bacteria or fungi to degrade contaminants (the latter is also called *mycoremediation*; cf. Singh 2006), approaches that have garnered growing popularity for more than 30 years already and, in some cases, are the only applicable option (Madigan et al. 2008).

Microorganisms are known to degrade many organic compounds in natural soils (e.g. Wackett 2003; Díaz 2004). Therefore, one approach to treat contamination is degradation without human intervention, often referred to as *natural attenuation*. This does not require any external energy supply and is applicable for large sites. However, degradation rates are often lower than immission rates, which is why the contaminants accumulate in the soils. Furthermore, given that natural conditions allow degradation, it may require a very long time until bioremediation targets are met, as well as expensive and time consuming monitoring efforts (e.g. Alvarez and Illman 2006). Hence, particularly when trying to improve the performance of bacterial degradation, the major task is to increase the rates at which contaminants are consumed by bacteria. To do this, the presence and well-being of contaminant-degrading bacteria should be assured, for instance, by additional supply of nutrients, or by modifications of the soil's pH-value and temperature (Harms and Wick 2006). In many soils, however, biodegradation performance is predominantly limited by the contact probability of contaminants and bacteria (Semple et al. 2007), which can often be very low due to heterogeneous spatial distributions of both contaminants and bacteria in the subsurface. Typical causes for such heterogeneities include variations in water content (which is paramount for bacterial growth and motility, but also for contaminant diffusion; cf. Harshey 2003; Schroll et al. 2006; Madigan et al. 2008), air-filled soil pores of various structures, and

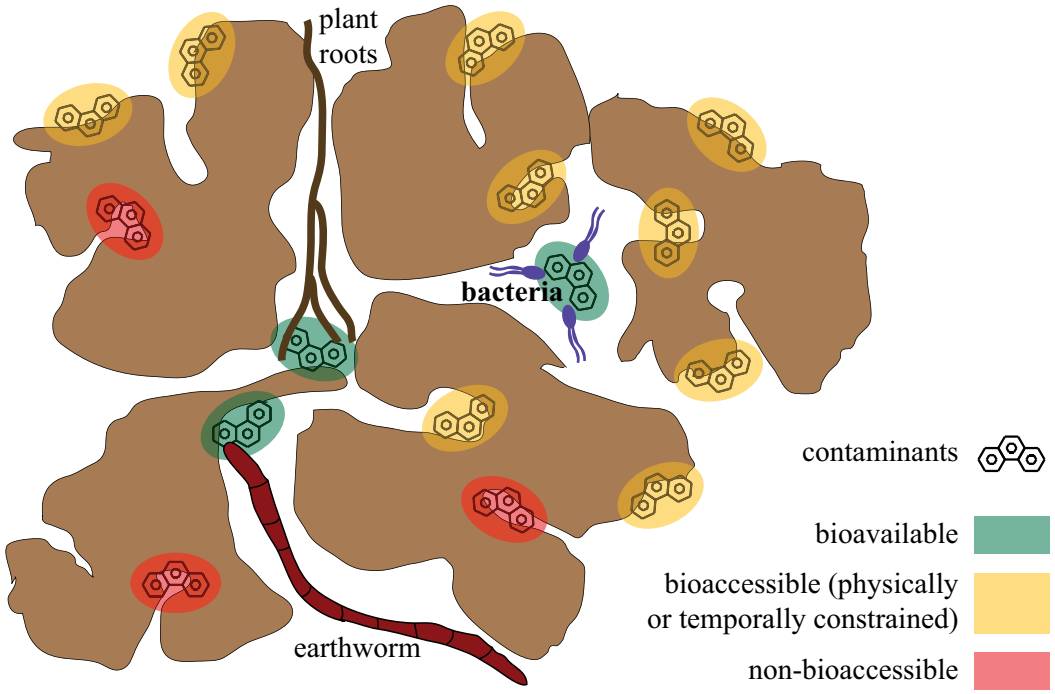

Figure 1.2 Visualisation of contaminant bioavailability at the microscale (source: Semple et al. 2004). Merely a fraction of contaminants is bioavailable to degrading organisms in heterogeneous soils. A substantial part is only bioaccessible, denoting that it is physically or temporally constrained, but could become bioavailable. Contaminants can also be occluded and, thence, are non-bioaccessible (cf. legend).

discontinuous paths for bacterial dispersal (e.g. Semple et al. 2003; Young and Crawford 2004; Boswell et al. 2007). If the contact probability is low, the *bioavailability* of the contaminants to the bacteria, that is, the quantity freely available for bacterial uptake within a given time interval (cf. Semple et al. 2004; Fig. 1.2), will be low, too. Therefore, many approaches to stimulate successful biodegradation focus on increasing the bioavailability of contaminants (Ehlers and Luthy 2003).

Various strategies have been suggested to improve the bioavailability of contaminants to degrading bacteria in soils. Several of them aim at actively homogenising the whole soil by excavation and mechanical treatment and have the same disadvantages as other *ex situ* methods (cf. above). Given this unsatisfying situation, new approaches to improve the bioavailability of contaminants *in situ* by stimulating the dispersal of bacteria (and partly also contaminants) have been investigated recently. Such *enhanced natural attenuation* approaches include the application of weak electric fields to migrate bacteria in electro-bioremediation (e.g. Wick et al. 2007b; Lohner and Tiehm 2009; Kim et al. 2010), the stimulation of chemotactic bacteria that are able to move actively towards higher contaminant concentrations (cf. Harms and Wick 2006 for a review of target contaminants and chemotactic strains applied), and the use of soil animals (e.g. cf. Sizmur and Hodson 2009 for a review of earthworm impacts on metal bioavailability), plant roots (e.g. Kuiper et al. 2001) or fungi (cf. Sec. 1.1.3) as dispersal vectors for bacteria and/or contaminants (cf. Harms and Wick 2006 for an overview of eukaryotes as bacterial dispersal vectors). All these strategies do not require excavation and physical or

chemical treatment of soil. Given the growing recognition of the importance of *sustainable remediation* (e.g. Wackett and Bruce 2000; Dellens 2007; Bardos et al. 2011), they are promising for the design and future application of economically, environmentally and socially sound bioremediation technologies.

1.1.3 Mobilisation of bacteria by fungi

Unfavourable conditions and environmental heterogeneities in the subsurface often limit the motility of bacteria (cf. Sec. 1.1.2). Therefore, one of the enhanced natural attenuation approaches to remedy contaminated soil sites is the specific stimulation of the establishment of filamentous fungi that can mobilise bacteria and, thus, increase the bioavailability of contaminants. Fungi are often much less sensitive to soil heterogeneities than bacteria (e.g. Boswell et al. 2003; 2007). For instance, they may be able to grow in air-filled pores or to breach air-water interfaces (Wösten et al. 1999; Singh 2006). Furthermore, hydrophilic fungi induce the formation of continuous liquid films around their hyphae (Wösten and Willey 2000). It was hypothesised and shown in experiments that bacteria can use the *fungal networks* formed by these liquid films (cf. Fig. 1.3) as paths for accelerated dispersal and, thus, spread efficiently in soil (Kohlmeier et al. 2005; Wick et al. 2007a; Furuno et al. 2010). Hence, improving the biodegradation performance *in situ* via stimulating the active growth of fungal hyphae seems a promising strategy for sustainable bioremediation in the future (Wick et al. 2010). However, there is still a high demand for a better understanding of the factors that influence biodegradation performance in relation to fungal networks, for instance, concerning the impact of environmental conditions, the network architecture, or the suitable combinations of soil fungi and contaminant degrading bacteria.

1.1.4 An ecological perspective

The microbiological context of bacterial colony growth, fungal networks and biodegradation relates to several prominent topics of ecological research, such as consumer-resource dynamics (e.g. Ernest et al. 2000; Johst and Schöps 2003; Murdoch et al. 2003), dispersal behaviour (e.g. Clobert et al. 2001), dispersal in heterogeneous environments (e.g. Hanski and Ovaskainen 2000; Dewhirst and Lutscher 2009) and resource allocation (e.g. Piceno and Lovell 2000; Brown et al. 2004). Furthermore, bacterial dispersal networks may be compared to dispersal corridors in animal ecological systems (e.g. Hill 1995; Tischendorf and Wissel 1997). Other ecology-related research questions concern the impact of environmental conditions on population dynamics (e.g. Pena et al. 2005; Berryman and Lima 2006) and subsequent bacterial degradation performance. Regarding various spatiotemporal distributions and patterns of bacteria, potential analogies to patterns known from general ecology (e.g. Johst and Brandl 1997b; Banitz et al. 2008) can be investigated.

Finally, and more broadly, microbial ecosystems may provide insights about the validity and generalisability of ecological theory, and new theory may originate from studying these ecosystems that is also relevant to animal and plant ecology (cf. Prosser et al. 2007).

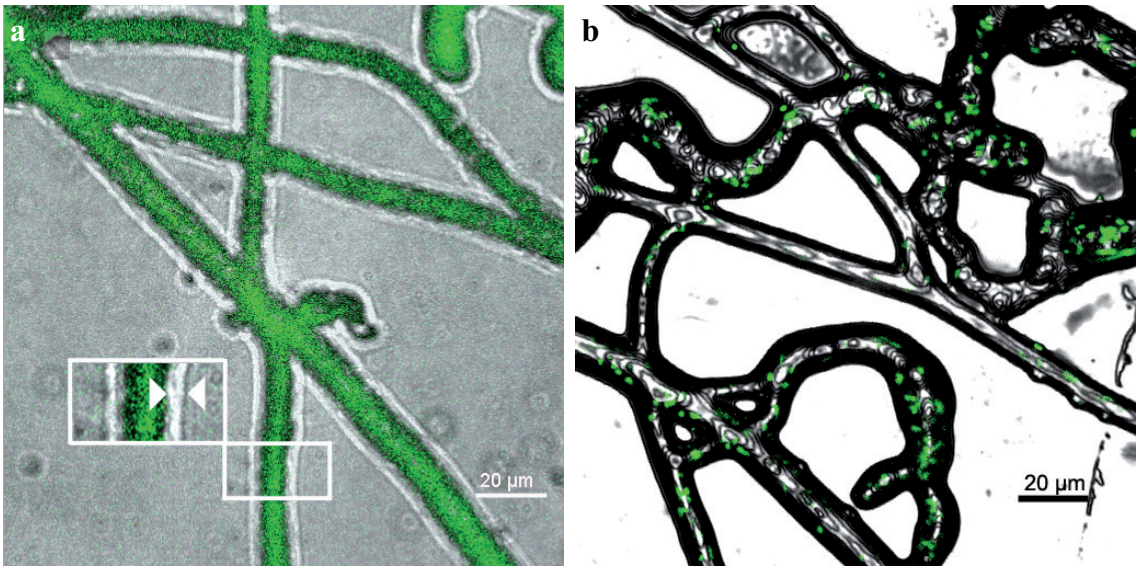

Figure 1.3 Confocal laser scanning microscopy images of *Pythium ultimum* filaments growing on glass surfaces (source: Furuno et al. 2010). **a** Visualisation of the presence of liquid films (light grey) along fungal hyphae. Arrows in the insert indicate the dimensions of the liquid film (3-4 µm). **b** Visualisation of the presence of *Pseudomonas putida* PpG7 (green) within the liquid films.

1.2 Research objectives

Drawing on the research requirements stated in section 1.1, this doctoral thesis aims at understanding the mechanisms and conditions that determine the success of increasing contaminant bioavailability and biodegradation performance with networks facilitating bacterial dispersal. The ecological perspective given in section 1.1.4 suggests integrating theoretical knowledge from ecology into these investigations of microbial degradation processes. Therefore, the studies of this thesis include the development of an integrative approach to combine simulation modelling and laboratory experiments, based on both ecological and microbiological theory (cf. Sec. 8.1). The main research objectives are:

- To derive relevant processes, ecological and microbiological, for appropriately modelling bacterial colony growth and achieving a high accordance of the simulation model with experimentally observed patterns.
- To find out whether bacterial dispersal networks can considerably improve the performance of contaminant degradation.
- To examine the consequences of different environmental conditions for the effects of bacterial dispersal networks on the performance of contaminant degradation.
- To test if and characterise how the spatial structure of dispersal networks influences their effects on the performance of contaminant degradation.

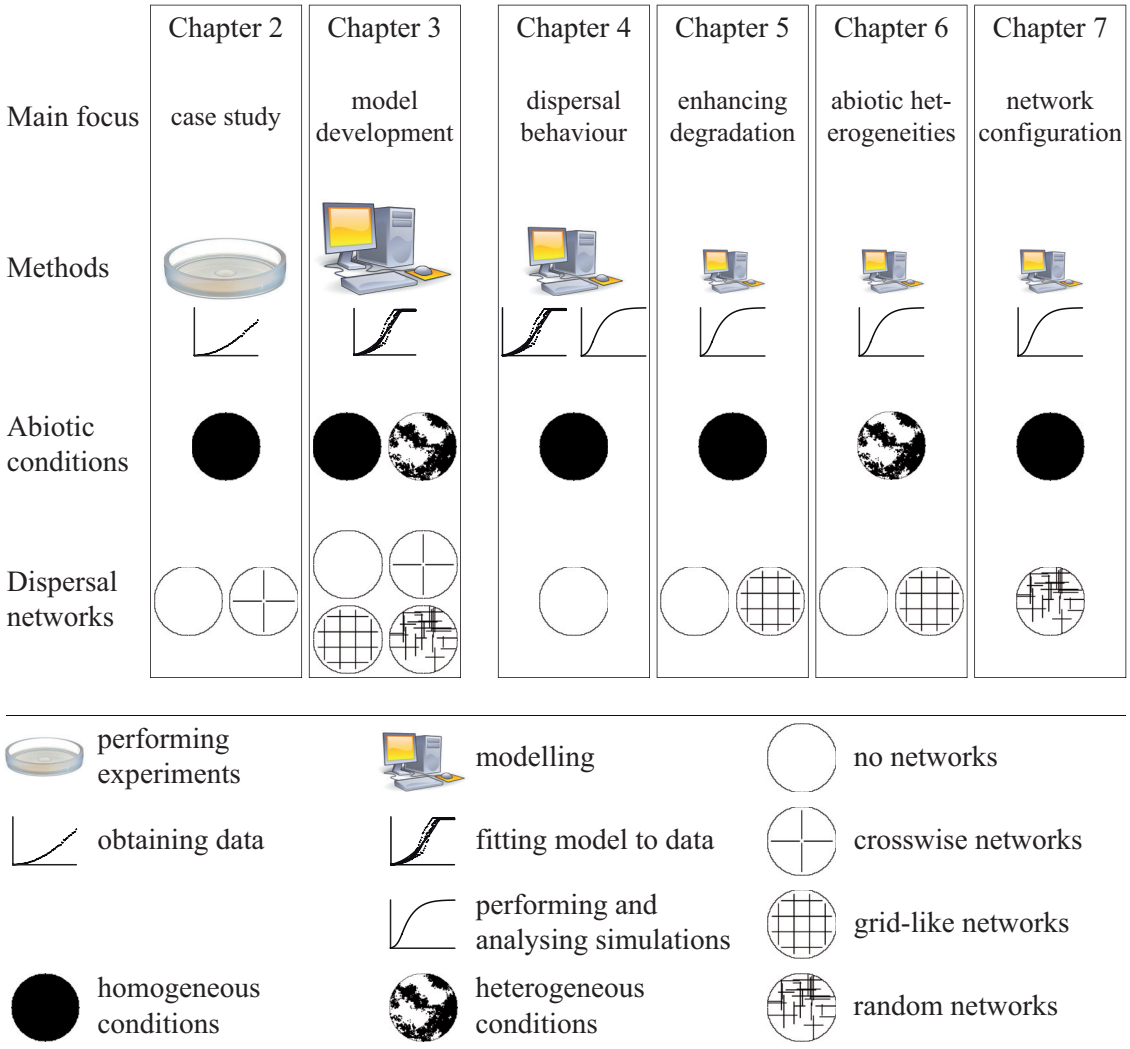

Figure 1.4 Overview of the following chapters, regarding the categories focus, methods, abiotic conditions and dispersal networks. The size of the 'modelling' icons indicates the share of programming work comprised in the respective chapters.

1.3 The chapters at a glance

1.3.1 Synopsis

Here, we summarise the major aspects covered in the following chapters of this thesis, including the methods applied and the crucial findings obtained. An overview of main focus as well as methods and assumptions for each chapter is provided in figure 1.4. First, we describe microbiological experiments that let us observe bacterial behaviour (Ch. 2). Second, we develop a mechanistic, process-based and spatially explicit computer model that enables us to simulate and interpret this behaviour (Ch. 3). This model serves as a tool for testing the validity and relevance of certain ecological concepts (conditional dispersal, resource allocation; Ch. 4) in the context of bacterial degradation. Most important, it allows for predictions of the ecosystem behaviour, also under conditions that cannot easily be examined in laboratory experiments (Ch. 5; 6; 7).

Finally, the approach developed in this thesis, the results obtained with this approach, and potential directions for future research are discussed (Ch. 8).

1.3.2 Chapter 2

Data for this thesis were derived from laboratory experiments with *Pseudomonas putida* PpG7 colonies growing on agar-plates. These experiments, which are described in detail in chapter 2, are a specific case study for consumer-resource systems that consist of organic substrate as resources and degrading bacteria as consumers. Spatiotemporal dynamics of bacterial colonies have been observed under various environmental conditions. Different abiotic conditions were investigated via different agar and glucose concentrations, and bacterial dispersal networks were mimicked with glass fibres.

1.3.3 Chapter 3

In chapter 3, the bacterial simulation model is presented. The model was developed to describe microbial consumer-resource systems, to understand their key behavioural mechanisms, and to predict the performance of an ecosystem service they provide – biodegradation of organic contaminants – under various environmental conditions. Fundamental to this model is the use of reaction-diffusion equations incorporating individual behavioural rules to describe spatiotemporal dynamics of bacterial colony growth and depletion of organic substrate. Furthermore, the integration of theoretical concepts from two disciplines, ecology and microbiology, is a specific feature. This simulation model is a major element of the thesis used for all subsequent analyses. It provides the means for fulfilling the research objectives stated in section 1.2.

1.3.4 Chapter 4

Chapter 4 addresses the question whether the theoretical ecological concept of conditional dispersal, denoting that the dispersal strategy depends on environmental conditions, is crucial for accurately assessing the dynamics and efficiency of bacterial degradation of contaminants. Different dispersal strategies, which either incorporate or neglect this concept, are implemented in the model and simulation results compared to the laboratory case study (Ch. 2). The results show that, with respect to the condition resource uptake, the model's correspondence to observation data is significantly higher for conditional than for unconditional bacterial dispersal. One aspect of conditional dispersal in particular accounts for a major part of the improvement: the cessation of bacterial dispersal at high resource levels. It is also shown that the bacterial dispersal strategy has a significant impact on model predictions for bacterial degradation of resources: Disregarding conditional bacterial dispersal can lead to overestimations when assessing the performance of this ecosystem service.

1.3.5 Chapter 5

In chapter 5, the general effects of some simple exemplary bacterial dispersal networks on the performance of contaminant degradation are explored, with focus on abiotic conditions, particularly on the agar concentration. As biodegradation performance in soil often depends on the bioavailability of organic contaminants to degrading bacteria (cf. Sec. 1.1.2), this performance is analysed (and predicted) under various abiotic conditions and in response to dispersal networks with different spatial configurations,

including scenarios that are not easily feasible in experiments. It is shown that conditions of restricted bacterial dispersal also limit degradation performance. Under such unfavourable conditions, dispersal networks have the highest potential for improving the bioavailability of contaminants to bacteria. Furthermore, the biodegradation performance significantly varies with the spatial configuration of the dispersal networks applied and the time horizon over which performance is assessed.

1.3.6 Chapter 6

Chapter 6 takes into account the heterogeneity of environmental conditions, which is known to limit the bioavailability of contaminants to degrading bacteria in many cases (cf. Sec. 1.1.2). To match situations regarded as being typical in contaminated soils, two types of abiotic conditions are studied: heterogeneous bacterial dispersal conditions, that is, a mix of areas where bacterial movement is efficient or restricted, and heterogeneous initial resource distributions, that is, a mix of areas of low and high contaminant concentrations. The simulation model predicts that bacterial dispersal networks can enhance the performance of biodegradation for a wide range of spatial heterogeneities under these conditions. Also here, the time horizon considered for assessing biodegradation performance and the spatial configuration of networks are key factors determining the degree of biodegradation improvement by dispersal networks.

1.3.7 Chapter 7

The focus of chapter 7 is the spatial configuration of bacterial dispersal networks. Since the spatial structure of real fungal networks can be very complex, several aggregated metrics for handling this complexity and distinguishing networks with regard to their impact on biodegradation performance are investigated. To this end, we develop a method to test single metrics and combinations of two metrics for their suitability to assess biodegradation performance. It is shown that a particular combination of two metrics allows for capturing most of the network's characteristics that determine respective biodegradation improvements: Network coverage and accessibility lead to reliable assessments and should therefore be considered when developing enhanced bioremediation strategies based on stimulating the establishment of fungal mycelia on contaminated soil sites.

1.3.8 Chapter 8

Finally, chapter 8 concludes with a discussion of methods and results, and gives an outlook on planned research. First, a summary of the developed approach highlights the fundamental elements contributing to this thesis, how they are connected, and which benefits were derived from the approach. This integrative approach can serve as a basis for future research on ways to explore and understand microbial ecosystems, and also to generalise and answer fundamental ecological questions. Second, the main findings are summarised and discussed shortly. These results highlight the potential of applying fungal networks for enhancing bacterial degradation of soil contaminants, as well as key factors that will determine the success of strategies based on such enhancements. Third, the outlook covers topics of future studies that are planned in succession of this doctoral thesis, and collaborative research activities relating to topics beyond its scope that have been started already.

Chapter 2

Laboratory Experiments*

2.1 Organism and culture conditions

Pseudomonas putida PpG7 (NAH7) bacteria (Dunn and Gunsalus 1973) and glucose (Fluka, Switzerland) were used as model organism and model substrate. Bacterial colonies were grown at a constant temperature of 30 °C in Petri dishes on minimal medium agar MMA (Harms and Zehnder 1994; Wick et al. 2001) under various abiotic conditions in terms of agar and glucose concentrations. We varied the agar concentration C_a, which limits the potential dispersal of bacteria, and the initial concentration of glucose C_s^0, which was the sole energy resource (3, 4 and 5 g/l agar concentration; 0.1 and 1 g/l glucose concentration). The applied conditions ranged from 'swimming agar' (below 3.5 g/l agar concentration) to 'swarming agar' (above 3.5 g/l agar concentration; cf. Harshey 2003). Four replicate experiments were performed for each combination of C_a and C_s^0.

2.2 Observation data

Each agar plate was inoculated in its centre with approximately 6×10^7 bacterial cells pregrown on glucose. The colonies were observed for 66 h by hourly image scanning (e.g. Fig. 2.1a) using a commercial flatbed scanner (HP Jetset 7400c). From these images, the total area of the bacterial colonies was calculated with image analysis software ImageJ (Rasband 1997). Thus, subsequent image sequences provided the colony areas as a function of time for each combination of the two varied abiotic factors C_a and C_s^0 (Fig. 2.2). The observation data were used for validating and parameterising the simulation model (cf. Ch. 3; 4).

Contrary to studies with other bacterial strains (*Bacillus subtilis* (Ohgiwari et al. 1992; Wakita et al. 1994), *Pseudomonas aeruginosa* (Köhler et al. 2000; Rashid and Kornberg 2000), *Mycobacterium gilvum* (Fredslund et al. 2008)), in which diverse morphological growth patterns under various conditions could be identified, we observed a homogeneous circular colony growth over the whole range of abiotic conditions examined.

---

* Dr. Ingo Fetzer, Dr. Daniela Inkrot and Susann Pleger contributed substantially to conducting and observing laboratory experiments.

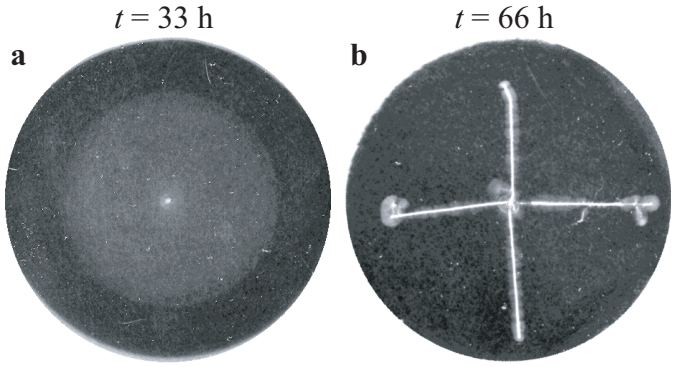

Figure 2.1 Observed spatial patterns of bacteria on agar plates (image scans). Bacterial concentrations are indicated by grey shading, increasing from black (no bacteria) to white. **a** After 33 h under 0.1 g/l initial glucose concentration and 3 g/l agar concentration. **b** After 66 h under 0.1 g/l initial glucose concentration and 5 g/l agar concentration, with a crosswise dispersal network of four glass fibres (cf. Sec. 2.3).

2.3 Bacterial dispersal networks

In order to simulate the effects of dispersal networks, we used disposable polymer coated glass fibres based on Mayer et al. (2000) as well-controlled substitutes for fungal networks. Glass fibres mimic the attributes of fungal hyphae, as thin films of water emerge around the glass fibres and provide dispersal corridors for the bacteria. They were placed on MMA, and experiments with 0.1 g/l initial glucose concentration and 3, 4 and 5 g/l agar concentration were conducted (e.g. Fig. 2.1b).

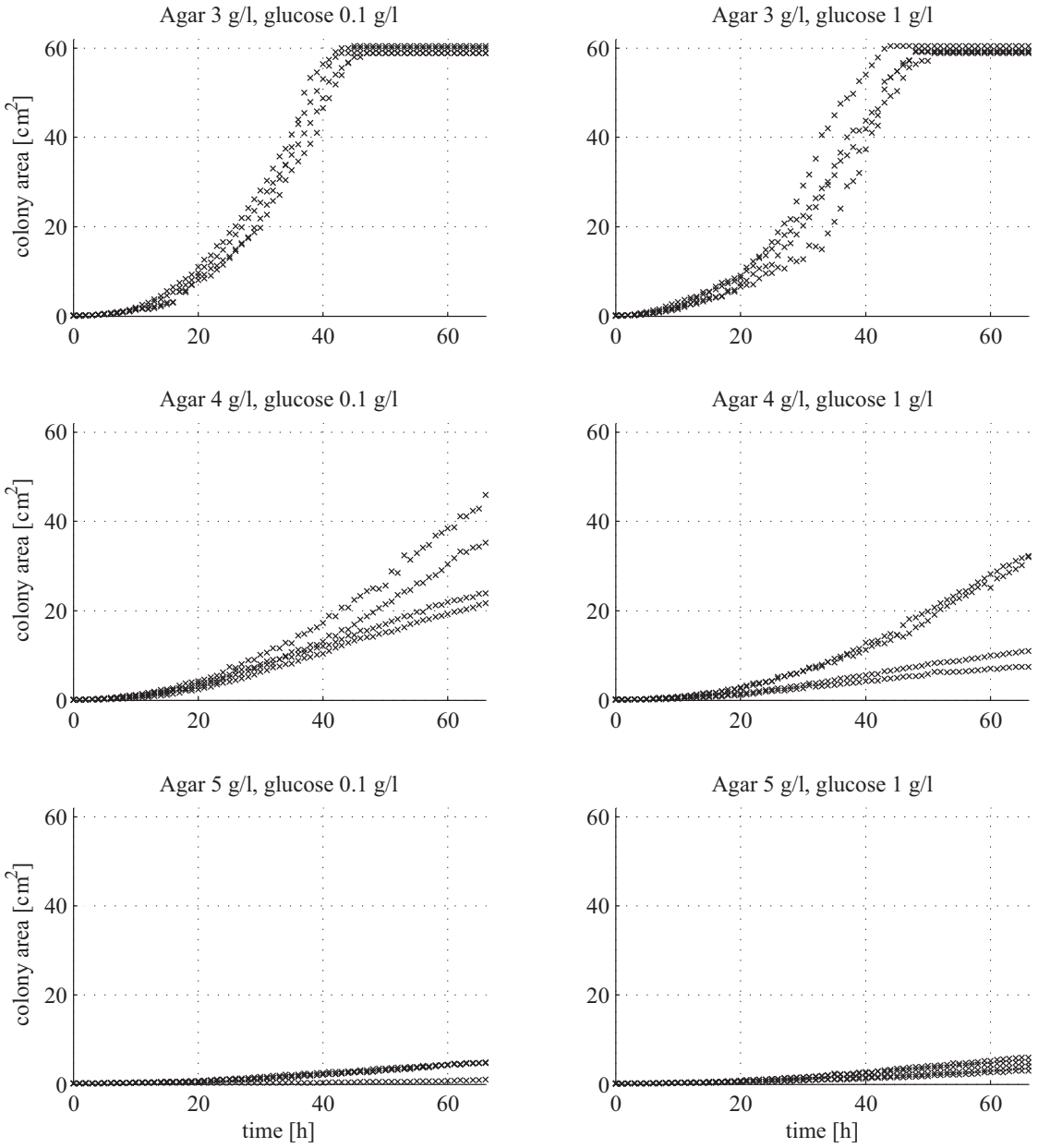

Figure 2.2 Total area measurements of bacterial colonies plotted versus time. Columns show different initial glucose concentrations, increasing from left to right. Rows show different agar concentrations, increasing from top to bottom (cf. graph titles). Four experimental replicates for each scenario are plotted as black crosses. Note that at approximately 60 cm² the size of the agar plates is reached.

Chapter 3

Simulation Model

3.1 Overview

The purpose of the simulation model is to describe consumer-resource systems consisting of organic contaminants as resource and degrading bacteria as consumers, in order to analyse their spatiotemporal dynamics and assess their degradation performance in response to various dispersal networks and under various abiotic conditions. Therefore, the model spatially explicitly describes the dynamics of bacterial colony growth and substrate depletion, using the following set of reaction-diffusion equations (cf. Symbols table on page 87 for units):

$$\frac{\partial C_x}{\partial t} = \nabla\left(D_x(C_a, C_x, q(C_s))\nabla C_x\right) + \left(q(C_s)Y_g - a - d(D_x)\right)C_x, \tag{3.1}$$

$$\frac{\partial C_s}{\partial t} = D_s\nabla^2 C_s - q(C_s)\, C_x, \tag{3.2}$$

$$\frac{\partial C_y}{\partial t} = \max\left(0, a - q(C_s)Y_g\right)C_x, \tag{3.3}$$

where C_x is the concentration of active bacteria, C_s is the concentration of substrate, and C_y is the concentration of inactive bacteria. D_x is the bacterial diffusion coefficient for a given (constant) agar concentration C_a. It varies with C_x and C_s. D_s is the constant diffusion coefficient of substrate. The bacterial reaction term includes the substrate uptake rate q, the growth yield Y_g, and biomass loss rates due to maintenance a and dispersal d.

According to this system, the explicit spatiotemporal dynamics of concentrations of bacteria and substrate are approximated with a finite difference method, inspired by the BacSim model (Kreft et al. 1998), on a two-dimensional simulation area SA representing an 88 mm diameter agar plate with reflective boundaries. This area is divided into rectangular grid cells, which are indexed with (i, j) starting from (0,0) in the centre of the simulation area (Fig. 3.1).

From a process-based point of view, one simulation time step Δt comprises the following sequence of processes: substrate uptake by bacteria, uptake allocation, bacterial dispersal, bacterial growth and reproduction, and substrate diffusion (cf. Fig. 3.2 for an overview; Sec. 3.2 for a detailed description of these processes). Examples of bacterial colonies simulated with the model can be found in figures 3.3 and 3.4a.

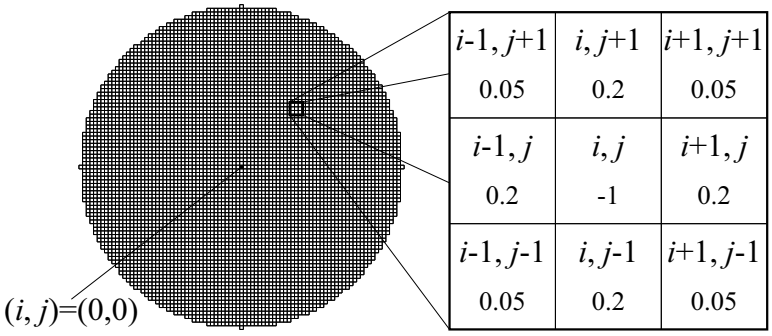

Figure 3.1 The circular simulation area *SA* is divided into rectangular grid cells. Indexing starts from $(i, j) = (0, 0)$ in the centre of the agar plate. The enlargement shows the 9 point neighbourhood $NBH_{i,j}$ of a grid cell (i, j) including the grid cell itself (cf. Eq. (3.8)), and the weights for diffusion $w_{k,l}$ (cf. Eq. (3.9)).

3.2 Model processes

3.2.1 Substrate uptake

In agreement with other bacterial models (e.g. Panikov 1996; Kreft et al. 2001; Grijspeerdt et al. 2005; Schuler 2005; Picioreanu et al. 2007; Xavier and Foster 2007) the Monod kinetic function (Monod 1949) is used for calculating the substrate uptake in cell (i, j) at time t:

$$q^{i,j,t} = q_{\max} \frac{C_s^{i,j,t}}{K_s + C_s^{i,j,t}}, \tag{3.4}$$

where K_s is the Monod half-saturation constant. The maximum uptake rate $q_{\max}$ is calculated according to equation (3.18) below. The corresponding change in substrate concentration is:

$$\left.\frac{C_s^{i,j,t+1} - C_s^{i,j,t}}{\Delta t}\right|_{react} = -q^{i,j,t} C_x^{i,j,t}. \tag{3.5}$$

3.2.2 Uptake allocation

The substrate uptake $q^{i,j,t}$ is divided into fractions for maintenance, dispersal and growth. The fraction for maintenance $\tilde{a}$ is constant. The fraction for dispersal $\tilde{d}_{eff}^{i,j,t}$ depends on resource uptake according to the conditional dispersal strategy described in detail in chapter 4. These two fractions are related to corresponding biomass loss rates ($a = \tilde{a} Y_g$, $d = \tilde{d}_{eff}^{i,j,t} Y_g$, cf. Eq. (3.1)). The fraction for growth is left:

$$q_{eff}^{i,j,t} = q^{i,j,t} - \tilde{a} - \tilde{d}_{eff}^{i,j,t}. \tag{3.6}$$

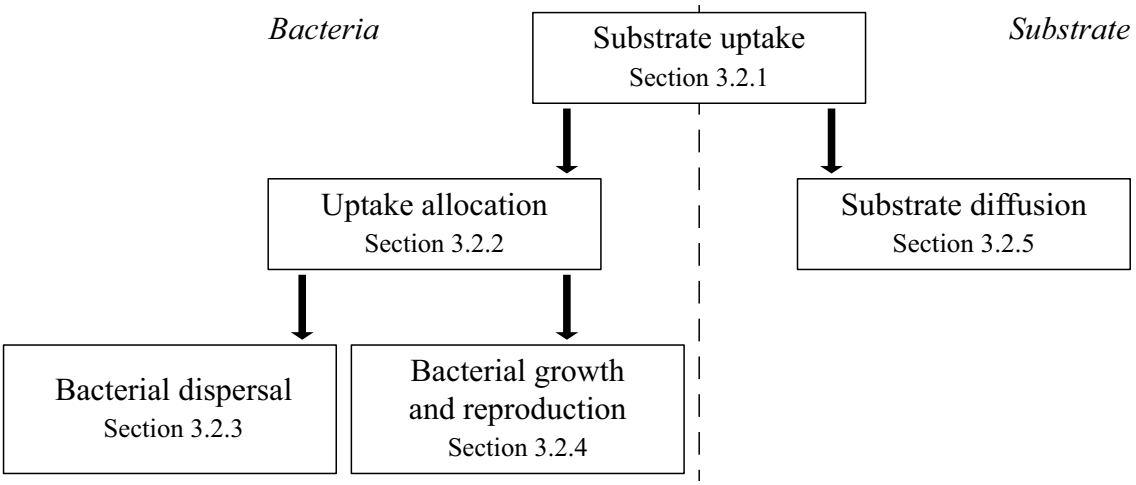

Figure 3.2 Scheme of processes comprised in the bacterial simulation model. Processes on the left affect bacterial dynamics, processes on the right affect substrate dynamics, the process of substrate uptake by bacteria affects both.

3.2.3 Bacterial dispersal

The dispersal of bacteria is modelled as diffusion. For this purpose the finite difference approximation from the BacSim model (Kreft et al. 1998) is adapted to our simulation model. The original diffusion algorithm is:

$$\left.\frac{C_x^{i,j,t+1} - C_x^{i,j,t}}{\Delta t}\right|_{diff} = \frac{D_x}{cl^2}\,\overline{C}_x^{i,j,t}, \tag{3.7}$$

where $\overline{C}_x^{i,j,t}$ is the weighted average of bacterial concentrations $C_x^{k,l,t}$ in the 9 point neighbourhood of a regarded grid cell (i,j) (cf. Fig. 3.1):

$$NBH_{i,j} = \{(k,l) : (i-1 \le k \le i+1) \wedge (j-1 \le l \le j+1)\} \tag{3.8}$$

and cl is the side length of one grid cell. As in the BacSim model, the weights $w_{k,l}$ accord to the following stencil (cf. Fig. 3.1):

$$\forall (k,l) \in NBH_{i,j} : w_{k,l} = \begin{cases} \frac{1}{20} & (k \ne i) \wedge (l \ne j) \\ -1 & (k,l) = (i,j) \\ \frac{1}{5} & otherwise \end{cases}. \tag{3.9}$$

Thus, equation (3.7) reads:

$$\left.\frac{C_x^{i,j,t+1} - C_x^{i,j,t}}{\Delta t}\right|_{diff} = \frac{D_x}{cl^2} \sum_{(k,l)\in NBH_{i,j}} w_{k,l} C_x^{k,l,t} \,, \tag{3.10}$$

which can be written as:

$$\left.\frac{C_x^{i,j,t+1} - C_x^{i,j,t}}{\Delta t}\right|_{diff} = \frac{D_x}{cl^2} \sum_{\substack{(k,l)\in NBH_{i,j} \\ (k,l)\neq(i,j)}} w_{k,l} \left(C_x^{k,l,t} - C_x^{i,j,t}\right). \tag{3.11}$$

In our system, the effective bacterial diffusion coefficient $D_{x,eff}^{i,j,t,C_a}(C_x^{i,j,t}, q^{i,j,t})$ may vary in space and time depending on the bacterial concentration and the conditional bacterial dispersal strategy (cf. Ch. 4), and on the presence of dispersal networks (cf. Sec. 3.5). Its maximum $D_{x,\max}^{C_a}$ is determined by the agar concentration C_a. Adapting to spatiotemporally varying bacterial diffusion coefficients $D_{x,eff}^{i,j,t,C_a}$, the approximation algorithm for the changes in bacterial concentration needs to be modified. With regard to the finite difference scheme, the effective diffusivity between two neighbour grid cells is given by the harmonic mean of their diffusion coefficients:

$$\overline{h}(D_{x,eff}^{i,j,t,C_a}, D_{x,eff}^{k,l,t,C_a}) = \frac{2 D_{x,eff}^{i,j,t,C_a} D_{x,eff}^{k,l,t,C_a}}{D_{x,eff}^{i,j,t,C_a} + D_{x,eff}^{k,l,t,C_a}}. \tag{3.12}$$

The harmonic mean is used, because it provides the average velocity over a distance, when half the distance is travelled with one and the other half with another velocity. Inserting these diffusivities (Eq. (3.12)) for D_x into equation (3.11) results in:

$$\left.\frac{C_x^{i,j,t+1} - C_x^{i,j,t}}{\Delta t}\right|_{diff} = \frac{1}{cl^2} \sum_{\substack{(k,l)\in NBH_{i,j} \\ (k,l)\neq(i,j)}} w_{k,l} \left(C_x^{k,l,t} - C_x^{i,j,t}\right) \overline{h}(D_{x,eff}^{i,j,t,C_a}, D_{x,eff}^{k,l,t,C_a}) \,. \tag{3.13}$$

In addition to varying diffusion coefficients, which depend on bacterial concentration and substrate uptake (cf. Ch. 4), this algorithm allows for the incorporation of very high diffusion coefficients for grid cells, which belong to dispersal networks (cf. Sec. 3.4). It also allows for spatially heterogeneous bacterial dispersal conditions (cf. Ch. 6).

3.2.4 Bacterial growth and reproduction

The processes of growth and reproduction are not distinguished but modelled simultaneously as the growth of bacterial biomass. This growth is related to the substrate uptake – the more uptake is available for growth (cf. Eqs. (3.4); (3.6)) the more the bacteria can grow. The effective bacterial growth rate is given by:

$$\mu_{eff}^{i,j,t} = \mu_{\max}^{eff} \frac{q_{eff}^{i,j,t}}{q_{\max} - \tilde{a}}, \tag{3.14}$$

where $\mu_{\max}^{eff}$ is the maximum effective growth rate, and $q_{\max} - \tilde{a}$ is the potential maximum effective uptake rate, calculated by assuming maximum uptake, which is exclusively used for maintenance and growth. Hence, the change in biomass through growth is given by:

$$\left.\frac{C_x^{i,j,t+1} - C_x^{i,j,t}}{\Delta t}\right|_{react} = \mu_{eff}^{i,j,t} C_x^{i,j,t}, \tag{3.15}$$

which can be negative, if the maintenance rate is not met (i.e. $q_{eff}^{i,j,t} < 0$). In this case bacterial cells become inactive – they do not consume substrate, disperse, or grow any more but do remain in the system, which leads to an increase in the concentration of inactive biomass:

$$\left.\frac{C_y^{i,j,t+1} - C_y^{i,j,t}}{\Delta t}\right|_{react} = \max\left(0, -\mu_{eff}^{i,j,t}\right) C_x^{i,j,t}. \tag{3.16}$$

To determine the maximum uptake rate $q_{\max}$ we use the growth yield coefficient corrected for maintenance, which only considers the substrate consumption for growth (cf. van Bodegom 2007):

$$Y_g = \frac{\mu_{eff}^{i,j,t}}{q_{eff}^{i,j,t}} \tag{3.17}$$

and, by inserting equation (3.14), get:

$$q_{\max} = \frac{\mu_{\max}^{eff}}{Y_g} + \tilde{a}. \tag{3.18}$$

3.2.5 Substrate diffusion

The substrate diffusion is modelled with the same approximation algorithm as the bacterial dispersal (cf. Sec. 3.2.3), but with a spatially and temporally invariant diffusion coefficient. Hence, the finite difference equation is (cf. Eqs. (3.7); (3.10)):

$$\left.\frac{C_s^{i,j,t+1} - C_s^{i,j,t}}{\Delta t}\right|_{diff} = \frac{D_s}{cl^2} \sum_{(k,l)\in NBH_{i,j}} w_{k,l} C_s^{k,l,t}. \tag{3.19}$$

3.2.6 Summary

Summing up all processes, we can write the following discrete equations which correspond to the reaction-diffusion model given by equations (3.1), (3.2) and (3.3):

$$\left.\frac{C_x^{i,j,t+1}-C_x^{i,j,t}}{\Delta t}\right|_{diff+react} = \frac{1}{cl^2}\sum_{\substack{(k,l)\in NBH_{i,j}\\(k,l)\neq(i,j)}} w_{k,l}\left(C_x^{k,l,t}-C_x^{i,j,t}\right)\bar{h}\left(D_{x,eff}^{i,j,t,C_a}, D_{x,eff}^{k,l,t,C_a}\right) + q_{eff}^{i,j,t} Y_g C_x^{i,j,t}, \tag{3.20}$$

$$\left.\frac{C_s^{i,j,t+1}-C_s^{i,j,t}}{\Delta t}\right|_{diff+react} = \frac{D_s}{cl^2}\sum_{(k,l)\in NBH_{i,j}} w_{k,l} C_s^{k,l,t} - q^{i,j,t} C_x^{i,j,t}, \tag{3.21}$$

$$\left.\frac{C_y^{i,j,t+1}-C_y^{i,j,t}}{\Delta t}\right|_{react} = \max\left(0, -q_{eff}^{i,j,t}\right) Y_g C_x^{i,j,t}. \tag{3.22}$$

3.3 Model inputs and outputs

The simulation model for the consumer-resource system was implemented in Delphi 5.0 (Borland 1999), including a graphical user interface (Fig. 3.3).

In accordance with the laboratory experiments (Ch. 2), the model inputs (cf. Fig. 3.3) include the abiotic conditions (agar concentration C_a: 3, 4, 5 g/l; initial substrate concentration C_s^0: 0.01-1 g/l) and the bacterial biomass inoculated (the average wet mass of 1 bacterial cell is assumed to be 2.5 pg, i.e. 6×10^7 cells (as inoculated in the experiments; cf. Sec. 2.2) relate to 0.15 mg). The simulation time can be chosen up to 2000 h. The standard grid cell side length cl is 1 mm, but the mesh is variable from 0.25-2 mm. The standard time step Δt of 60 s can be reduced down to 10 s, in particular, to simulate very fast bacterial diffusion along dispersal networks (cf. Sec. 3.5). The presence of dispersal networks and their spatial configuration (cf. Ch. 5; 6; 7) also belong to the model inputs. Finally, the relative abundance and spatial autocorrelation of fractal patterns for heterogeneous abiotic conditions (cf. Ch. 6) can be specified.

All model outputs (cf. Fig. 3.3) are time-dependent. Most important are the simulated spatial patterns of bacteria and substrate. From the bacterial distribution, the bacterial colony area, its growth velocity, the mean, minimum, maximum and total population (biomass) of bacteria in the system and the population growth rate are calculated. From the substrate distribution the mean, minimum, maximum and total amount of substrate in the system are derived. This allows for determining the amount of substrate consumed by bacteria at any given time in the simulation, which is an operationalisation of the ecosystem service of interest – the biodegradation of organic contaminants. Bacterial substrate consumption (proportional to the initial amount of substrate) serves as a measure of biodegradation performance throughout the following chapters.

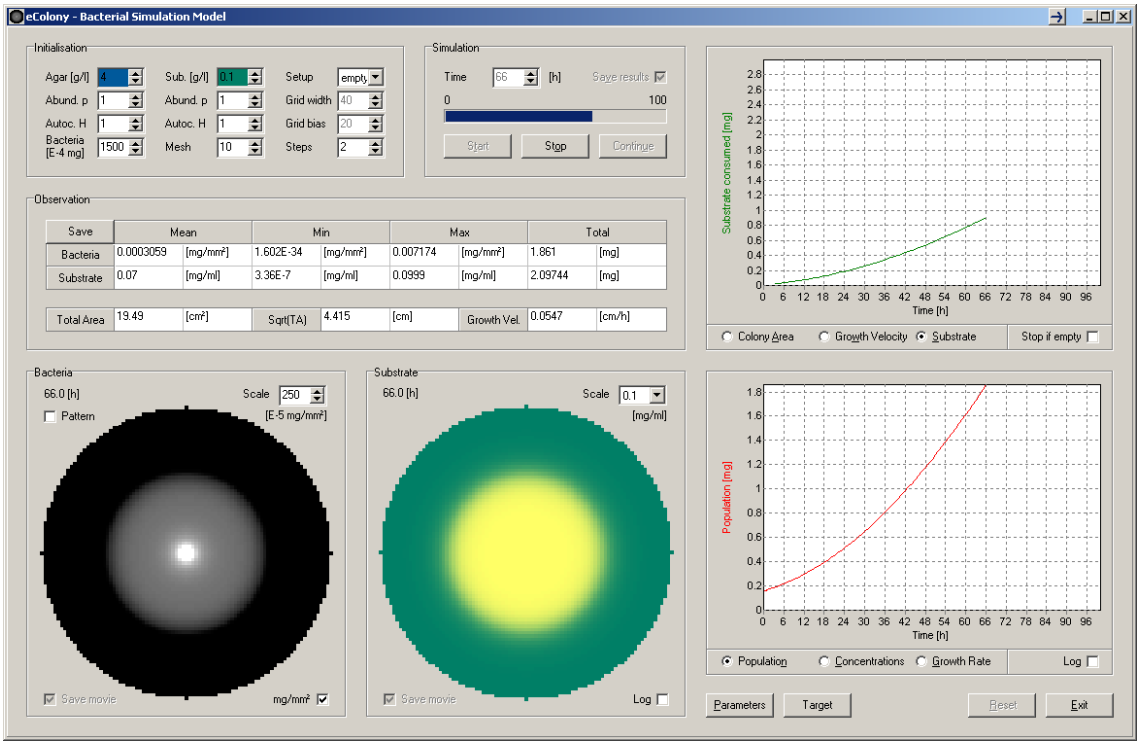

Figure 3.3 Graphical user interface of the bacterial simulation model.

3.4 Model parameterisation

The maximum effective growth rate $\mu_{\max}^{eff}$ of *Pseudomonas putida* PpG7 bacteria was approximated for growth on liquid minimal medium in presence of 2 g/l glucose (Fluka, Switzerland) as sole energy source, as described earlier by Wick et. al. (2001). Moreover, the model contains a number of parameters that were approximated from literature (cf. Table 3.1). Following the approach of pattern-oriented modelling (Grimm et al. 2005), the remaining parameter values are indirectly determined by optimising the fit of the model output to particular patterns observed from the laboratory experiments – the total area covered by the bacterial colony as a function of time and abiotic conditions (cf. Ch. 2).

To fit a selected set of simulation model parameter values to the data we define bound constraints for the parameter values and perform a pattern search within these constraints (Lewis and Torczon 1998; 1999). For this purpose, the objective value R to be minimised during the pattern search is defined as the sum of weighted squared residuals:

$$R = \sum_{\substack{C_a=3,4,5 \\ C_s^0=0.1,1}} \sum_{\substack{m=1,2..4 \\ t=0,1..66}} \frac{\left(TA_{mdl}^{C_a,C_s^0}(t) - TA_{msr}^{C_a,C_s^0}(m,t)\right)^2}{VAR_{smth}^{C_a,C_s^0}(t) + 0.5}. \qquad (3.23)$$

This R-value provides a measure of the model's agreement to the data, that is, the model performance (low R means high performance and vice versa). The residuals are

the differences between model output $TA_{mdl}^{C_a,C_s^0}(t)$ and the four replicate measurements $TA_{msr}^{C_a,C_s^0}(m,t)$ at each point in time ($m = 1, 2..4$; $t = 0, 1..66$ h) and for each combination of initial conditions ($C_a = 3, 4, 5$; $C_s^0 = 0.1, 1$ g/l). The weights for each point are obtained from the variance of the measurement data at this point $VAR_{smth}^{C_a,C_s^0}(t)$, which is smoothed with a fourth-order polynomial Savitzky-Golay filter (Orfanidis 1995) with a frame width of 15 points, and biased with a default variance of 0.5 cm^4.

According to the different model configurations (e.g. different bacterial dispersal strategies; cf. Ch. 4) specific subsets of simulation model parameters are included in the optimisations. The excluded parameters are fixed to standard values (cf. Ch. 4 for details). The high correspondence between simulation model and observation data is exemplified in figure 3.4.

Table 3.1 Simulation model parameters.

Parameter	Symbol	Values	Units[a]	Source
time step	Δt	30-60	s	-
minimum dispersal fraction	$\lambda_{\min}$	0.5[b] 0.05[c]	-	qualitative fit to experiments, (cf. Golding et al. 1998)
maximum effective growth rate	$\mu_{\max}^{eff}$	0.4142	1/h	own measurement
maintenance rate	$\tilde{a}$	0.0005	$g_s/g_x/h$	parameter testing[d]
strategy thresholds	c_0	0.0005	$g_s/g_x/h$	parameter optimisation[e]
	c_1	0.0055	$g_s/g_x/h$	
	c_2	0.581	$g_s/g_x/h$	
	c_3	0.6684	$g_s/g_x/h$	
dispersal reduction limit[f]	$C_{x,\lambda}$	0.125×10^{-6}	g_x/mm^2	qualitative fit to experiments, (cf. Golding et al. 1998)
maximum dispersal concentration[f]	$C_{x,\max}$	0.25×10^{-6}	g_x/mm^2	qualitative fit to experiments, (cf. Golding et al. 1998)
grid cell side length	cl	1	mm	-
maximum dispersal consumption rate	$\tilde{d}_{\max}$	0.005	$g_s/g_x/h$	parameter testing[d]
substrate diffusion coefficient	D_s	2.33	mm^2/h	(Zhang and Fang 2005)
maximum bacterial diffusion coefficients	$D_{x,\max}^{3\,g_a/l}$	5.58	mm^2/h	parameter optimisation[e]
	$D_{x,\max}^{4\,g_a/l}$	1.81	mm^2/h	

Parameter	Symbol	Values	Units[a]	Source
maximum bacterial diffusion coefficients	$D_{x,\max}^{5\,g_a/l}$	0.21	mm^2/h	parameter optimisation[e]
	$D_{x,\max}^{DN}$	144	mm^2/h	qualitative fit to experiments
Monod half-saturation constant	K_s	0.09	g_s/l	approximated from literature (cf. Hardy et al. 1993)
maximum substrate uptake rate	$q_{\max}$	0.6908	$g_s/g_x/h$	calculated from Eq. (3.18)
growth yield coefficient	Y_G	0.6	g_x/g_s	approximated from literature (cf. Isken et al. 1999)
fraction of protein mass in dry biomass		0.5	-	
fraction of dry biomass in wet biomass		0.25	-	

[a] g_s – grams of substrate, g_x – grams of dry biomass
[b] On swimming agar (agar concentration < 3.5 g/l; cf. Sec. 4.2).
[c] On swarming agar (agar concentration > 3.5 g/l; cf. Sec. 4.2).
[d] Cf. Sec. 4.2.2.
[e] Cf. Sec. 4.3; Table 4.3.
[f] Cf. Sec. 4.2.1; Eq. (4.3). Not on dispersal networks.

3.5 Bacterial dispersal networks

In the simulation model, high diffusivity corridors are implemented through a high bacterial diffusion coefficient $D_{x,\max}^{DN}$ in the corresponding grid cells (cf. Table 3.1). The value of the bacterial diffusion coefficient along these dispersal networks DN was determined by qualitative comparison of the simulation model outcome (e.g. Fig. 3.4c) to the observations from the laboratory experiments with glass fibres (e.g. Fig. 3.4d; cf. Sec. 2.3). Throughout this thesis, different spatial configurations of dispersal networks are applied: crosswise networks for adjusting the model to experiments (e.g. Fig. 3.5a; cf. Sec. 3.4), grid-like networks for simulating general effects of networks and obtaining indications about the role of their spatial configuration (e.g. Fig. 3.5b, c; cf. Ch. 5; 6) and random networks for analysing the spatial configuration's impact on biodegradation performance in detail (e.g. Fig. 3.5d, e, f; cf. Ch. 7).

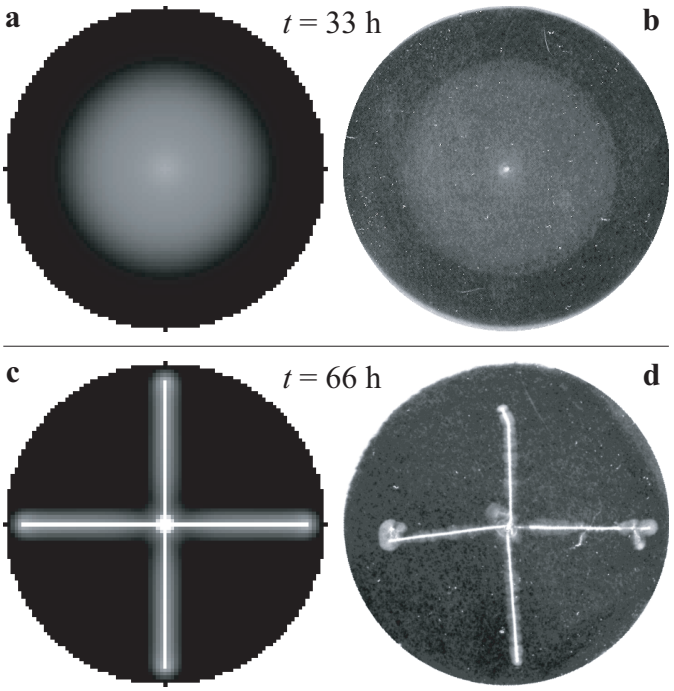

Figure 3.4 Spatial patterns of bacteria on agar plates. Bacterial concentrations are indicated by grey shading, increasing from black (no bacteria) to white. **a, b** After 33 h under 0.1 g/l initial glucose concentration and 3 g/l agar concentration. **a** Simulation model result. **b** Experimental result (cf. Fig. 2.1a). **c, d** After 66 h under 0.1 g/l initial glucose concentration and 5 g/l agar concentration, with a dispersal network of four glass fibres. **c** Simulation model result (cf. Sec. 3.5). **d** Experimental result (cf. Sec. 2.3; Fig. 2.1b).

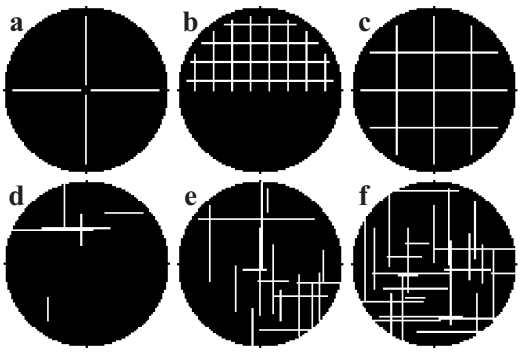

Figure 3.5 Examples of different bacterial dispersal networks in the model, implemented as high diffusivity corridors (white grid cells) on the simulation area (visualised in black). **a** Crosswise configuration (cf. Fig. 3.4). **b, c** Grid-like configurations (cf. Ch. 5; 6). **d-f** Random configurations (cf. Ch. 7).

Chapter 4

Conditional Bacterial Dispersal*

4.1 Conditional dispersal

Ecological studies have shown that mode of dispersal has a fundamental impact on the dynamics, spatial distribution and survival of populations in many ecosystems (e.g. Roughgarden et al. 1988; Hastings 1993; Hovestadt and Poethke 2006; Münkemüller and Johst 2008). In microbiology, however, its role is largely unexplored. Hence, we investigate the impact of dispersal mode on bacterial colony growth and its relevance for subsequent resource consumption and, in turn, biodegradation performance. In particular, we study the ecological concept of conditional dispersal (e.g. Ims and Hjermann 2001; Bowler and Benton 2005; Armsworth 2009; Cosner 2009; Hovestadt et al. 2010).

Generally, unconditional dispersal refers to the assumption of a constant dispersal rate, irrespective of biotic and abiotic factors. By contrast, conditional dispersal refers to dispersal rates with functional dependence on these factors. Various internal and external conditions can be considered to determine a conditional dispersal function (Ims and Hjermann 2001; Bowler and Benton 2005), for instance, habitat quality (Armsworth 2009), habitat dynamics (Travis and Dytham 1999), population density (Johst and Brandl 1997a; Poethke and Hovestadt 2002; Ims and Andreassen 2005; Travis et al. 2009; Münkemüller et al. 2011), and different more or less complex functional relationships can be assumed (Hovestadt et al. 2010).

To analyse whether conditional dispersal is a relevant aspect of the bacterial behaviour we use the bacterial simulation model described in chapter 3. Bacterial models are known to provide excellent possibilities for investigating ecological concepts in a microbiological context (e.g. Jessup et al. 2004; Kreft 2004), which can benefit both ecology (Kerr et al. 2002; Cadotte et al. 2005; Jessup et al. 2005; Benton et al. 2007) and microbiology (Battin et al. 2007; Prosser et al. 2007). They have been used successfully to interpret experimental observations (Wimpenny and Colasanti 1997; van Loosdrecht et al. 2002; Matsushita et al. 2004; Picioreanu et al. 2007) and to predict bacterial behaviour (Lega and Passot 2004; Zorzano et al. 2005).

The simulation model translates bacterial dispersal into a bacterial diffusion coefficient (cf. Sec. 3.2.3). Two aspects of conditional dispersal can be regarded in this context: (a) the dependence of bacterial dispersal on bacterial density, and (b) the dependence of bacterial dispersal on resource uptake. Both aspects are included in the

* A research paper with analogous content to this chapter was submitted (title: The relevance of conditional dispersal for bacterial colony growth and biodegradation).

model as variable functional dependencies of the bacterial diffusion coefficient on (a) bacterial concentration and (b) substrate uptake rate. The focus of our study lies on aspect (b), because in existing bacterial colony models (e.g. Kreft et al. 1998; Mimura et al. 2000; Ginovart et al. 2002a) bacterial dispersal is often considered to be uncoupled from resource uptake. Kawasaki et al. (1997) proposed a simple linear relationship between the bacterial diffusion coefficient and resource uptake. We consider several functional relationships of increasing complexity.

Drawing on the corresponding model results, implications can be derived about the sensitivity of the spatiotemporal bacterial colony dynamics to differences in the dispersal process. Pivotal to our approach is the incorporation of well-controlled laboratory experiments into the analysis with *Pseudomonas putida* PpG7 organisms growing under a variety of environmental conditions on glucose agar (cf. Ch. 2). The different model configurations are fitted to multiple colony growth patterns obtained from these laboratory experiments (cf. Sec. 2.2) in the sense of pattern-oriented modelling (Grimm et al. 2005). Based on goodness of fit, we show the extent to which conditional dispersal with respect to resource uptake improves the accuracy of the simulation model compared with unconditional dispersal. We also show that disregarding conditional dispersal may have a considerable impact on bacterial degradation in the model and derive a conditional dispersal mode for reliably assessing the performance of this ecosystem service.

Furthermore, we discuss how the implementation of conditional bacterial dispersal with respect to resource uptake is related to the ecological concept of resource allocation (e.g. Piceno and Lovell 2000; Ernest et al. 2003; Brown et al. 2004; Johst et al. 2008). This concept describes the division of resource uptake into fractions allocated to different energy-demanding processes, such as reproduction, movement or maintenance. In the given context of bacterial colony growth and biodegradation, the relation is based on the assumption that bacterial dispersal requires energy expenditure.

4.2 Methods

4.2.1 Bacterial dispersal strategies

In the simulation model, bacterial dispersal at agar concentration C_a is related to two conditions: bacterial concentration and substrate uptake via

$$D_{x,eff}^{i,j,t,C_a}(C_x^{i,j,t}, q^{i,j,t}) = \alpha(C_x^{i,j,t}, C_a) \cdot D_x(q^{i,j,t}, C_a). \tag{4.1}$$

Omitting indices, this formula can be simply written as:

$$D_{x,eff}(C_x, q) = \alpha(C_x) \cdot D_x(q). \tag{4.2}$$

The first term defines how bacterial dispersal depends on bacterial concentration:

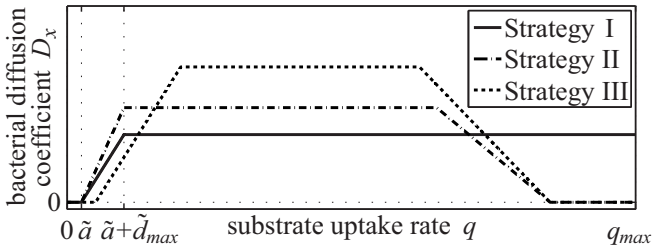

Figure 4.1 Functional dependence of bacterial dispersal on substrate uptake in general form (cf. Eq. (4.4); Table 4.1). Bacterial dispersal strategies I, II and III (cf. legend, definitions on page 36).

$$\alpha(C_x^{i,j,t}, C_a) = \begin{cases} \lambda_{\min}^{C_a} + \left(1 - \lambda_{\min}^{C_a}\right) \dfrac{C_x^{i,j,t}}{C_{x,\lambda}} & C_x^{i,j,t} \le C_{x,\lambda} \\ 1 & C_{x,\lambda} < C_x^{i,j,t} \le C_{x,\max} \\ \dfrac{C_{x,\max}}{C_x^{i,j,t}} & \textit{otherwise} \end{cases} . \tag{4.3}$$

At high bacterial concentrations the access of the bacteria to the dispersal medium is limited and the probability of collisions between bacteria increases (Golding et al. 1998). At low bacterial concentrations the bacteria suffer from the limited provision of dispersal-facilitating substances (to disperse on swarming agar (agar concentration above 3.5 g/l) bacteria need to produce a lubrication fluid (Golding et al. 1998; Cohen et al. 1999), also referred to as wetting agents (Matsuyama and Nakagawa 1996; Bees et al. 2000; Harshey 2003); to disperse in swimming agar (agar concentration below 3.5 g/l) bacteria secrete materials which make the liquid more suitable for swimming (Golding et al. 1998)). Hence, dispersal is reduced in both cases, at high ($C_x^{i,j,t} > C_{x,\max}$) and at low ($C_x^{i,j,t} < C_{x,\lambda}$) bacterial concentrations.

The second term in equation (4.1) defines the general dependence of bacterial dispersal on substrate uptake (cf. Fig. 4.1):

$$D_x(q^{i,j,t}, C_a) = D_{x,\max}^{C_a} \cdot \begin{cases} 0 & q^{i,j,t} < c_0 \vee q^{i,j,t} > c_3 \\ \dfrac{q^{i,j,t} - c_0}{c_1 - c_0} & c_0 \le q^{i,j,t} < c_1 \\ 1 & c_1 \le q^{i,j,t} < c_2 \\ \dfrac{q^{i,j,t} - c_3}{c_2 - c_3} & \textit{otherwise} \end{cases} . \tag{4.4}$$

This relationship is given by a piecewise linear function, defined by the strategy parameters $D_{x,\max}^{C_a}$, c_0, c_1, c_2 and c_3. The explicit values of these parameters were determined by optimisation (cf. Sec. 3.4). As our focus lies on conditional bacterial dispersal with respect to substrate uptake, we analysed three different *bacterial*

Table 4.1 Bacterial dispersal strategies – parameters included in the optimisations.

Strategy	Fixed parameters	Optimised parameters
I	$c_0 = \widetilde{a}$, $c_1 = \widetilde{a} + \widetilde{d}_{\max}$, $c_2 = q_{\max}$, $c_3 = q_{\max}$	$D_{x,\max}^{C_a}$
II	$c_0 = \widetilde{a}$, $c_1 = \widetilde{a} + \widetilde{d}_{\max}$	$D_{x,\max}^{C_a}$, c_2 , c_3
III	-	$D_{x,\max}^{C_a}$, c_2 , c_3 , c_0 , c_1

dispersal strategies of increasing complexity with regard to functional dependence on substrate uptake. These were defined in the following way:

- *Strategy I* – Dispersal is unconditional with respect to substrate uptake (black curve in Fig. 4.1). The bacteria always disperse as much as they can. Only if the uptake falls below the energy demand for dispersal and maintenance ($q^{i,j,t} < \widetilde{a} + \widetilde{d}_{\max}$) will dispersal be reduced. Then the bacteria cannot grow, because the whole uptake is allocated to (reduced) dispersal and maintenance. If the uptake falls below the maintenance rate ($q^{i,j,t} < \widetilde{a}$), it will be allocated to (reduced) maintenance only. This leads to no bacterial dispersal and negative growth (cf. Eqs. (3.6); (3.14)).

- *Strategy II* – Simple conditional dispersal with respect to substrate uptake is implemented (red curve in Fig. 4.1). The bacteria can reduce their dispersal at high uptake rates ($q^{i,j,t} > c_2$). The uptake, which is not used for dispersal, is allocated to bacterial growth instead.

- *Strategy III* – More complex conditional dispersal with respect to substrate uptake (in comparison to strategy II) is implemented (blue curve in Fig. 4.1). The bacteria can reduce their dispersal at high uptake rates ($q^{i,j,t} > c_2$) as well as at low uptake rates ($q^{i,j,t} < c_1$), allocating the available uptake to growth instead.

The effective bacterial diffusion coefficient $D_{x,eff}^{i,j,t,C_a}$ (cf. Eq. (4.1)) also determines the fraction of uptake allocated to dispersal (cf. Sec. 3.2.2; Eq. (3.6)):

$$\widetilde{d}_{eff}^{\,i,j,t} = \widetilde{d}_{\max} \frac{D_{x,eff}^{i,j,t,C_a}}{D_{x,\max}^{C_a}} . \tag{4.5}$$

Table 4.2 Energy setups.

$\widetilde{d}_{\max}$ [$g_s/g_x/h$]	0	0.005	0.01
$\widetilde{a}$ [$g_s/g_x/h$]			
0.0005	A	B	C
0.001	D	E	F

According to the different bacterial dispersal strategies specific subsets of parameters of the dispersal function were included in the optimisations (Table 4.1; cf. Sec. 3.4). The excluded parameters were fixed to the values given in table 4.1.

4.2.2 Selected dispersal model configurations

To compare the bacterial dispersal strategies, it was necessary to specify the model parameter values for the maintenance rate $\widetilde{a}$ and the maximum energy demand for dispersal $\widetilde{d}_{\max}$. We call a combination of values for $\widetilde{a}$ and $\widetilde{d}_{\max}$ an *energy setup*. Based on the outcome of several test parameter optimisations 6 different energy setups, comprising reasonable ranges of values for $\widetilde{a}$ and $\widetilde{d}_{\max}$, were analysed (A-F; cf. Table 4.2). As many microbial models neglect energy demands for bacterial dispersal, we also investigated the performance of the different strategies when a $\widetilde{d}_{\max}$-value of 0 $g_s/g_x/h$ was assumed (energy setups A and D; cf. Table 4.2).

For each energy setup, we optimised the model parameter values of the three different bacterial dispersal strategies (cf. Table 4.1; Fig. 4.1). We defined a *dispersal model configuration* as the combination of an energy setup (A-F) and a bacterial dispersal strategy (I, II, III). The comparison of dispersal model configurations comprised the goodness-of-fit measure R (cf. Eq. (3.23)), the number of optimised parameters N_{pars}, and the graphical congruence to the experimental data (e.g. Fig. 4.2).

Since we focussed on the functional dependence on substrate uptake $D_x(q)$, the functional dependence on bacterial concentration $\alpha(C_x)$ was not varied during strategy optimisation (cf. Eq. (4.2)). The following parameter values were applied: $\lambda_{\min}^{C_a=3} = 0.5$ g_x/mm^2, $\lambda_{\min}^{C_a=4,5} = 0.05$ g_x/mm^2, $C_{x,\lambda} = 0.125\times10^{-6}$ g_x/mm^2, $C_{x,\max} = 0.25\times10^{-6}$ g_x/mm^2 (cf. Eq. (4.3)). To test the robustness of our findings to variations in this functional dependence, values of $C_{x,\max} = 0.5\times10^{-6}$ g_x/mm^2 and $C_{x,\max} = 1.25\times10^{-6}$ g_x/mm^2 were applied, too, but did not alter our results qualitatively.

4.3 Results

The fixed and the optimised parameter values, and the sum of weighted squared residuals R for each dispersal model configuration are given in table 4.3. These

Table 4.3 Optimisation results for each dispersal model configuration. The small-written values were fixed during optimisation (cf. Table 4.1). The bold values indicate the dispersal model configurations shown in figures 4.2 and 4.3.

Model configuration		A I	A II	A III	B I	B II	B III	C I	C II	C III
$\tilde{a}$	[g_s/g_x/h]		0.0005			0.0005			0.0005	
$\tilde{d}_{\max}$	[g_s/g_x/h]		0			0.005			0.01	
$D_{x,\max}^{3\,g_a/l}$	[mm²/h]	4.99	5.54	7.24	5.03	5.58	7.17	5.1	5.69	7.2
$D_{x,\max}^{4\,g_a/l}$	[mm²/h]	1.19	1.75	2.94	1.19	1.81	2.92	1.19	1.82	2.87
$D_{x,\max}^{5\,g_a/l}$	[mm²/h]	0.18	0.21	0.25	0.18	0.21	0.26	0.18	0.21	0.26
c_2	[g_s/g_x/h]	0.6908	0.5857	0.5625	0.6908	0.581	0.5537	0.6908	0.583	0.5444
c_3	[g_s/g_x/h]	0.6908	0.6654	0.663	0.6908	0.6684	0.6684	0.6908	0.6656	0.6737
c_0	[g_s/g_x/h]	0.0005	0.0005	0.1892	0.0005	0.0005	0.178	0.0005	0.0005	0.1643
c_1	[g_s/g_x/h]	0.0005	0.0005	0.2875	0.0055	0.0055	0.2733	0.0105	0.0105	0.2874
N_{pars}	[]	3	5	7	3	5	7	3	5	7
R	[]	9306	4198	4056	**9404**	**4215**	**4004**	9501	4252	3990

Model configuration		D I	D II	D III	E I	E II	E III	F I	F II	F III
$\tilde{a}$	[g_s/g_x/h]		0.001			0.001			0.001	
$\tilde{d}_{\max}$	[g_s/g_x/h]		0			0.005			0.01	
$D_{x,\max}^{3\,g_a/l}$	[mm²/h]	4.97	5.54	7.18	5.05	5.6	7.25	5.09	5.7	7.27
$D_{x,\max}^{4\,g_a/l}$	[mm²/h]	1.19	1.74	2.94	1.19	1.8	2.98	1.2	1.85	3
$D_{x,\max}^{5\,g_a/l}$	[mm²/h]	0.18	0.2	0.26	0.18	0.21	0.26	0.18	0.21	0.25
c_2	[g_s/g_x/h]	0.6913	0.5898	0.5571	0.6913	0.584	0.5527	0.6913	0.593	0.5625
c_3	[g_s/g_x/h]	0.6913	0.6624	0.6674	0.6913	0.6664	0.6693	0.6913	0.6583	0.6625
c_0	[g_s/g_x/h]	0.001	0.001	0.1843	0.001	0.001	0.1855	0.001	0.001	0.178
c_1	[g_s/g_x/h]	0.001	0.001	0.2787	0.006	0.006	0.2797	0.011	0.011	0.288
N_{pars}	[]	3	5	7	3	5	7	3	5	7
R	[]	9327	4214	4007	9414	4228	4002	9512	4295	4081

optimisation results show a significant increase in model accuracy for the conditional bacterial dispersal strategies II and III (R-values 3990-4295) in comparison to the unconditional bacterial dispersal strategy I (R-values 9306-9512). Furthermore, the model accuracy is slightly lower for strategy II than for strategy III. The latter, however, comprises two additional optimisation parameters. These results are robust for all energy setups A-F, and the optimised parameter values are very similar. Hence, the graphical comparison of dispersal model configurations B I-III and the measurement data (Fig. 4.2) is representative for all energy setups.

Inspecting the optimised parameter values, we found a general trend of increasing bacterial diffusion coefficients from unconditional dispersal strategy I to conditional dispersal strategies II and III (cf. Table 4.3). The reason for this is that the range of substrate uptake rates at which the bacteria disperse is smaller for strategies II and III than for strategy I. Consequently, the bacterial diffusion coefficients have to increase to fit the same experimental colony growth curves.

The model output deviates significantly from the empirical data for 4 g/l agar concentration (Fig. 4.2). This is due to the fact that the model is optimised to the whole dataset at once and the residuals are weighted according to the variances of the data (cf. Sec. 3.4; Eq. (3.23)). These variances are comparatively high for 4 g/l agar concentration. Hence, the corresponding data have less influence on the optimisation than the data obtained with 3 g/l and 5 g/l agar concentration.

Figure 4.3 shows an example of the simulated substrate (glucose) consumption resulting from the dispersal model configurations B I, B II and B III (for 3 g/l agar concentration and 1 g/l initial substrate concentration). Substrate consumption depends sensitively on the assumed bacterial dispersal strategy. Unconditional bacterial dispersal according to strategy I results in higher substrate consumption than conditional dispersal according to the strategies II and III. Similar to the colony areas (Fig. 4.2), the differences in the dispersal model configurations B II and B III are rather small.

4.4 Discussion

The motivation for studying the theoretical ecological concept of conditional dispersal (e.g. Travis and Dytham 1999; Bowler and Benton 2005; Armsworth 2009) was to investigate and improve the accuracy of the process-based bacterial simulation model (cf. Ch. 3), which was developed to assess the ecosystem service of biodegradation of organic contaminants in terms of the bacterial consumption of resources during colony growth. This requires a reliable model structure that includes all ecological processes relevant for the bacterial system dynamics. Therefore, we examined three bacterial dispersal strategies differing in their functional response to resource uptake with regard to their impacts on colony growth and biodegradation performance. A fundamental aspect of our approach was to confront the simulation data resulting from the different dispersal strategies with empirical bacterial colony growth data from adequate laboratory experiments (cf. Ch. 2) in order to estimate model accuracy (e.g. cf. Hilborn and Mangel 1997). We analysed which bacterial dispersal strategy and which parameter combinations fit best to the laboratory results. This allowed us to identify the relevance of the ecological concept of conditional dispersal and the parameter values for correctly

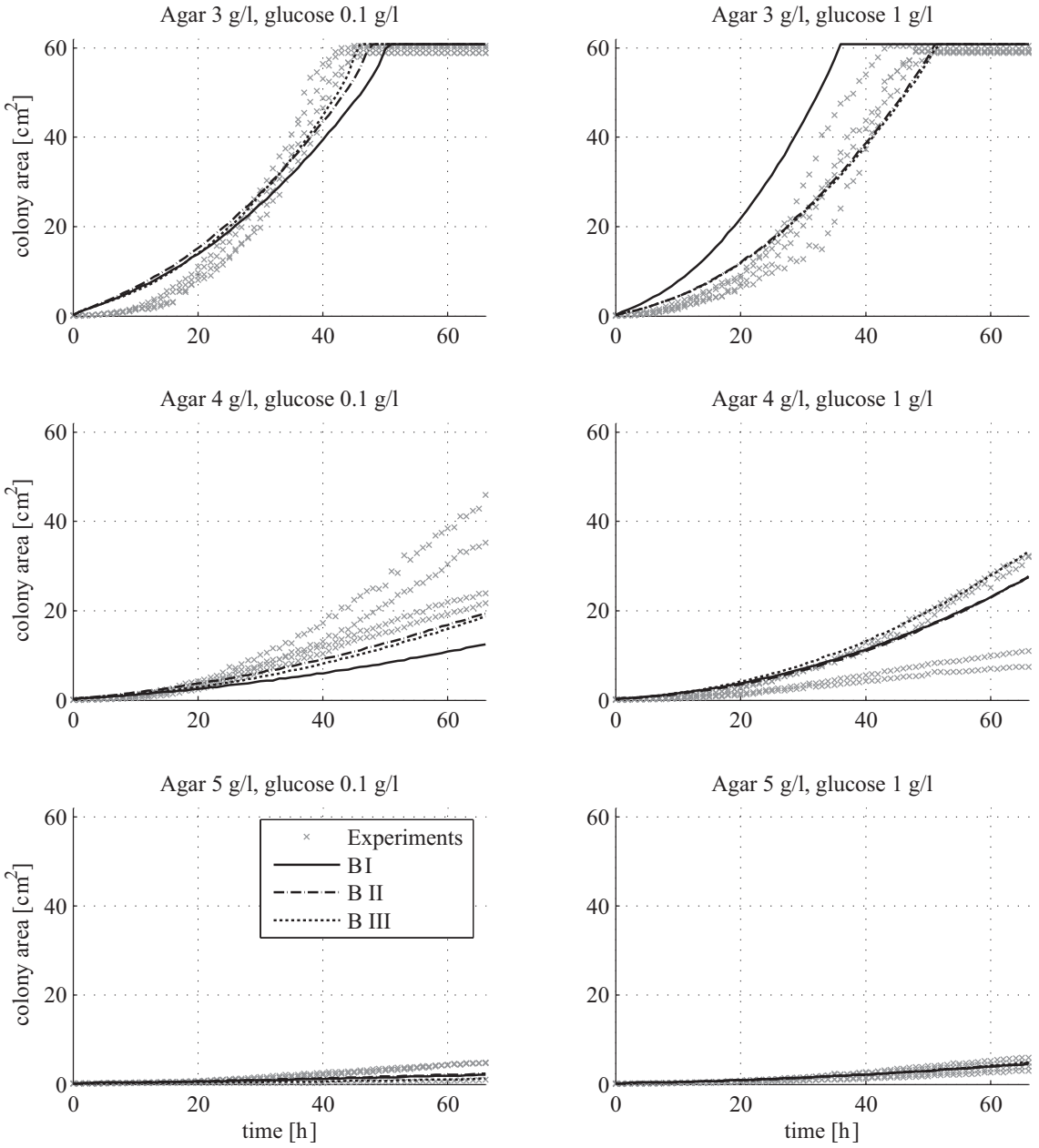

Figure 4.2 Experimental measurement data (grey crosses; cf. Fig. 2.2) and simulation model results with the energy setup B and three different bacterial dispersal strategies I, II and III (different line types; cf. legend). Total area of bacterial colonies plotted versus time. Different subplots display different combinations of agar concentration and initial glucose concentration (cf. subplot titles).

describing bacterial colony growth with the simulation model and, more importantly, for reliably assessing the performance of biodegradation.

4.4.1 The necessity to incorporate conditional dispersal

Comparison of the simulation results to empirical data (cf. Fig. 4.2) revealed that the accuracy of the model can be significantly enhanced when conditional, rather than

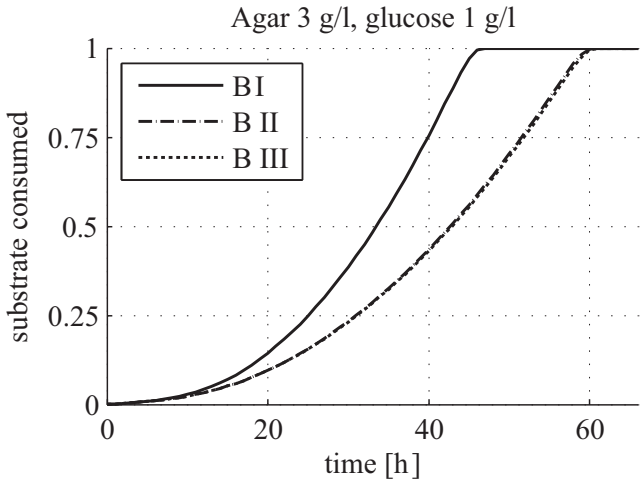

Figure 4.3 Simulated consumption of substrate (glucose) with the bacterial dispersal configurations B I, B II and B III (different line types; cf. legend), for 3 g/l agar concentration and 1 g/l initial substrate concentration. Proportion of substrate consumed plotted against time.

unconditional, bacterial dispersal with respect to resource uptake is assumed. In particular, it proved to be very important that bacterial dispersal ceases at high resource uptake rates (i.e. conditional dispersal strategy II fitted much better than unconditional dispersal strategy I). The additional assumption of the cessation of bacterial dispersal at low resource uptake rates (conditional dispersal strategy III) only led to minor improvements (compared to conditional dispersal strategy II). Hence, the two additional optimisation parameters c_0 and c_1 included in strategy III did not add significant benefit. For this reason, we use the conditional bacterial dispersal strategy II for subsequent applications of the simulation model (cf. Table 3.1).

Most important for the assessment of biodegradation performance is our finding that, in addition to significantly improving the agreement with laboratory experiments and the reliability of the model, conditional dispersal may result in markedly different resource consumption curves compared to unconditional dispersal (Fig. 4.3). Hence, assuming unconditional instead of conditional bacterial dispersal can lead to biased model predictions on the performance of the ecosystem service of bacterial degradation.

The impact of conditional dispersal has rarely been studied in microbial systems. In experimental studies, Friedenberg (2003) tested it in microcosms for bacteriophagous nematodes, and Taylor and Buckling (2010) used resource-free zones to limit bacterial dispersal. Also, some colony growth modelling studies introduced a simple functional dependence of the bacterial diffusion coefficient on resource uptake using a linear function (e.g. Kawasaki et al. 1997; Lega and Passot 2003). But this is the first study to include different forms of this functional dependence on resource uptake, where unconditional versus conditional dispersal strategies (cf. Eq. (4.4); Fig. 4.1) are compared in the analytical framework of bacterial colony growth modelling and in relation to empirical data from experiments.

4.4.2 Relating conditional dispersal to resource allocation

Our results help to clarify the interrelations between the ecological concepts of conditional dispersal and resource allocation (e.g. Piceno and Lovell 2000; Ernest et al. 2003; Brown et al. 2004; Johst et al. 2008) in the given microbiological context. By considering bacterial energy demands for maintenance, dispersal and reproduction, the bacterial colony simulation model implicitly incorporates the ecological concept of resource allocation to these processes. The fraction of resource uptake which is allocated to dispersal is determined by the bacterial dispersal strategy. Thus, if dispersal is reduced conditionally, fewer resources will be allocated to dispersal and, consequently, more resources will be allocated to reproduction. In this way, the two ecological concepts of conditional dispersal and resource allocation are linked. Ultimately, resource allocation turned out to be a key process for bacterial colony growth and biodegradation performance.

4.4.3 The potential of the approach presented

The central idea behind the approach presented in this chapter was:

- To consider model configurations that either incorporate the ecological concept of interest (here: conditional dispersal depending on resource uptake) in a certain way or neglect it.

- To compare the results of these model configurations based on their goodness of fit to a variety of empirical data from laboratory experiments in order to investigate whether the concept considered actually matters and should be incorporated.

- To assess the relevance of this concept for reliably assessing the performance of the ecosystem service of interest (here: biodegradation).

Thus, we optimised the analytical framework for assessing bacterial ecosystems and their services. Simulation model (cf. Ch. 3) and laboratory experiments (cf. Ch. 2) had different roles in this approach with complementary benefits.

- *Simulation model* – The model allowed us to test different scenarios of incorporating the ecological concept. This variation of behavioural mechanisms such as the bacterial dispersal strategy is impossible in experiments. But it is possible in the model and we gained insight into the extent to which the ecological concept matters by comparing its effects on bacterial colony growth and on the ecosystem service of interest (resource consumption).

- *Laboratory experiments* – The experiments were essential for parameterising the different model configurations. Of major importance was the fact that the experiments comprised a broad range of abiotic conditions (here: agar concentration determining bacterial dispersal potential, and glucose concentration determining resource supply). For each combination of abiotic conditions the colony growth curves form an independent empirical pattern

and the model configurations were optimised to fit the whole variety of these patterns at once (cf. Fig. 4.2). Therefore, the approach corresponds to the strategy of pattern-oriented modelling widely used in ecology (cf. Grimm et al. 2005, and references therein). Only by fitting to multiple empirical patterns at once it was possible to reveal the relevance of conditional dispersal for bacterial colony growth and biodegradation.

Evidently, the approach allowed the analysis of bacterial ecosystem services on different levels of abstraction: concepts, models and experiments. Therefore, it can be viewed as a rigorous implementation of the scientific principle of combining pure rationalism (abstract concepts) and radical empiricism (concrete experiments), with models mediating between them. This combination is known to be crucial for gaining an understanding of the principles of complex systems, which is a precondition for both theory building and management support.

4.4.4 Main conclusion

Summing up, our study shows that the ecological concept of conditional dispersal can significantly improve the agreement of a bacterial simulation model to corresponding experimental observations. Our results specifically suggest that the propensity of bacteria to disperse may not be constant, but may depend on resources in such a way that bacterial dispersal ceases when resource uptake is high. Therefore, considering the ecological concept of conditional dispersal in microbiology can be beneficial and, in particular, of key importance for reliable predictions of bacterial degradation performance.

By following the presented approach, microbiology and theoretical ecology can benefit from each other: Microbiological models can be made more theoretically sound by founding them on general ecological concepts. On the other hand, the validity and reliability of general ecological concepts can be tested in microbiological contexts.

Chapter 5

Biodegradation Benefits from Dispersal Networks*

5.1 Assessing biodegradation performance in response to bacterial dispersal networks

Several experimental studies suggest that fungal hyphae can act as dispersal networks, increasing the performance of biodegradation *in situ* (Kohlmeier et al. 2005; Wick et al. 2007a; Furuno et al. 2010). This in turn is pivotal for developing more energy-efficient and environmentally friendly biotechnologies for remediation of contaminated soil sites (cf. Ch. 1). Such technologies require a comprehensive understanding of the dynamics, functioning and services of soil-bacteria-fungi ecosystems. Particularly, when applying dispersal networks, the impact of both their spatial configuration and the abiotic conditions on biodegradation performance have been rarely studied. These factors, however, may be essential for efficient biodegradation.

Here, we study the impact of different dispersal networks with various spatial configurations and under various abiotic conditions on the spatiotemporal dynamics of the consumer-resource system consisting of organic substrate as resource and bacteria as consumers (cf. Ch. 3; 4), with particular focus on the performance of bacterial degradation. In order to gain a mechanistic understanding of the system's spatiotemporal dynamics, we use the simulation model (cf. Ch. 3) to investigate scenarios which are not experimentally feasible, due to their complex spatial configurations. Thus, we are able to make predictions of biodegradation performance in response to dispersal network configurations and abiotic conditions. We show that bacterial dispersal, and thus contaminant uptake and degradation, strongly depend on abiotic conditions, and that dispersal networks can efficiently improve degradation performance, especially under otherwise adverse conditions.

5.2 Methods

To analyse bacterial degradation performance as a function of abiotic conditions, time and dispersal network configurations, we monitored the amount of substrate consumed by bacteria in the simulation model. According to the experimental setup in the

* A research paper with analogous content to this chapter was published (Banitz et al. 2011a).

particular case study considered (cf. Ch. 2 for a description of the laboratory experiments performed), we varied the abiotic conditions in terms of agar concentrations from 3 to 5 g/l. The initial substrate concentration was set to 0.1 g/l. We applied three different dispersal networks with grid-like structures (Networks 1, 2 and 3) as shown in figure 5.1. By simulating the combined dynamics of bacteria and substrate over a total period of 120 h without and with different dispersal networks, we analysed, if and how such networks may change the biodegradation performance. We varied the coverage of the networks and the networks' position relative to the bacterial inoculum to test, whether these factors change the simulation results significantly.

5.3 Results

Figure 5.1 shows the biodegradation performance in response to dispersal networks, measured in terms of substrate consumption during bacterial colony growth, as a function of abiotic conditions (different agar concentrations, compare graphs a, b and c), time (x-axis), and dispersal network configurations (different line colours in the graphs, cf. legend) over a total period of 120 h, and the spatial patterns of bacteria and substrate after 120 h (images).

First, figure 5.1 highlights the impact of varying abiotic conditions, in terms of different agar concentrations: The results without dispersal networks (black curves; cf. legend) clearly indicate a decrease in biodegradation performance with an increasing concentration of agar, and so with an increasingly limited bacterial dispersal. This model outcome is robust to a wide range of changes in initial substrate concentration. While the addition of dispersal networks generally leads to minor improvements under favourable bacterial dispersal conditions (i.e. low agar concentration; Fig. 5.1a), they are found to significantly improve glucose consumption under unfavourable bacterial dispersal conditions (i.e. high agar concentration; Fig. 5.1c).

Second, the graphs in figure 5.1 demonstrate the importance of specifying the time horizon over which biodegradation performance is assessed. For instance, as depicted in figure 5.1a, there are significant differences among the four simulated network configurations after 40 h, but no differences occur after 120 h. Whereas in figure 5.1c, three of the four scenarios show the same performance after 40 h, but significant differences after 120 h.

Third, the impact of different dispersal network configurations (different line colours; cf. legend) on glucose consumption, in comparison to consumption without dispersal networks, is visualised. Adding a grid-like dispersal network on half of the plate's area (Network 1) lets the bacteria disperse faster on the plates and hence, they do degrade faster than without the dispersal network. This effect gets stronger when the network covers almost the whole plate (Network 2) or when the initial distance between the network's branches and the bacterial inoculum is reduced (Network 3). The differences in degradation performance, resulting from the four different dispersal network scenarios presented, increase with an increasing concentration of agar and vary over time.

Taking everything into account, these results are a strong indication that, in addition to the presence of dispersal networks, three factors will affect biodegradation performance in reality: the abiotic conditions, the time horizon over which performance is assessed, and the structure and location of the dispersal networks.

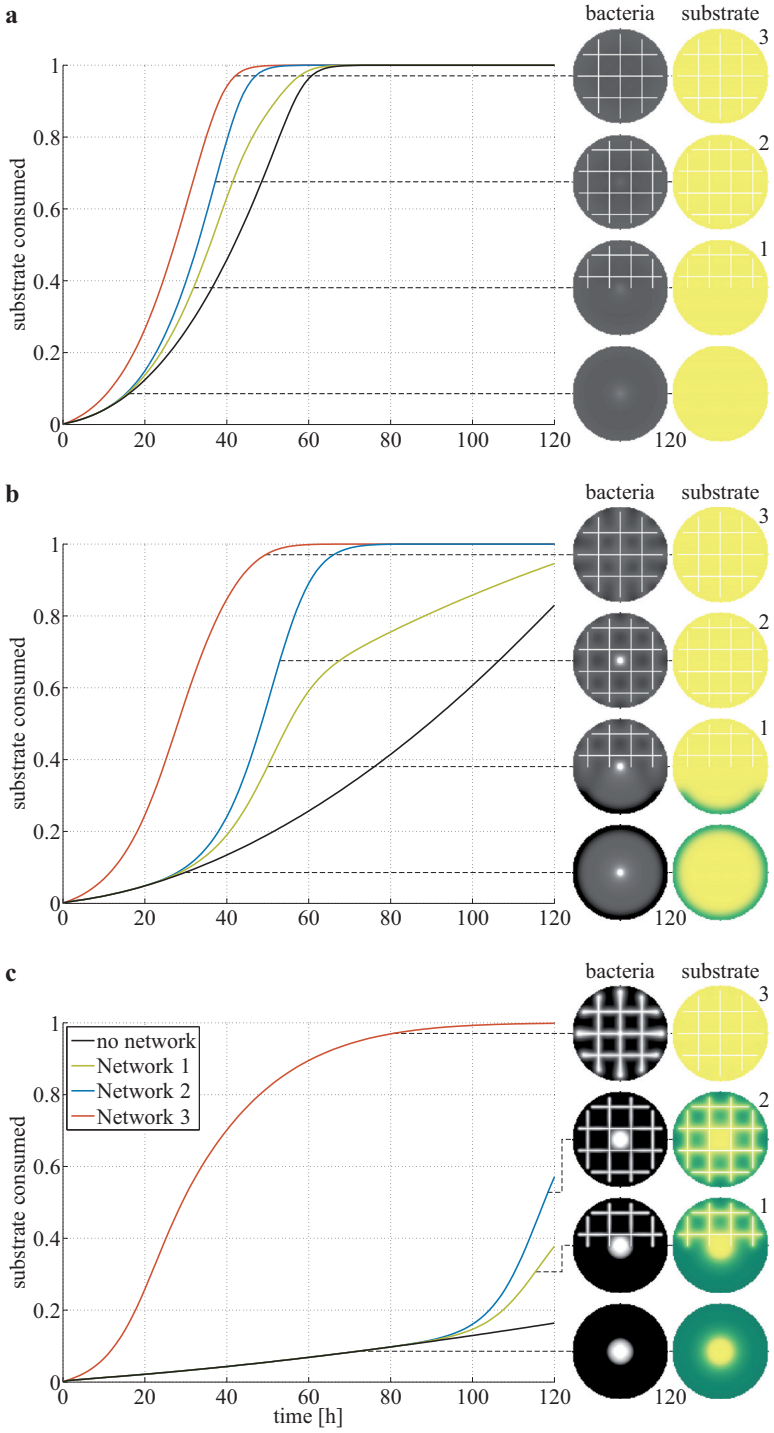

Figure 5.1 Simulated consumption of substrate (glucose) under 0.1 g/l initial glucose concentration, plotted versus time. No dispersal network – black curves, Network 1 – ochre curves, Network 2 – blue curves, Network 3 – red curves (cf. legend). The images on the right show the corresponding dispersal network configurations (white grids), and simulated spatial patterns of bacteria (left column) and substrate (right column) after 120 h. Bacterial concentrations are indicated by grey shading, increasing from black (no bacteria) to white. Substrate concentrations are indicated by colour shading, decreasing from green (0.1 g/l) to yellow (0 g/l). **a** Agar concentration 3 g/l. **b** Agar concentration 4 g/l. **c** Agar concentration 5 g/l.

5.4 Discussion

In this chapter, we presented simulations of the spatiotemporal dynamics of contaminant degrading bacteria, growing on agar plates with and without various dispersal networks and under various abiotic conditions. A number of studies have modelled bacterial colony growth on agar plates using reaction-diffusion equations (Kawasaki et al. 1997; Kitsunezaki 1997; Golding et al. 1998; Kessler and Levine 1998; Mimura et al. 2000), reaction-diffusion equations coupled with a hydrodynamic equation (Lega and Passot 2003; 2004), individual-based modelling (Ben-Jacob et al. 1994; Kreft et al. 1998; Ginovart et al. 2002b; Krone et al. 2007), or individual-based modelling coupled with reaction-diffusion equations (Golding et al. 1999). Selected aspects of these bacterial studies have been adapted to our model. For instance, we used finite difference algorithms to approximate the solutions of a set of reaction-diffusion equations for the concentrations of bacteria and organic substrate (cf. Sec. 3.2.3; 3.2.5) and we used the Monod kinetic function (cf. Sec. 3.2.1). However, our model differs from existing studies in two aspects. First, we implemented the ecological concepts of conditional dispersal and resource allocation (cf. Ch. 4) as we explicitly considered division of consumer energy uptake into fractions for bacterial maintenance, dispersal and growth (cf. Eqs. (3.6); (4.4); (4.5)). Second, our model is first and foremost focussed on the degradation of organic contaminants, and its performance in response to dispersal networks and abiotic conditions. This ecosystem service of bacteria in soil is of high relevance (Whitman et al. 1998), as contaminated soils are known to severely influence human food production, health, recreation or even reproduction (Harms and Bosma 1997; Ehlers and Luthy 2003).

The modelling approach has major advantages for investigating the bacterial colony dynamics: It permits to simulate a large number of scenarios with different conditions, it provides a mechanistic understanding of the ecosystem service of interest – the bacterial degradation of organic contaminants, and it allows for directly measuring the performance of this ecosystem service – in terms of the simulated glucose consumption. This is unfeasible in laboratory experiments, as indicator compounds added to make the glucose consumption quantifiable bear the risk of modifying the bacterial behaviour (cf. Sec. 8.3.1).

We identified three important factors influencing the performance of bacterial degradation in response to dispersal networks: the abiotic conditions, the time horizon, and the dispersal network's spatial configuration.

- *Abiotic conditions* – The agar concentration was identified as a key factor limiting the biodegradation performance. The more fluid the medium is, the easier the flagellated bacteria can disperse, and the faster the contaminants can be accessed and, hence, become bioavailable for degradation. This is in accordance with the general dependence of bacterial motility on moist conditions (Harshey 2003; Schroll et al. 2006).

  We have also shown that the abiotic conditions are essential for the relative improvement of biodegradation performance, which dispersal networks can cause: The more difficult it is for the bacteria to disperse, the more crucial the dispersal networks are for reaching remote areas. This does not imply that the biodegradation under unfavourable abiotic conditions will outperform the biodegradation under favourable abiotic conditions (cf. Fig.

5.1), but that dispersal networks have the potential to compensate for the detrimental effects unfavourable abiotic conditions have on biodegradation.

- *Time horizon* – The time horizon considered proved to be an essential aspect for assessing the ecosystem service's performance. Our results reveal that contrasting findings can arise when not specifying this time horizon (cf. Fig. 5.1). Hence, when assessing the performance of biodegradation in response to different abiotic conditions and dispersal networks, one should always be aware of the time horizon's impact.

- *Dispersal network's spatial configuration* – The results show that the dispersal network's ability to enhance contaminant degradation is highly sensitive to its spatial configuration. Both the network coverage and the initial distance from the bacterial inoculum to the network appear to be important criteria for determining the potential improvement of biodegradation performance.

We used an integrative approach combining the simulation model with laboratory experiments. In a case study, *Pseudomonas putida* colonies were grown under different well-defined abiotic conditions (cf. Ch. 2). The simulation model (Ch. 3) shows high accordance with real bacterial colonies. It is able to reproduce the observed bacterial behaviour qualitatively, in terms of the colony patterns (cf. Fig. 3.4a, b), and quantitatively, in terms of the increase of colony areas over time (cf. Fig. 4.2). We also included simple dispersal networks in the laboratory experiments. The model qualitatively reproduces the corresponding bacterial colony patterns too (e.g. Fig. 3.4c, d), in particular as it was designed to incorporate bacterial diffusion coefficients, which vary temporally and spatially in structured environments (cf. Sec. 3.2.3).

Chapter 6

Spatially Heterogeneous Environments*

6.1 Considering spatially heterogeneous abiotic conditions

In situ bioremediation is a promising strategy for energy-efficient treatment of contaminated soil. Nonetheless, biodegradation performance is often limited by low bioavailability of contaminants to bacteria (cf. Ch. 1). Experimental studies have shown that fungal mycelia can act as bacterial dispersal networks, facilitating bacterial access to the contaminants (Kohlmeier et al. 2005; Wick et al. 2007a; Furuno et al. 2010). More generally, simulation modelling has demonstrated that bacterial dispersal networks have the potential to improve biodegradation performance (Ch. 5). These simulations revealed that abiotic conditions, by governing the ability of bacteria to disperse and the bioavailability of contaminants, have a strong impact on biodegradation benefits from bacterial dispersal networks. However, in chapter 5 abiotic conditions were assumed to be homogeneous in space, which is unlikely in soil systems, where water-air interfaces and pores are prevalent and contaminants (i.e. bacterial resources) are often heterogeneously distributed (Boswell et al. 2002; Semple et al. 2003; Boswell et al. 2003; Young and Crawford 2004; Harms and Wick 2006; Or et al. 2007; Boswell et al. 2007; Wick et al. 2010). Whether biodegradation benefits from dispersal networks in homogeneous environments are maintained in heterogeneous environments, for instance, with a mix of areas where bacterial movement is efficient or restricted or a mix of high and low contaminant concentrations, remained an open question.

In this chapter we therefore explicitly assume spatial heterogeneity of abiotic conditions and investigate the effects of bacterial dispersal networks on biodegradation performance. We extend the simulation model developed in chapter 3 and include (a) spatially heterogeneous bacterial dispersal conditions and (b) spatially heterogeneous initial resource distributions. In particular, we use fractal landscapes (With 1997; With and King 1999) to create heterogeneous patterns which vary in two attributes: relative abundance and spatial autocorrelation of abiotic conditions of a certain quality. We simulate bacterial consumption of resources without and with different dispersal networks. This allows us to derive predictions about the impacts of dispersal networks on biodegradation under the more realistic assumption of environmental heterogeneity. Our results show that dispersal networks facilitate the colonisation of areas otherwise restricting bacterial dispersal and enable the bacteria to reach even remote resource-rich

* A research paper with analogous content to this chapter was published (Banitz et al. 2011b).

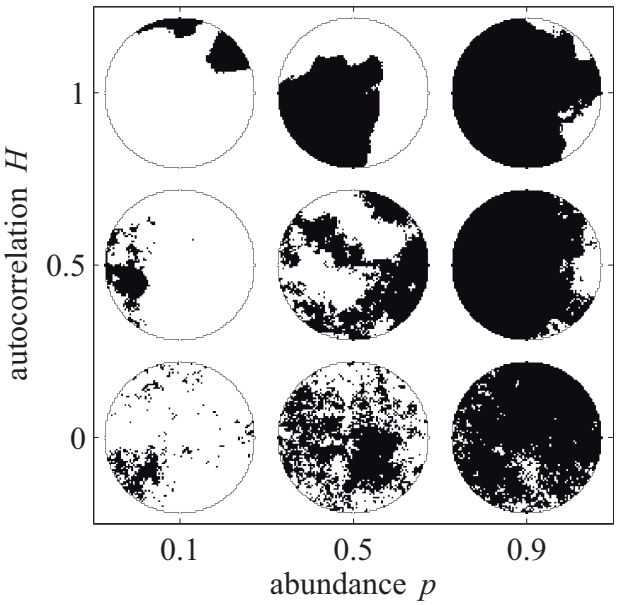

Figure 6.1 Examples of heterogeneous fractal patterns, created with the midpoint displacement algorithm. Both attributes, relative abundance p (x-axis) and spatial autocorrelation H (y-axis), can be varied from 0 to 1.

areas quickly. Concerning the attributes of the heterogeneities investigated, we find that relative abundance (i.e. quantity) of favourable abiotic conditions is much more relevant for biodegradation improvements than spatial autocorrelation (i.e. degree of clumping). Altogether, bacterial dispersal networks (mimicking the effects of fungal mycelia) greatly accelerate resource consumption and improve biodegradation performance in most instances of heterogeneous abiotic conditions.

6.2 Methods

Using the simulation model (cf. Ch. 3), we investigated the interaction of heterogeneous abiotic conditions and bacterial dispersal networks in relation to biodegradation performance. This performance was assessed from determining the amount of substrate consumed as a proportion of the initial amount (cf. Sec. 3.3). We tested (a) spatially heterogeneous bacterial dispersal conditions and (b) spatially heterogeneous initial resource distributions. To apply spatial heterogeneity, we systematically generated fractal patterns with the midpoint displacement algorithm (Saupe 1988). The two input attributes for this algorithm are the relative abundance (as a proportion $p \in [0,1]$ of the simulation area) and the spatial autocorrelation (determined by parameter $H \in [0,1]$) of the pattern of grid cells (Fig. 6.1).

Simulations were performed without and with bacterial dispersal networks, the latter using three different spatial configurations varying in network coverage and initial distance between bacterial inoculum and network (the same configurations as in Ch. 5).

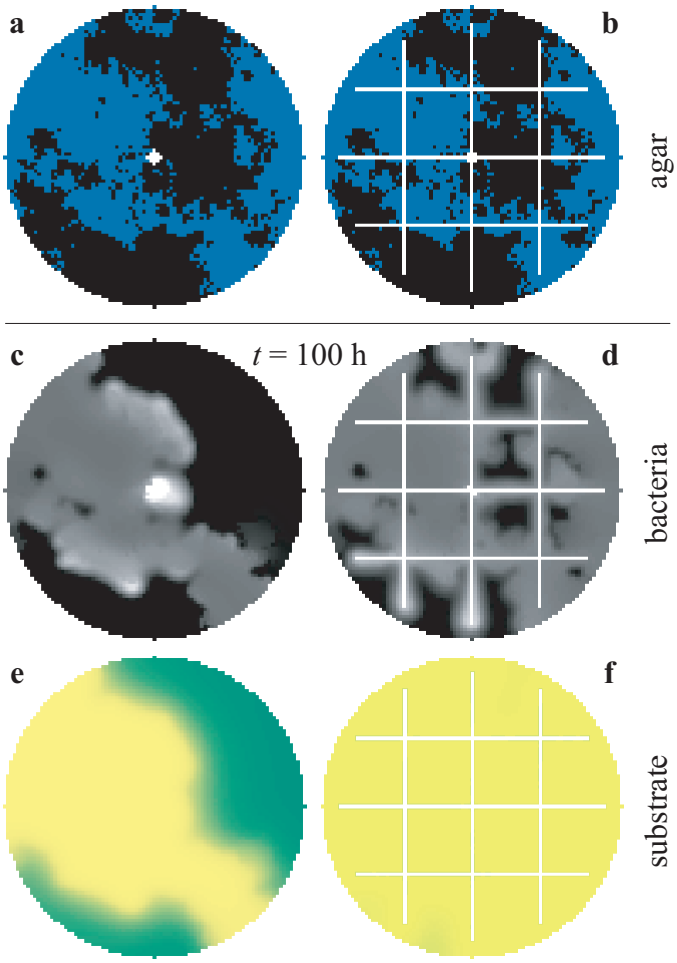

Figure 6.2 Example of heterogeneous bacterial dispersal conditions without a dispersal network (left panel) and with dispersal Network 3 (white grid; right panel). The initial substrate concentration was set to 0.1 g/l. **a, b** Pattern of agar concentrations, blue grid cells – low agar concentration (3 g/l, i.e. favourable bacterial dispersal conditions), black grid cells – high agar concentration (5 g/l, i.e. unfavourable bacterial dispersal conditions). **c, d** Simulated spatial patterns of bacteria after 100 h. Bacterial concentrations are indicated by grey shading, increasing from black (no bacteria) to white. **e, f** Simulated spatial patterns of substrate after 100 h. Substrate concentrations are indicated by colour shading, decreasing from green (0.1 g/l) to yellow (0 g/l).

6.2.1 Spatially heterogeneous bacterial dispersal conditions

Patterns of grid cells with favourable bacterial dispersal conditions (corresponding to bacterial dispersal at 3 g/l agar) were created and unfavourable bacterial dispersal conditions (5 g/l agar) were assigned to the remaining grid cells. Values of p and H were varied from 0 to 1 with a step width of 0.05. Figure 6.2 shows an example of heterogeneous agar concentrations and resulting bacterial and substrate distributions, without and with one specific bacterial dispersal network. For each combination of p and H, and for each of the four dispersal network configurations, 20 random spatial patterns of heterogeneous agar concentrations were simulated over 200 h. From these 20 simulation runs, mean values and standard deviations of consumed substrate were

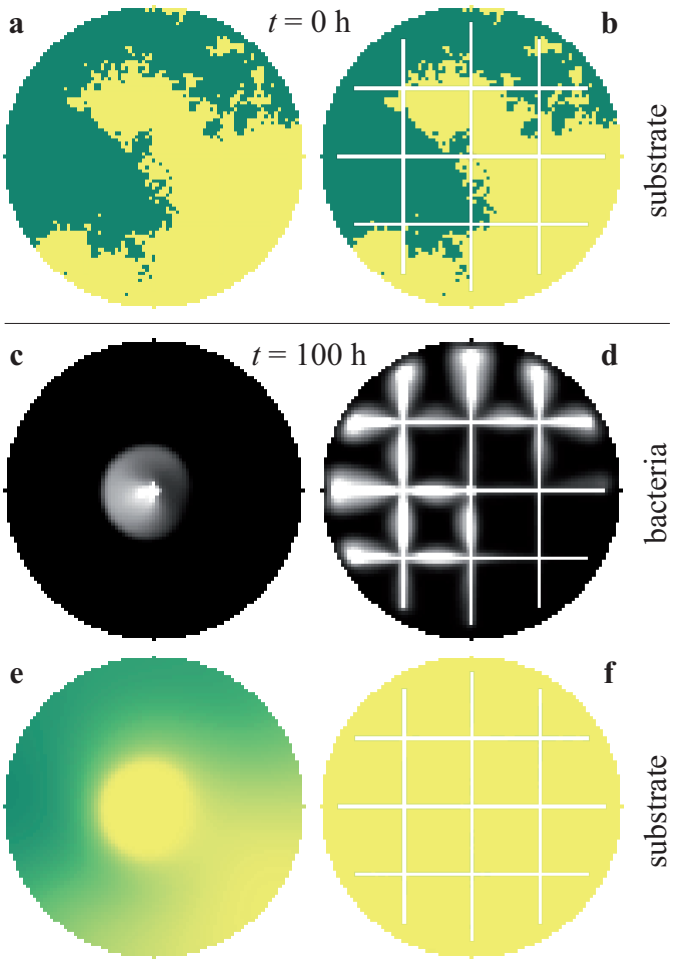

Figure 6.3 Example of heterogeneous initial resource concentrations, without a dispersal network (left panel) and with dispersal Network 3 (white grid; right panel). The agar concentration was set to 5 g/l. **a, b** Pattern of initial substrate concentrations, green grid cells – high initial substrate concentration (1 g/l), yellow grid cells – no initial substrate concentration (0 g/l). **c, d** Simulated spatial patterns of bacteria after 100 h. Bacterial concentrations are indicated by grey shading, increasing from black (no bacteria) to white. **e, f** Simulated spatial patterns of substrate after 100 h. Substrate concentrations are indicated by colour shading, decreasing from green (1 g/l) to yellow (0 g/l).

calculated. For one particular combination ($p = 0.5$; $H = 0.5$), we compared the mean consumption curves to a reference case of homogeneous moderate bacterial dispersal conditions (4 g/l agar; cf. Ch. 5). Moreover, at a given point in time (e.g. after 100 h), the mean values provided a measure of degradation performance, as a function of autocorrelation H and abundance p of the patterns, for different dispersal network configurations.

6.2.2 Spatially heterogeneous initial resource distributions

Patterns of grid cells with high substrate concentration (1 g/l) were created, the remaining grid cells were left without substrate at the start of the simulations. The value

of p was varied from 0.05 to 1 and the value of H from 0 to 1, both with a step width of 0.05. If p were set to 0, the bacteria could neither grow nor disperse in the simulations, as they need to consume substrate for both processes. An example of heterogeneous initial substrate concentrations and the resulting bacterial and substrate distributions, without and with a dispersal network, is given in figure 6.3. Note that substrate diffuses to initially empty grid cells during simulation. Thus, bacteria located on these grid cells can consume substrate after some time and use the energy uptake to disperse and grow. Degradation performance was assessed from mean values of substrate consumption in the same way as for heterogeneous agar concentrations. For comparison, we also simulated a homogeneous initial substrate concentration of 0.5 g/l.

6.3 Results

6.3.1 Spatially heterogeneous bacterial dispersal conditions

Figure 6.2a, b shows an example pattern of spatially heterogeneous agar concentrations. Half of the grid cells ($p = 0.5$) have a low agar concentration (3 g/l, i.e. favourable bacterial dispersal conditions) while the remaining grid cells have a high agar concentration (5 g/l, i.e. unfavourable bacterial dispersal conditions). The spatial autocorrelation H (cf. Sec. 6.2) is set to 0.5. Without a dispersal network, the bacteria predominantly colonise areas with favourable dispersal conditions within 100 h (Fig. 6.2c). Most of the areas with unfavourable dispersal conditions and, also, some remote areas with favourable dispersal conditions remain inaccessible to the bacteria. The spatial pattern of substrate corresponds to that of bacteria (Fig. 6.2e). With a dispersal network, the bacteria colonise almost all areas within 100 h (Fig. 6.2d) and substrate is consumed completely (Fig. 6.2f).

In figure 6.4a-d, substrate consumption is plotted against time for heterogeneous patterns of favourable dispersal conditions (as in the example in Fig. 6.2). For each dispersal network configuration, the outcomes of 20 simulation runs and their mean values show a considerable improvement in biodegradation performance through the introduction of dispersal networks (e.g. from 64% up to 100% after 100 h; compare red spots). The degree of improvement and, thus, the differences between the four dispersal network configurations varies with the time horizon considered. Moreover, except for Network 3, the outcomes of the single simulation runs vary distinctly. The simulated substrate consumption for the homogeneous reference pattern (cf. Sec. 6.2) with 4 g/l agar assumed (dashed cyan curves) shows some similarity to the mean values under heterogeneous conditions (thick black curves), but also a notably deviating curve shape.

The lower panels in figure 6.4 display biodegradation improvements by bacterial dispersal networks for the whole range of heterogeneous patterns examined (Fig. 6.4e-h). Network 3 leads to highest benefits, followed by Network 2 and Network 1. Regarding the attributes of the different spatial patterns, mean biodegradation performance generally increases with increasing abundance p of favourable dispersal conditions, but is much less sensitive to variations in their spatial autocorrelation H. Also, the differences among the single simulation runs depend on p and H: Standard deviations (Fig. 6.4i-k) vary greatly with the relative abundance p and, to a minor

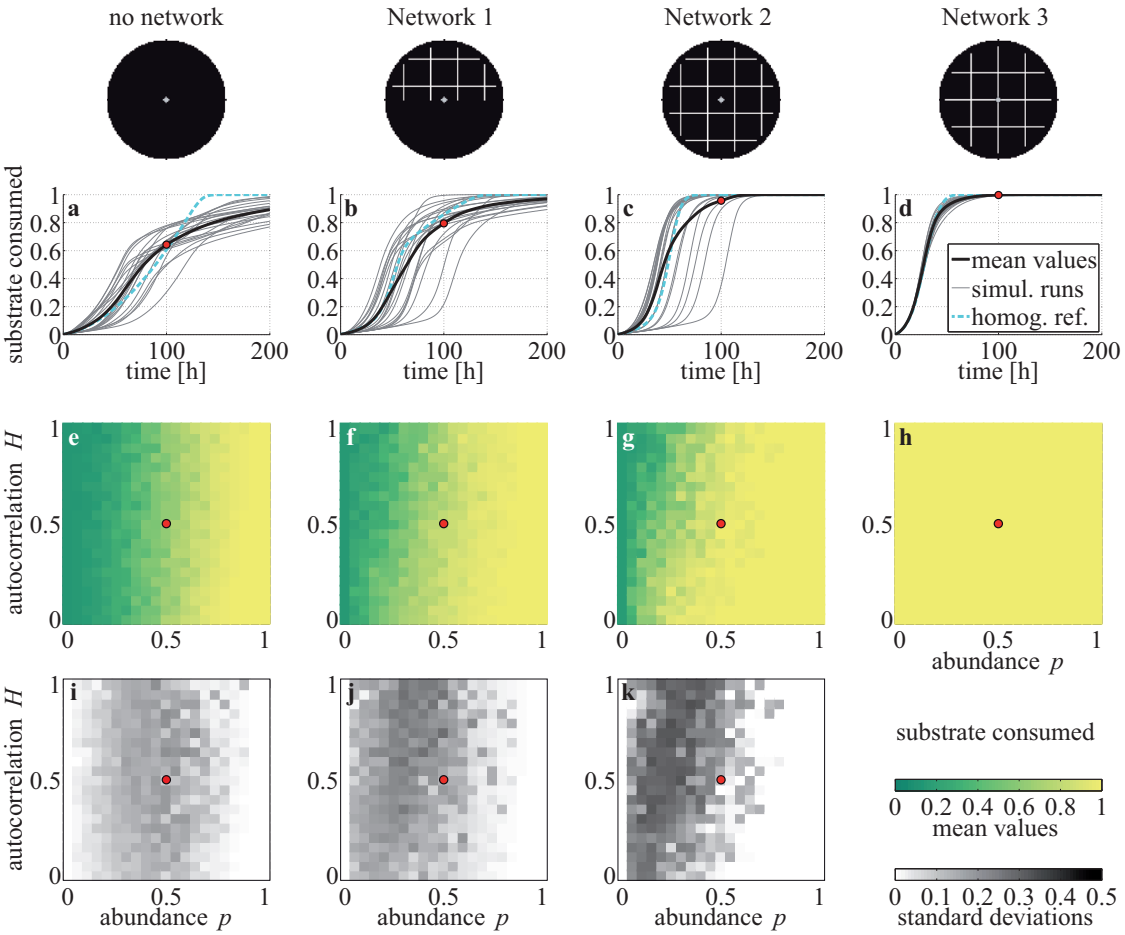

Figure 6.4 Simulated biodegradation performance under heterogeneous bacterial dispersal conditions. Each column shows a different bacterial dispersal network configuration (cf. images and titles on top). Within these columns, the red spots in the different subplots correspond to each other. **a-d** Substrate consumption over time for exemplary patterns with a relative abundance $p = 0.5$ and a spatial autocorrelation $H = 0.5$ (cf. example in Fig. 6.2). Each subplot shows 20 simulation runs (thin grey curves), their mean values (thick black curves), and the reference simulation results with homogeneous bacterial dispersal conditions (dashed cyan curves; cf. legend). **e-h** Mean values of substrate consumption at 100 h, increasing from green (no substrate consumed) to yellow (all substrate consumed; cf. colour bar), for multiple heterogeneous patterns differing in the attributes relative abundance p (x-axes) and spatial autocorrelation H (y-axes). **i-k** Standard deviations of substrate consumption at 100 h, increasing from white to black (cf. colour bar), for the same heterogeneous patterns. For Network 3 the simulation runs did not deviate from the mean values.

degree, with the spatial autocorrelation H of heterogeneous bacterial dispersal conditions.

6.3.2 Spatially heterogeneous initial resource distributions

Figure 6.3a, b shows an example pattern of spatially heterogeneous substrate concentrations, where high initial substrate concentration (1 g/l) covers half of the grid

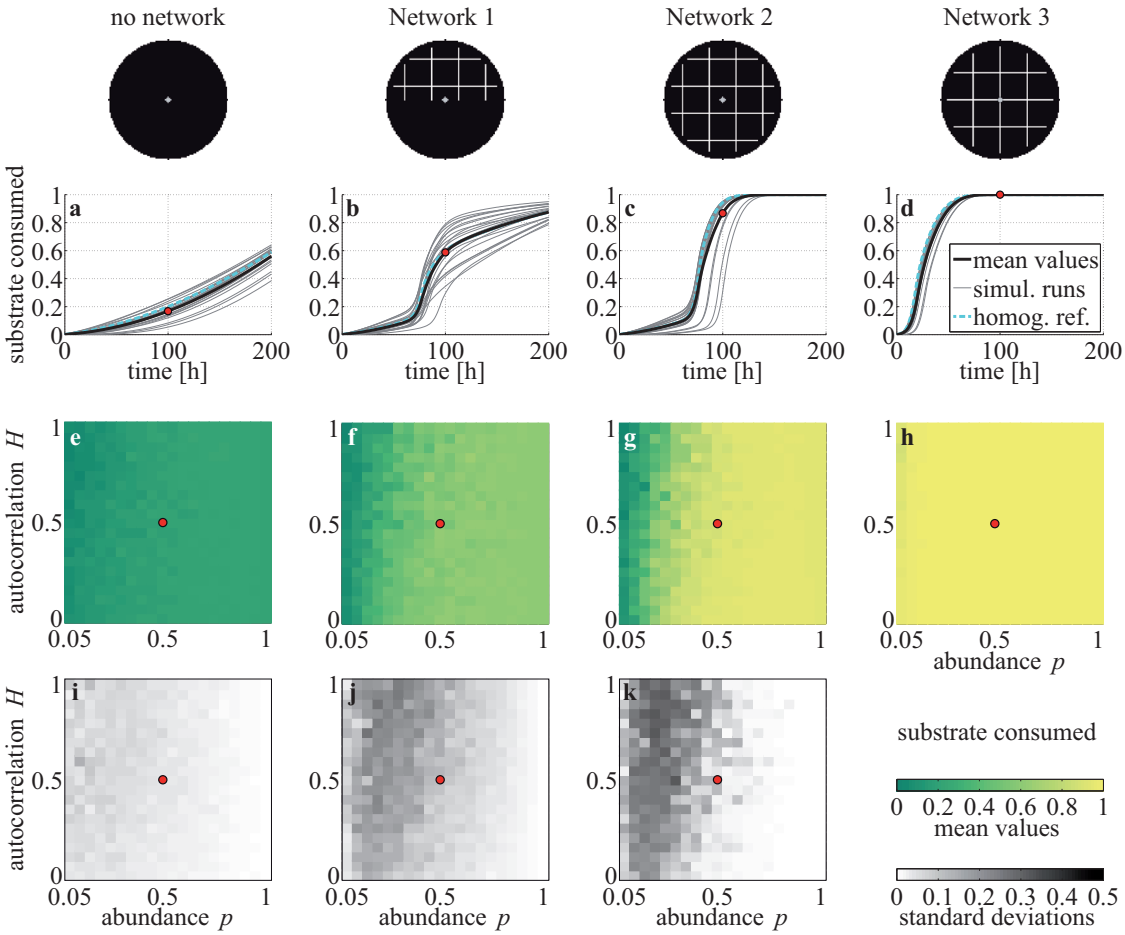

Figure 6.5 Simulated biodegradation performance under heterogeneous initial resource distributions. Each column shows a different bacterial dispersal network configuration (cf. images and titles on top). Within these columns, the red spots in the different subplots correspond to each other. **a-d** Substrate consumption over time for exemplary patterns with a relative abundance $p = 0.5$ and a spatial autocorrelation $H = 0.5$ (cf. example in Fig. 6.3). Each subplot shows 20 simulation runs (thin grey curves), their mean values (thick black curves), and the reference simulation results with homogeneous initial resource distributions (dashed cyan curves; cf. legend). **e-h** Mean values of substrate consumption at 100 h, increasing from green (no substrate consumed) to yellow (all substrate consumed; cf. colour bar), for multiple heterogeneous patterns differing in the attributes relative abundance p (x-axes) and spatial autocorrelation H (y-axes). **i-k** Standard deviations of substrate consumption at 100 h, increasing from white to black (cf. colour bar), for the same heterogeneous patterns. For Network 3 the simulation runs did only negligibly deviate from the mean values.

cells ($p = 0.5$) and has a spatial autocorrelation H of 0.5 (cf. Sec. 6.2). The remaining grid cells are empty at the start of the simulations. Due to the high agar concentration assumed (5 g/l, i.e. unfavourable dispersal conditions), without a dispersal network bacterial colony growth towards substrate-rich regions is substantially limited and the colony covers a very small area after 100 h (Fig. 6.3c). Only substrate initially located in the vicinity of the bacteria can be consumed (Fig. 6.3e). Contrarily, with a dispersal

network the bacteria are able to reach even remote substrate-rich regions within 100 h (Fig. 6.3d) and consume this substrate (Fig. 6.3f).

Figure 6.5a-d shows substrate consumption against time for heterogeneous patterns of grid cells initially containing substrate (as in the example in Fig. 6.3). Bacterial dispersal networks improve mean biodegradation performance greatly (e.g. from 17 % up to 100 % after 100 h; compare red spots). Also, variations with the time horizon considered can be observed. For instance, after 50 h bacterial substrate consumption is only improved by Network 3 in comparison to the configuration without a dispersal network. Differences between single simulation runs occur, but are smaller than under heterogeneous agar concentrations (cf. Fig. 6.4a-d). The simulation outcomes for the same initial amount of substrate, but homogeneously distributed, i.e. 0.5 g/l in each grid cell (dashed cyan curves), are very similar to the mean values under heterogeneous initial substrate distributions (thick black curves).

Mean substrate consumption after 100 h (Fig. 6.5e-h) is highly improved by the introduction of dispersal networks for almost any initial substrate distribution, with the improvement increasing from Network 1 via Network 2 to Network 3. Biodegradation performance generally increases when the abundance p of substrate-rich grid cells, and thus also the total amount of substrate, increases. It is, however, not very sensitive to the spatial autocorrelation H of these grid cells. Again, the standard deviations of the single simulation runs from the mean values after 100 h (Fig. 6.5i-k) vary greatly with the attributes abundance p and autocorrelation H of spatially heterogeneous initial resource distributions.

6.4 Discussion

The aim of the studies in this chapter was to systematically investigate whether bacterial dispersal networks can considerably improve the performance of biodegradation under spatially heterogeneous environmental conditions, which are characteristic for contaminated soils (e.g. Semple et al. 2003; Young and Crawford 2004; Boswell et al. 2007). Although it had been shown that dispersal networks have the potential to greatly improve bacterial degradation under (various) homogeneous abiotic conditions (cf. Ch. 5), the question of whether the benefits of dispersal networks also hold true for heterogeneous abiotic conditions, and if so, depending on which factors, remained open. This knowledge, however, is of major importance for an appreciation of the natural role of dispersal networks for bioremediation and even more so for their practical application.

6.4.1 Simulation model

To test the impact of bacterial dispersal networks under spatially heterogeneous abiotic conditions we used a suitable simulation model, which was designed to gain a mechanistic understanding of the spatiotemporal dynamics of bacterial colony growth and to investigate the performance of bacterial contaminant degradation (cf. detailed description in Ch. 3). Heterogeneous bacterial dispersal conditions and contaminant distributions were incorporated via agar concentrations and initial substrate concentrations, both varying in space. Thereby, we took advantage of the following strengths of this model:

- It provides a conceptually sound spatially explicit framework for analysing bacterial colony growth in any type of (homogeneous or heterogeneous) environment. The model integrates theoretical concepts from both ecology and microbiology and it was comprehensively validated and parameterised by means of empirical data from controlled laboratory experiments (cf. Ch. 3; 4).

- The model allows for directly measuring the performance of an ecosystem service of interest represented by simulated bacterial substrate consumption (cf. Sec. 3.3). This operationalisation facilitates a mechanistic understanding of this ecosystem service and a focussed analysis of the roles of abiotic conditions and bacterial dispersal networks for its performance.

- The model permits the simulation of a large number of scenarios of abiotic conditions and different bacterial dispersal networks. Therefore, we were able to analyse a huge variety of conceivable heterogeneities which are hard to cover in laboratory experiments. Even if it were technically possible to realise such conditions experimentally, the number of experiments required would be enormous (in this chapter we presented the results of ca. 70.000 simulation runs over 200 h, each, and we performed more than 500.000 simulation runs relating to this study). Only by harnessing this major advantage of the simulation model were we able to obtain the findings discussed below.

6.4.2 Biodegradation benefits from bacterial dispersal networks

We found that bacterial dispersal networks accelerate substrate consumption for most of the heterogeneities tested. The networks allow bacteria to bridge areas of unfavourable dispersal conditions and reach remote areas quickly. This effect is similar to that of dispersal corridors in macro-ecological systems, which may facilitate species dispersal across unfavourable regions in heterogeneous landscapes (e.g. Hill 1995; Tischendorf and Wissel 1997; Tischendorf et al. 1998). When initial substrate distributions are heterogeneous, the networks let the bacteria reach and consume remote substrate quickly (in particular when the bacterial inoculum directly adjoins the network, e.g. Network 3).

Key factors for biodegradation improvements in the presence of bacterial dispersal networks under homogeneous abiotic conditions (cf. Sec. 5.4) are also important under heterogeneous abiotic conditions: The improvements depend on the given abiotic conditions, the time horizon, and the spatial configuration of the dispersal network applied. Under initially adverse abiotic conditions the degree of improvement is highest as dispersal networks can compensate for the negative effects of these conditions. Assessments of biodegradation performance can vary greatly for different time horizons considered, which may lead to contrasting findings. Regarding spatial configurations, biodegradation performance increases with a high network coverage and a short initial distance between bacterial inoculum and network. However, it is important to highlight that these three factors are interrelated. Their effects on biodegradation performance depend complexly on each other and cannot always be disentangled.

By including spatially heterogeneous conditions typical for unsaturated subsurface soils, our study elevates the recent finding that biodegradation benefits from bacterial

dispersal networks to a much higher level of reliability and generalisability. Stimulating the establishment of fungal networks, for instance by planting trees associated with mycorrhizal fungi, to achieve energy-efficient and environmentally sound bioremediation appears to be a robust and promising strategy for many contaminated soil sites.

6.4.3 Inspecting the attributes of spatial heterogeneities – relative abundance

Our simulations revealed that substrate consumption is positively correlated to the relative abundance (cf. Sec. 6.2) of favourable dispersal conditions (cf. Fig. 6.4). This is plausible as the bacteria have access to more substrate when larger areas are easy to colonise. Similarly, with an increasing initial abundance of substrate, biodegradation performance increases as well (cf. Fig. 6.5). On the one hand, less substrate in the system demands less bacterial efforts to degrade it. On the other hand, more substrate fosters bacterial colony growth, since it is the sole energy source for bacterial maintenance, dispersal and reproduction. Apparently, the latter effect dominates the former and leads to better biodegradation performance when more substrate is initially present in the system.

6.4.4 Inspecting the attributes of spatial heterogeneities – spatial autocorrelation

Interestingly, the spatial autocorrelation (cf. Sec. 6.2) in the patterns of heterogeneous abiotic conditions only affects the mean substrate consumption to a minor degree (cf. Figs. 6.4; 6.5). For heterogeneous dispersal conditions, the explanation is that the mean diffusion rate over an area of slow and fast sections does not depend on the spatial arrangement of these sections. Hence, the mean area colonised by the bacteria at a given time, and consequently the mean amount of substrate consumed, remain very similar for different spatial autocorrelations, provided that the abundance of favourable dispersal conditions is the same. Of course, patches of favourable dispersal conditions are more (less) beneficial when they are close to (far away from) the bacterial inoculation point. Hence, the explicit consideration of spatial heterogeneities and randomly chosen patch distributions can lead to varying outcomes of individual simulation runs (cf. Fig. 6.4a-d). However, it should be sufficient to consider the mean biodegradation performance, since bacterial dispersal from scattered indigenous microcolonies or multiple, distributed inoculations with bacteria are very likely in bioremediation measures.

For heterogeneous initial substrate distributions, a high spatial autocorrelation leads to substrate-rich patches which support high bacterial growth, sometimes close to the inoculation point and sometimes far away, but this does not alter the mean substrate consumption very much in comparison to less correlated initial substrate distributions.

6.4.5 Homogeneous approximations for heterogeneous conditions

Because it is known from ecological theory that, under certain conditions, some characteristics of complex heterogeneous systems can be predicted by simpler homogeneous systems with appropriate parameters (Frank and Wissel 2002; Drechsler 2009), we also tested whether mean biodegradation performance under heterogeneous

conditions could be adequately represented by homogeneous conditions, on the example of one specific scenario of spatial heterogeneities (Fig. 6.4a-d). Our test, however, indicates qualitative differences in biodegradation performance between homogeneous and heterogeneous bacterial dispersal conditions. Only an easily accessible and widespread bacterial dispersal network can largely homogenise spatially heterogeneous bacterial dispersal conditions and lead to a considerable overlap of the biodegradation performance curves under homogeneous and heterogeneous conditions, respectively (Network 3; cf. Fig. 6.4d). This suggests that spatially heterogeneous bacterial dispersal conditions should be taken into account explicitly to obtain reliable predictions of biodegradation performance.

Spatially heterogeneous initial substrate distributions are smoothed over time by substrate diffusion. This important difference to spatially heterogeneous bacterial dispersal conditions, which are temporally invariant, has two consequences: First, single simulation runs with equal attributes of spatial heterogeneity vary less than those under spatially heterogeneous bacterial dispersal conditions (compare Figs. 6.5a-d, i-k and 6.4a-d, i-k). Second, our comparison on the example of one specific heterogeneous scenario suggests that a spatially homogeneous initial resource distribution might adequately represent a heterogeneous one, in terms bacterial degradation performance. This is due to the homogenising effect of resource diffusion. However, when diffusion of resources is limited, it is very likely that, similar to temporally invariant bacterial dispersal conditions, spatial heterogeneities need to be taken into account explicitly. A detailed analysis of the general validity of homogeneous approximations is beyond the scope of this chapter and a topic for future investigations (cf. Sec. 8.3.1).

Chapter 7

Spatial Configuration of Dispersal Networks

7.1 Multiple complex spatial configurations of bacterial dispersal networks

Simulation results with grid-like bacterial dispersal networks have shown that, in addition to the prevalent abiotic conditions and the time horizon considered for assessing biodegradation performance, the spatial configuration of networks may significantly affect potential enhancement of biodegradation (Ch. 5; 6). Understanding the role of this spatial configuration is important for developing effective bioremediation strategies based on stimulating the establishment of fungal networks in contaminated soils. Beyond that, criteria to distinguish different spatial configurations are required for assessing biodegradation benefits from bacterial dispersal networks.

In this chapter, we therefore use the bacterial colony growth model (cf. detailed description in Ch. 3) to simulate complex, randomly created dispersal network configurations and analyse their impact on bacterial substrate consumption. We obtain indications about the dependence of biodegradation performance on the spatial configuration of bacterial dispersal networks. A methodological approach is developed to investigate the suitability of several spatial metrics, which characterise the manifold and complex explicit network configurations in an aggregated manner, for reliably assessing the biodegradation benefits created by different dispersal networks. Thus, our analysis provides the basis for selecting appropriate characteristics to focus on when dealing with the complexity of real fungal networks in future practical applications.

7.2 Methods

7.2.1 Abiotic conditions and dispersal networks applied

To investigate the dependence of biodegradation on the spatial configuration of bacterial dispersal networks, we used abiotic conditions of 5 g/l agar concentration (i.e. unfavourable bacterial dispersal conditions) and 0.1 g/l initial substrate concentration. The dispersal-enhancing effects of fungal networks were modelled with high-diffusivity corridors, as described earlier (cf. Sec. 3.5). We generated dispersal networks by randomly selecting the number (1-40) of dispersal corridors. For each of these corridors, length (11-51 mm), location (midpoint coordinates (i, j)), and orientation on the

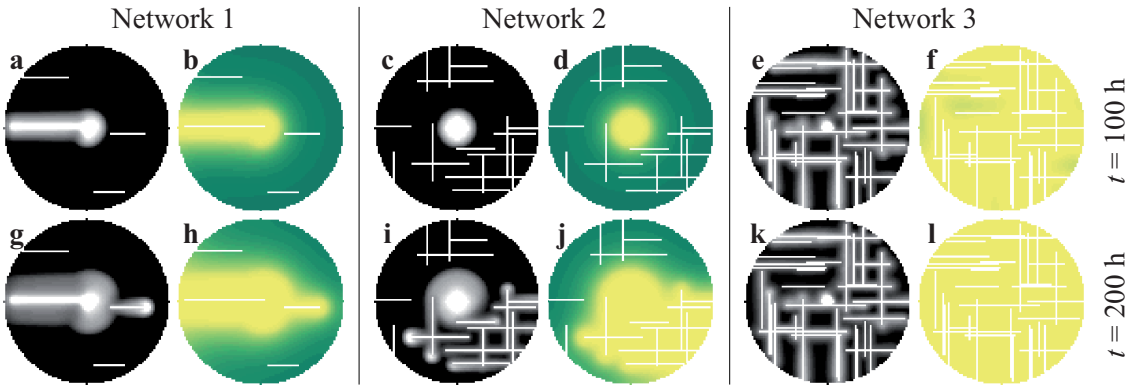

Figure 7.1 Simulation results for three exemplary, randomly created spatial configurations of dispersal networks (Networks 1-3; cf. titles; dispersal corridors visualised in white) under 5 g/l agar concentration and 0.1 g/l initial substrate concentration. **a-f** After 100 h. **g-l** After 200 h. **a, c, e, g, i, k** Spatial patterns of bacteria. Bacterial concentrations are indicated by grey shading, increasing from black (no bacteria) to white. **b, d, f, h, j, l** Spatial patterns of substrate. Substrate concentrations are indicated by colour shading, decreasing from green (0.1 g/l) to yellow (0 g/l).

simulated Petri dish (horizontal or vertical) were selected randomly too (see example network configurations in Fig. 7.1).

7.2.2 Metrics of spatial configuration of dispersal networks

As a variety of metrics can be considered for characterising the explicit spatial configurations of dispersal networks in an aggregated manner, we investigated the suitability of the following (cf. Symbols table on page 87 for units):

- *Network area* – The network area $na \in [0,1]$ is the area of grid cells (i, j) belonging to the dispersal network DN, as a proportion of the simulation area SA:

$$na = \frac{\sum_{(i,j)\in DN} cl^2}{\sum_{(i,j)\in SA} cl^2}, \tag{7.1}$$

  where cl is the side length of one grid cell ($1\,cl = 1$ mm; cf. Table 3.1).

- *Network coverage* – The network coverage nc is defined as the area of grid cells not more than 5 mm away from the network, as a proportion of the simulation area. For this purpose, the set NC containing these grid cells is defined:

$$NC = \left\{ (i,j) : \min_{(k,l)\in DN} \left\| \begin{pmatrix} i-k \\ j-l \end{pmatrix} \right\| \leq 5\ cl \right\}, \tag{7.2}$$

so that network coverage nc is:

$$nc = \frac{\sum_{(i,j)\in NC} cl^2}{\sum_{(i,j)\in SA} cl^2}. \tag{7.3}$$

- *Network connectivity* – For determining network connectivity, the Euler characteristic χ, a well-established measure in image analysis (e.g. Vogel 2002; Roth et al. 2005), is used:

$$\chi = n_o - n_l. \tag{7.4}$$

It counts the number of unconnected network objects n_o minus the number of closed loops in these objects n_l (cf. Roth et al. 2005). Hence, it leads to positive values for poorly connected structures and decreases far into negative when connectivity rises.

- *Mean distance to network* – For each grid cell in the simulation area, the distance to the nearest grid cell belonging to the dispersal network is calculated, as a proportion of the diameter of the simulation area $d_{SA} = \max_{(i,j),(k,l)\in SA} \left\| \begin{pmatrix} i-k \\ j-l \end{pmatrix} \right\|$. The mean value of these distances is given by:

$$mdn = \frac{\sum_{(i,j)\in SA} \min_{(k,l)\in DN} \left\| \begin{pmatrix} i-k \\ j-l \end{pmatrix} \right\|}{\sum_{(i,j)\in SA} d_{SA}}. \tag{7.5}$$

Additionally, we investigated one metric that takes into account the bacterial inoculation point:

- *Inoculum distance to network* – We calculate the distance from the centre $(i,j) = (0,0)$ of the simulation area (cf. Fig. 3.1), where the bacteria are inoculated, to the nearest grid cell belonging to the dispersal network, as a proportion of the diameter of the simulation area:

$$idn = \frac{\min_{(k,l)\in DN} \left\| \begin{pmatrix} k \\ l \end{pmatrix} \right\|}{d_{SA}}. \tag{7.6}$$

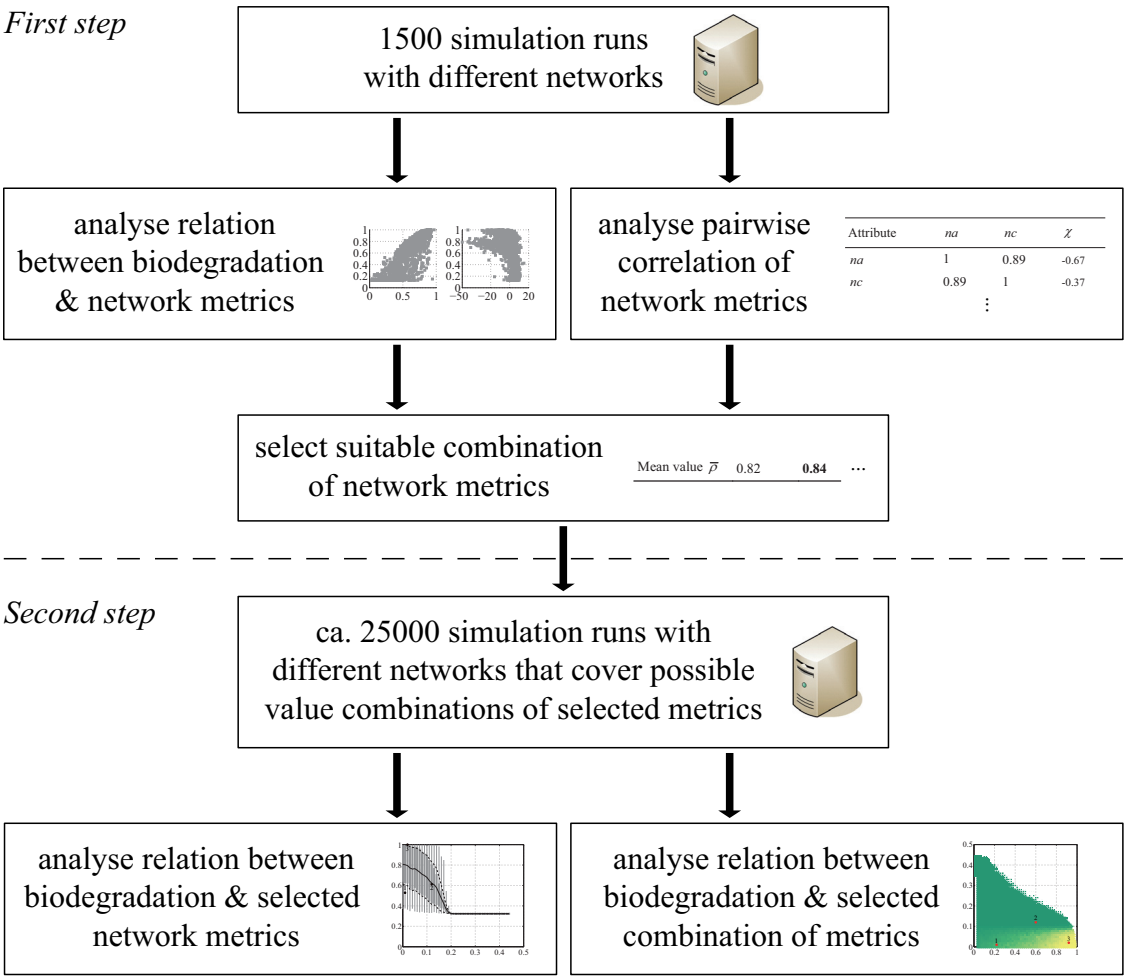

Figure 7.2 Scheme of the methodological approach developed in this chapter. The two network metrics selected for the second step are *nc* and *idn*.

7.2.3 Methodological approach

The approach we used for performing and analysing simulations with multiple spatial configurations of dispersal networks is visualised in figure 7.2.

In a first step (cf. Sec. 7.3.1), we simulated 1500 different random dispersal network configurations over 200 h. In order to increase the diversity of examined dispersal networks, 500 simulation runs had the additional restriction that the midpoints of the dispersal corridors forming a network all lie in the left half of the Petri dish. Thus, the right half remained nearly free of grid cells belonging to the network. We calculated Spearman's rank correlation coefficient ρ, a non-parametric measure of dependence (Hollander and Wolfe 1999; Gibbons and Chakraborti 2010), between each metric and the simulated substrate consumption at four points in time (after 50, 100, 150 and 200 h), as well as the mean values of these correlation coefficients $\bar{\rho}$ (cf. Table 7.1). Thus, we estimated the metrics' suitability for assessing biodegradation performance based on the spatial configurations of networks. Substrate consumption was plotted against the metrics (cf. Fig. 7.3).

To improve the assessment, we also analysed the combination of two metrics (cf. second step below). To this end, we calculated Spearman's rank correlation coefficient ρ pairwise between the metrics (cf. Table 7.2) and selected two metrics with a comparatively low correlation between each other, but both having a comparatively high correlation to substrate consumption.

In a second step (cf. Sec. 7.3.2), we changed our perspective on how to create the dispersal networks. Instead of generating many different random spatial configurations and calculating resulting metrics afterwards as in the first step (cf. above), we deliberately generated random spatial configurations that cover all possible value combinations of the two metrics selected (nc, idn). To this end, the possible values for these metrics were grouped into classes (nc: 0, 0.02, 0.04 .. 1, idn: 0, 0.01, 0.02 .. 0.5). We constrained the number of networks allowed for each combination of classes of the two metric values to 20. Thus, a total of more than 25000 simulation runs were performed, each with a different explicit spatial configuration of dispersal networks. Note that not all combinations of classes of metric values could be simulated, since certain combinations did appear rarely or not at all, due to the random generation of network configurations according to Sec. 7.2.1.

Using box plots for the sets of simulation runs sharing the same class of metric values, we visualised the distributions of simulated substrate consumption against the single metrics at two points in time (after 100 and 200 h). This allowed for comparison to the results of the first step (Fig. 7.4). Moreover, due to the classification of metric values, it was possible to calculate mean values and standard deviations of substrate consumption for each class. To estimate how much of the variability in substrate consumption is explained by the respective network metric considered, we also calculated values of the coefficient of determination R^2 (Table 7.3) according to:

$$R^2 = 1 - \frac{\sum_{r=1,\,2\,..\,n_r} (y_r - \bar{y}_r)^2}{\sum_{r=1,\,2\,..\,n_r} (y_r - \bar{y})^2}, \tag{7.7}$$

where y_r is the substrate consumption of a single simulation run ($r = 1, 2, .. n_r$), $\bar{y}$ is the mean substrate consumption of all simulation runs, $\bar{y}_r$ is the mean substrate consumption of all simulation runs sharing the same class of metric values as y_r, and $R^2 \in [0, 1]$.

Finally, we analysed mean values and standard deviations of substrate consumption of the up to 20 simulation runs for each combination of classes of the two metric values, at two points in time (after 100 and 200 h; Fig. 7.5). Also here, R^2-values were calculated based on these mean values and the variation of single simulation runs sharing the same combination of classes of metric values (Table 7.3). This allowed for estimating the improvement gained by taking into account the selected combination of two metrics and the suitability of this combination for assessing biodegradation performance in an aggregated manner.

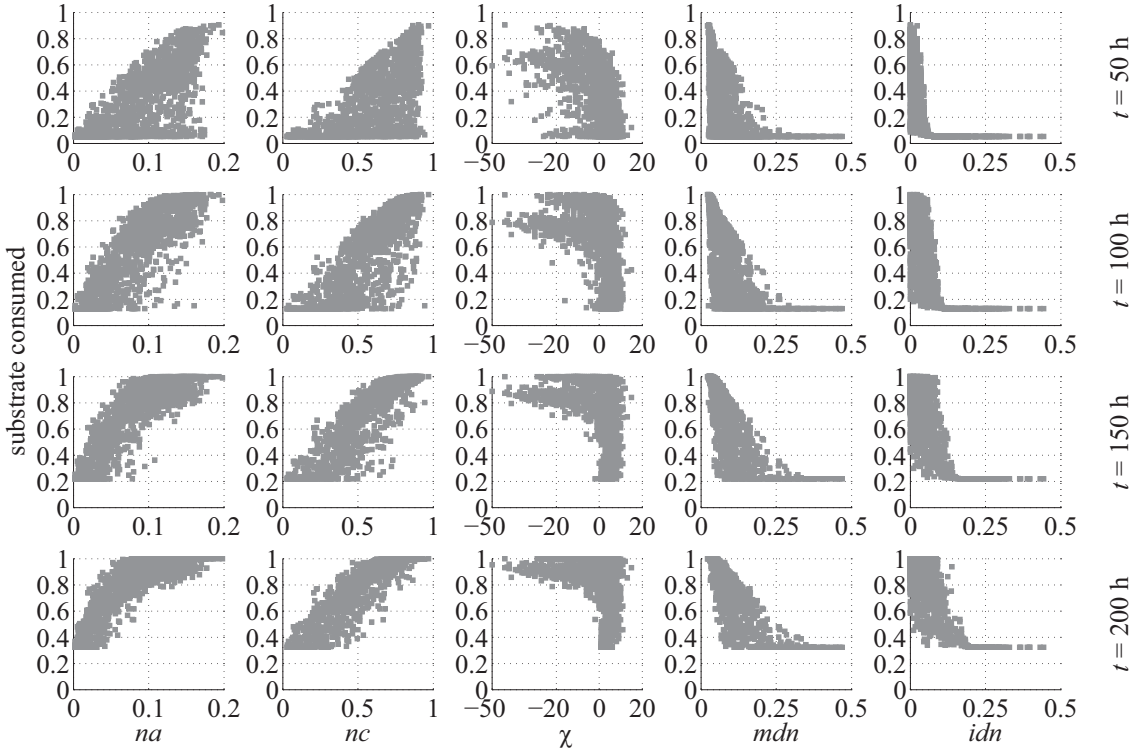

Figure 7.3 Substrate consumption of the first 1500 simulation runs under 5 g/l agar concentration and 0.1 g/l initial substrate concentration, plotted against five metrics of spatial configurations (different columns; cf. labels at bottom; Sec. 7.2) at four points in time (different rows; cf. labels at right). Corresponding Spearman's rank correlation coefficients are given in table 7.1.

7.3 Results

7.3.1 First step – single metrics

Figure 7.3 visualises the relations between the five metrics of spatial configuration of bacterial dispersal networks investigated and respective substrate consumption, that is, biodegradation performance, of the first 1500 simulation runs. Table 7.1 shows the corresponding correlation coefficients (cf. Sec. 7.2).

Network area *na* ($\bar{\rho} = 0.82$) and coverage *nc* ($\bar{\rho} = 0.84$) are highly positively correlated to substrate consumption, meaning that, on average, biodegradation performance increases when the values of these two metrics increase. The two metrics are similar to each other, but *nc* is slightly more suitable for assessing biodegradation performance. The other three metrics, Euler characteristic χ, mean distance to network *mdn* and inoculum distance to network *idn*, are negatively correlated to substrate consumption. On average, biodegradation performance increases when χ decreases (i.e. connectivity increases) and when *mdn* and *idn* decrease, respectively. The correlation between substrate consumption and χ is low ($\bar{\rho} = -0.5$), and particularly for high values of χ various significantly different simulation outcomes occur (cf. Fig. 7.3). Hence, the possibilities to assess biodegradation performance based on this metric

Table 7.1 Spearman's rank correlation coefficients ρ between five metrics of network configuration and substrate consumption from 1500 simulation runs (cf. Sec. 7.2), at four different points in time and mean values (cf. first column). The bold values indicate the two metrics selected for a combined analysis (cf. Sec. 7.3.2).

Metric	*na*	*nc*	χ	*mdn*	*idn*
t = 50 h	0.74	0.65	-0.55	-0.59	-0.86
t = 100 h	0.85	0.85	-0.56	-0.79	-0.7
t = 150 h	0.86	0.91	-0.48	-0.88	-0.63
t = 200 h	0.84	0.93	-0.42	-0.91	-0.59
Mean value $\overline{\rho}$	0.82	**0.84**	-0.5	-0.79	**-0.69**

are very limited. The absolute values of correlation are higher between substrate consumption and the remaining metrics *mdn* ($\overline{\rho} = -0.79$) and *idn* ($\overline{\rho} = -0.69$). The network's potential to enhance substrate consumption increases, when *mdn* decreases, but a low value of *mdn* does not necessarily lead to fast substrate consumption, in particular, at early points in time (cf. Fig. 7.3). The shorter the distance between bacterial inoculum and dispersal network *idn*, the higher is the potential for quick substrate consumption. Additionally, substrate consumption is only enhanced below a certain threshold of *idn*, which is increasing with time (cf. Fig. 7.3). Therefore, the metric *idn* is important for assessing biodegradation performance and, particularly, can be used to categorise into beneficial and non-beneficial configurations of dispersal networks, for a certain time horizon considered.

All metrics, except for χ, show a reasonable correlation to substrate consumption but also highly scattered simulation outputs for certain ranges of metric values and at several points in time (cf. Fig. 7.3). That is why we selected a combination of two metrics (out of the remaining four, i.e. excluding χ) for further investigations. This was done based on their pairwise correlations, which are given in Table 7.2. Although the combination of *idn* and *mdn* has the lowest absolute value of correlation ($\rho = 0.44$) we selected *idn* and *nc* ($\rho = -0.49$) since *nc* has the highest absolute value of mean correlation to substrate consumption ($\overline{\rho} = 0.84$; cf. Table 7.1).

7.3.2 Second step – a combination of two metrics

In figure 7.4, the box plots show the substrate consumption of the simulation runs performed in the second step of the methodological approach (cf. Fig. 7.2), classified with respect to the two aggregated metrics selected, that is, network coverage *nc* and inoculum distance to the network *idn* (cf. Sec. 7.2; 7.3.1). The relations between the two metrics and substrate consumption are similar to those in figure 7.3. Substrate consumption increases with increasing *nc*, and with decreasing *idn*, respectively. Again, a threshold in *idn* is clearly identifiable, increasing with the time horizon considered. Only spatial configurations of dispersal networks that are closer to the inoculation point than this threshold can enhance biodegradation performance.

Table 7.2 Pairwise Spearman's rank correlation coefficients ρ between metrics of network configurations. The bold values indicate the two metrics selected for a combined analysis (cf. Sec. 7.2). The small-written values were not considered for selection due to the low correlation between χ and substrate consumption (cf. Table 7.1).

Metric	*na*	*nc*	χ	*mdn*	*idn*
na	1	0.89	-0.67	-0.81	-0.53
nc	0.89	1	-0.37	-0.97	**-0.49**
χ	-0.67	-0.37	1	0.25	0.32
mdn	-0.81	-0.97	0.25	1	0.44
idn	-0.53	**-0.49**	0.32	0.44	1

The mean values of substrate consumed (solid curves in Fig. 7.4) underpin the trends observed in the first step (cf. Fig. 7.3), while standard deviations (dashed curves in Fig. 7.4) are high for many values of the metrics. Hence, when considered alone, each of the two metrics cannot capture all characteristics of the explicit spatial configurations relevant for biodegradation improvements. Also the corresponding R^2-values (Table 7.3) indicate that the two metrics on their own allow for a rough assessment of substrate consumption, but leave a substantial proportion of the variability unexplained.

The substrate consumption belonging to the three exemplary spatial configurations of dispersal networks (red spots in Fig. 7.4; cf. Fig. 7.1) highlights the importance of both metrics. Network 1 has a shorter *idn* than Network 2, leading to a higher biodegradation performance after 100 h (Fig. 7.4a, b). But since Network 2 has a higher *nc*, more substrate is consumed compared to Network 1 after 200 h (Fig. 7.4c, d). Network 3, having a high *nc* and a short *idn*, leads to a high biodegradation performance for both time horizons.

In figure 7.5, the mean values (Fig. 7.5a, c) and standard deviations (Fig. 7.5b, d) of substrate consumption are plotted against both metrics together, *nc* (x-axes) and *idn* (y-axes), at two points in time (after 100 and 200 h). Figure 7.5a shows a zone of high substrate consumption in the bottom right corner, that is, with a high *nc* and a short *idn*. The further away from this zone the network configurations are, the less substrate is consumed after 100 h. The threshold value of *idn*, above which substrate consumption cannot be enhanced by the dispersal networks because they are too far from the inoculation point (cf. Fig. 7.4b), is observable too. In figure 7.5c the zone of high substrate consumption is much larger, that is, more network configurations lead to improved biodegradation performance after 200 h. The standard deviations of substrate consumption of the up to 20 simulation runs for each combination of classes of metric values (Fig. 7.5b, d; cf. Sec. 7.2) are rather low, and the R^2-values (Table 7.3) are very high. Hence, the combination of the two metrics *nc* and *idn* captures most of the characteristics of the explicit spatial configurations relevant for biodegradation improvements, and is suitable for assessing biodegradation performance in an aggregated manner.

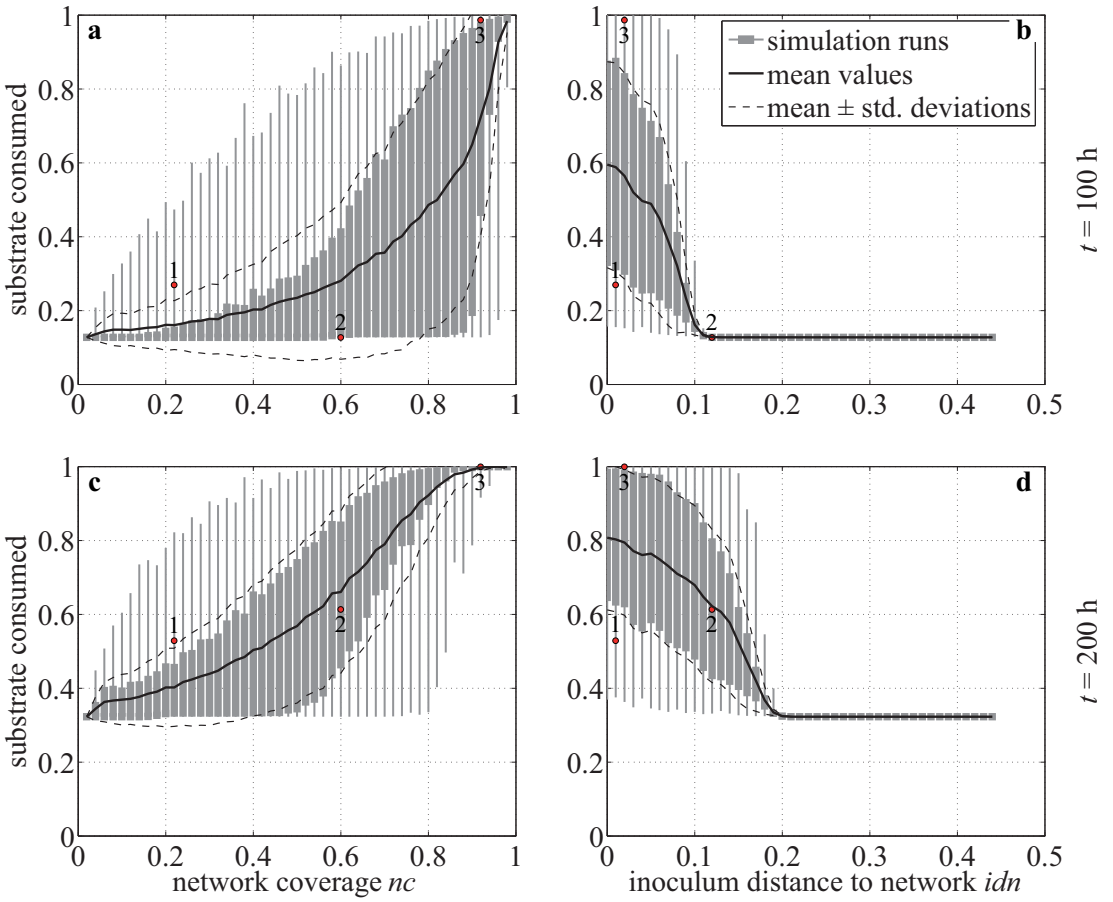

Figure 7.4 Box plots of substrate consumption of ca. 25000 simulation runs under 5 g/l agar concentration and 0.1 g/l initial substrate concentration, plotted against two metrics of spatial configurations (**a, c** network coverage, **b, d** inoculum distance to network; cf. Sec. 7.2). For each class of metric values (cf. Sec. 7.2), the boxes show the interquartile range (i.e. the spread of the middle 50 % of simulation runs). The whiskers (grey vertical lines) extend to the minimum and maximum values. Solid black curves show mean values, dashed black curves show standard deviations (cf. legend). Corresponding R^2-values are given in Table 7.3. Three red spots in each subplot belong to the three network configurations depicted in figure 7.1 (cf. spot labels). **a, b** After 100 h. **c, d** After 200 h.

The three exemplary dispersal network configurations are marked as before (red spots in Fig. 7.5; cf. Fig. 7.1). Also here, it is visualised that Network 1 leads to better biodegradation performance than Network 2 after 100 h (Fig. 7.5a), but not after 200 h (Fig. 7.5c). Network 3 is a much more beneficial spatial configuration, located in the zone of high biodegradation performance for both time horizons.

7.4 Discussion

In the simulation model, developed to investigate the spatiotemporal dynamics of bacterial colony growth and resulting substrate consumption, that is, biodegradation

Table 7.3 R^2-values (cf. Eq. (7.7)) for the two metrics network coverage and inoculum distance to network (cf. Fig. 7.4), and the combination of these two metrics (cf. Fig. 7.5).

Metric	*nc*	*idn*	*nc* and *idn*
t = 100 h	0.43	0.57	0.93
t = 200 h	0.66	0.6	0.94

performance, bacterial dispersal networks were used to model the dispersal-enhancing effects of fungal mycelia in microbial systems (cf. Ch. 3). Adding to experimental studies (Kohlmeier et al. 2005; Wick et al. 2007a; Furuno et al. 2010), it was shown earlier with the model that bacterial dispersal networks have the potential to improve biodegradation performance significantly (Ch. 5; 6). These studies revealed that biodegradation improvements will depend on the abiotic conditions under which bacteria degrade organic substrate and the time horizon considered for assessing biodegradation performance. Moreover, testing simple exemplary grid-like bacterial dispersal networks, these studies indicated that the spatial configuration of dispersal networks is an important factor determining biodegradation improvements (e.g. cf. Fig. 5.1).

Here, we used the simulation model and assumed initially unfavourable abiotic conditions, under which dispersal networks had shown highest potential for improvements (cf. Ch. 5). Taking great advantage of the model's spatial explicitness, we studied the impact of more complex spatial configurations of bacterial dispersal networks on biodegradation performance. We considered randomly generated network configurations in order to model fungal mycelia more realistically. Such mycelia might be widespread or narrow, highly or poorly connected, dense or sparse, close to or far away from the bacterial inoculum. The spatial characteristics of fungal mycelia were qualitatively represented by simulating multiple spatial configurations of bacterial dispersal networks. We developed a methodological approach to investigate the suitability of a set of aggregated spatial metrics for capturing the complex spatial characteristics of manifold dispersal networks that are relevant for biodegradation performance. In view of future practical applications, this is of particular importance for assessing potential biodegradation benefits from spatially complex fungal networks.

The first step of our approach showed that four of the five metrics considered allow for a rough characterisation of the dispersal network configurations' impact on biodegradation performance, whereas one of them, the Euler characteristic as a measure for connectivity, is not suitable (cf. Table 7.1). However, when considered alone, none of the metrics proved to capture the spatial characteristics relevant for biodegradation improvements completely. There were always additional aspects of the explicit spatial configurations of dispersal networks influencing biodegradation performance (cf. Fig. 7.3).

Therefore, in the second step of the approach, we selected two metrics, network coverage *nc* and initial distance between dispersal network and bacterial inoculum *idn*, for a detailed analysis, based on severalfold more simulation runs. The explicit spatial configurations of dispersal networks from these simulation runs were classified

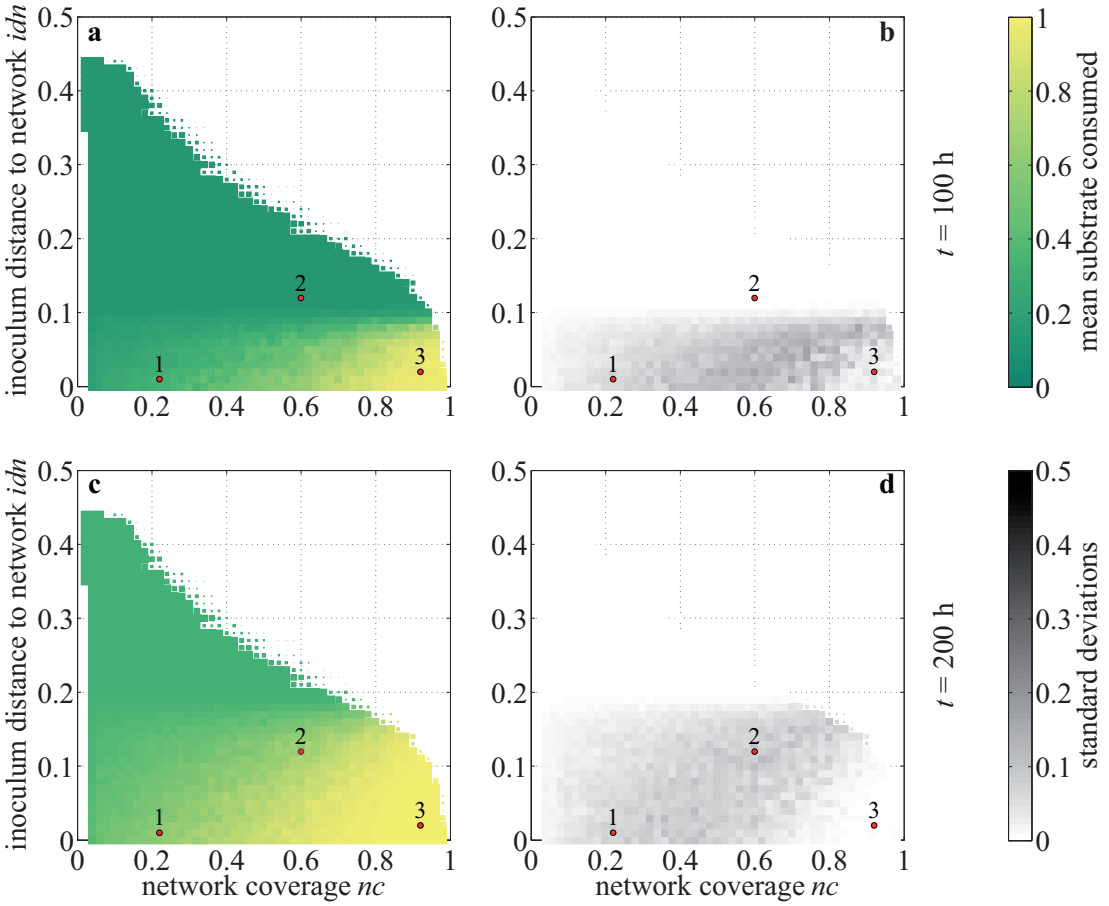

Figure 7.5 Mean substrate consumption (**a, c**) and standard deviations (**b, d**) of up to 20 simulation runs under 5 g/l agar concentration and 0.1 g/l initial substrate concentration, plotted in an aggregated manner against network coverage and inoculum distance to network (cf. axes labels). Mean values are indicated by colour, increasing from green (no substrate consumed) to yellow (all substrate consumed; cf. colour bar). Marker sizes indicate the number of simulation runs performed, increasing from 0 to 20. Standard deviations are indicated by grey shading, increasing from white to black (cf. colour bar). Corresponding R^2-values are given in Table 7.3. Three red spots in each subplot belong to the three network configurations depicted in figure 7.1 (cf. spot labels). **a, b** After 100 h. **c, d** After 200 h.

according to their values of the metrics. From analysing the mean values and standard deviations of substrate consumption within these classes (Fig. 7.4), we revealed how much of the networks' characteristics relevant for biodegradation performance were captured by the two aggregated spatial metrics, respectively. The values of R^2 (cf. Table 7.3) provided a good estimate of this relation, and confirmed our finding that each of the two metrics allows for a rough assessment of prospective biodegradation improvements, but also loses a substantial part of the characteristics of the explicit spatial configurations.

Thereupon, we showed that the combined consideration of the two aggregated metrics, network coverage *nc* and inoculum distance to network *idn*, is an appropriate choice for reliable assessments of biodegradation performance. From very high values

of R^2 (cf. Table 7.3), we observed that these two metrics cover the major part of the networks' spatial characteristics that influence biodegradation, irrespective of the explicit configurations.

The larger the area covered by the dispersal network, that is, the area made 'easily accessible' to the bacteria, the higher the potential biodegradation improvements. In addition to that, the distance from the point where bacteria were inoculated to the dispersal network needs to be covered before dispersal benefits are put into effect, which delays biodegradation improvements. The shorter this distance, the quicker the dispersal networks can improve biodegradation performance. The degree of improvement will then depend on network coverage. As a consequence, by taking into account the bacterial inoculation point, the metric *idn* allows for categorising into beneficial and non-beneficial spatial configurations of dispersal networks, for a certain time horizon considered. The importance of this time horizon for assessing biodegradation benefits from bacterial dispersal networks (cf. Sec. 5.4; 6.4) is also clearly detectable when comparing the exemplary dispersal network configurations (Fig. 7.1) and their impacts on biodegradation performance, respectively (Figs. 7.4; 7.5).

We conclude that the combination of two aggregated metrics of the spatial configuration of bacterial dispersal networks, network coverage and inoculum distance to the network, is best suited for assessing biodegradation performance, irrespective of explicit network configurations. It is likely that these two metrics are equivalently important for assessing biodegradation benefits from real fungal networks in future practical applications. They should, therefore, be taken into account when developing methods for stimulating the establishment of fungi and/or inoculating degrading bacteria on contaminated soil sites. These findings are planned to be further examined by experiments with real fungal networks and adequate simulation modelling, which go, however, beyond the scope of this study (cf. Sec. 8.3.1).

Chapter 8

Discussion and Outlook

8.1 The approach developed in this thesis

Addressing the research objectives of investigating key factors and processes for biodegradation performance in response to bacterial dispersal networks (as specified in Sec. 1.2), an integrative approach was developed in this doctoral thesis. It comprises the combination of simulation modelling and laboratory experiments, based on theoretical concepts from two disciplines: microbiology and ecology. The design of this approach is visualised in figure 8.1.

Of central interest was understanding and predicting the dynamics of microbial ecosystems, with a clear focus on the ecosystem service of biodegradation. To this end, laboratory experiments were conducted (cf. Sec. 8.1.1) and a simulation model was generated (cf. Sec. 8.1.2). In the experiments, we performed a case study of a microbial consumer-resource system under various conditions, driven by microbiological theoretical knowledge. Commencing from this case study, the fundamental element of the thesis was developed: a mechanistic, process-based and spatially explicit bacterial simulation model. A high agreement between experiments and model was achieved on the basis of systematic comparison of spatiotemporal patterns that characterise the microbial system dynamics (cf. Sec. 8.1.3). Concepts from microbiological and

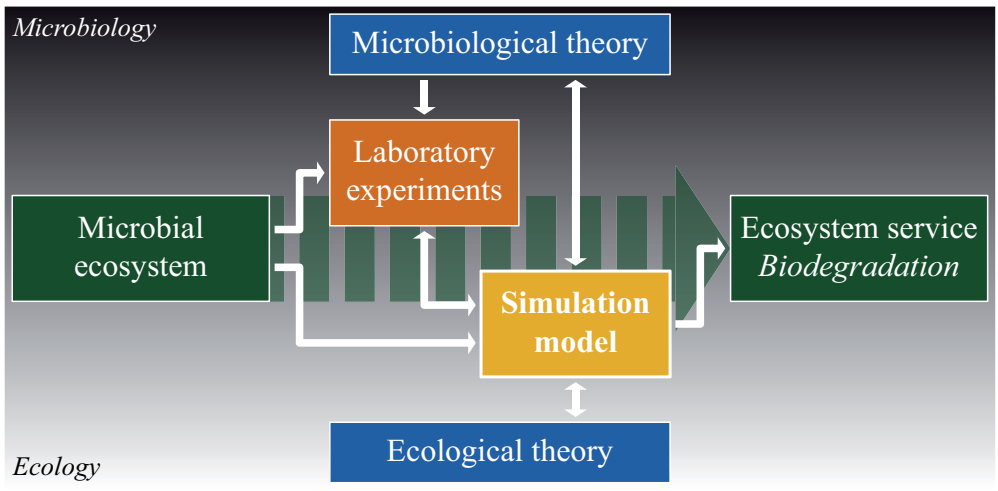

Figure 8.1 Scheme of the approach developed in this thesis, which is interdisciplinary between microbiology and ecology. Single arrows show direct impact of one element on another. Double arrows show direct impact and feedback.

ecological theory were incorporated into this model and, in return, new insights gained with the model contribute to microbiological and ecological theory. Most important, the simulation model provided the tool for assessing the performance of biodegradation under systematically varied environmental scenarios and determining key factors that control this performance (cf. Sec. 8.1.4). Hypotheses and findings that were derived with the simulation model can also be tested in microbial experiments. This potential to use simulation modelling for designing specific experiments is another important aspect of the integrative approach developed, and will be focussed on in future studies (cf. Sec. 8.3.1).

8.1.1 Laboratory experiments

Starting point of the thesis was a case study of a microbial consumer-resource system with *Pseudomonas putida* colonies growing on agar plates in well-controlled laboratory experiments (Ch. 2; cf. Fig. 8.1). In this context, the thesis benefited from the interdisciplinary cooperation with microbiologists and their expertise on how to perform and observe experimental assays, and to visualise the corresponding results. In particular, it was possible to mimic the dispersal-enhancing properties of fungal hyphae using glass fibres.

The applied abiotic conditions (agar concentration determining bacterial dispersal potential, initial glucose concentration determining resource supply) were varied systematically, such that the observations revealed characteristic spatial patterns of bacteria in response to all combinations of these abiotic conditions. High degree of control and short time spans for observing system dynamics exhibit a great advantage of microbial experiments in comparison to ecological field studies. This also allowed for performing replicate experiments, showing that bacterial behaviour resulting from equal conditions may be subject to variations. These variations provided a measure for the ‘degree of confidence’ in the experimental observations, which was directly incorporated into the process of model parameterisation later on (cf. Sec. 3.4).

8.1.2 Simulation model

We developed a simulation model (Ch. 3; cf. Fig. 8.1) to appropriately describe the spatiotemporal dynamics of bacterial colony growth and resulting biodegradation performance, and the specific microbial system studied in the experiments (cf. Sec. 8.1.1). With regard to our research objectives (Sec. 1.2), this model should be capable of modifying bacterial behavioural mechanisms, investigating bacterial dispersal networks of complex spatial structures, and simulating manifold scenarios with systematically varied abiotic conditions. It is therefore mechanistic, process-based and spatially explicit, and combines the advantages of *individual-based* and *continuous population modelling* (cf. Ferrer et al. 2009).

The method of individual-based modelling is highly valued for its ability to derive system dynamics from individual behaviour in ecology (Huston et al. 1988; Grimm and Railsback 2005; DeAngelis and Mooij 2005) and also in microbiology (Kreft et al. 2001; Picioreanu et al. 2004; Gregory et al. 2006; Ferrer et al. 2008; Hellweger and Bucci 2009). On the other hand, successful applications of *reaction-diffusion equations* (Murray 2002) for modelling sophisticated bacterial colony patterns (e.g. Golding et al. 1998; Mimura et al. 2000; Lega and Passot 2004) have proven that not every detail of individual variability is necessarily important to represent microbial consumer-resource

systems appropriately. These equations can comprise substrate consumption, growth and reproduction, linear or nonlinear diffusion, and even bacterial chemotaxis (cf. Murray 2002; Lega and Passot 2003).

Our simulation model is based on reaction-diffusion equations for organic contaminants as resources and degrading bacteria as consumers. Thus, restrictions concerning the spatial and temporal scale that result from high computational demands of discretely modelling huge numbers of individual bacteria (and sometimes also substrate particles) were avoided. Taking advantage of individual-based modelling, we also incorporated bacterial behavioural rules (e.g. conditional dispersal strategies; cf. Ch. 4). Concentrations of bacteria and organic substrate were modelled explicitly in space and time, such that various environmental conditions (e.g. heterogeneous bacterial motility; cf. Ch. 6) and bacterial dispersal networks (e.g. manifold spatial configurations of networks; cf. Ch. 7) could be taken into account.

To solve the reaction-diffusion equations for bacteria and substrate, a *finite difference approximation* was used (Press et al. 2007). This basic approach worked satisfactorily and did not lead to numerical instabilities. Testing more complex solving methods for partial differential equations may be subject to subsequent studies with the model (cf. Sec. 8.3).

8.1.3 Fitting the model to experiments

An important part of the integrative approach of this thesis (cf. Fig. 8.1) was to bring the simulation model into good accordance with observations from the laboratory case study, which required executing the following steps:

- For some general parameters, appropriate values could be directly obtained from literature or from specific experiments (e.g. glucose diffusion coefficient in agar, maximum effective growth rate of *P. putida* PpG7; cf. Sec. 3.4).

- Other, more specific parameter values were determined by qualitative fitting of model outcomes to experimental observations (e.g. bacterial diffusion coefficient along dispersal networks; cf. Fig. 3.4; Sec. 3.5). Also microbiological processes to be incorporated were selected in this way. For instance, parameter values for the reduction of dispersal at low or high bacterial densities, a concept based on microbiological theory (cf. Sec. 4.2), were tuned by qualitative fitting.

- Values for the remaining model parameters were determined by quantitative fitting to the experimental observations, in particular, to the bacterial colony area data (e.g. bacterial diffusion coefficients depending on agar concentration, bacterial dispersal strategy thresholds; cf. Sec. 3.4). At first, this inverse modelling task was executed with a Markov Chain Monte Carlo method (the Shuffled Complex Evolution Metropolis algorithm; Vrugt et al. 2003). This provided an idea of reasonable parameter values and distributions. Thereafter, a computationally less expensive bound constrained pattern search algorithm was finally applied (cf. Sec. 3.4).

  In this context, the availability of replicate measurements covering a variety of abiotic conditions was essential. By simultaneously fitting the

model to the corresponding variety of empirical patterns at once, thereby weighing the confidence in these patterns based on their variances (cf. Sec. 3.4), we determined a highly reliable model parameterisation. Moreover, this approach allowed for selecting ecological processes to be incorporated, by comparing different model versions on the basis of agreement between optimised model output and empirical patterns (cf. Sec. 8.1.4).

A comparison of experimental observations and simulation results for a scenario that was not used for parameterisation is given in figure 8.2. The model's capability to qualitatively reproduce the observed patterns endorses our fitting approach.

8.1.4 Model application

In chapter 4, the quantitative fitting method described above was used to test the validity of certain theoretical ecological concepts (conditional dispersal, resource allocation) for the microbial consumer-resource system and analyse their consequences for biodegradation performance assessments (cf. Fig. 8.1). To our knowledge, this was the first systematic comparison of different bacterial dispersal strategies varying in their functional dependence on resource uptake. The approach of confronting different model versions with multiple empirical patterns followed the strategy of pattern-oriented modelling (cf. Grimm et al. 2005) and is thoroughly discussed in section 4.4.3.

In subsequent chapters (Ch. 5; 6; 7), the appropriately implemented model served as a tool for simulating bacterial colony growth and analysing biodegradation performance under various environmental conditions, many of which can not be examined in the same way in laboratory experiments. The simulation model provided the great advantage that different scenarios of environmental conditions and bacterial dispersal networks could be controlled and tested systematically. As a consequence, the high number and variety of simulations performed allowed for general findings on a broad basis, which add substantially to the insights gained from experimental observations alone. Hence, this doctoral thesis also demonstrates the suitability and efficiency of simulation modelling for understanding ecosystem dynamics and predicting ecosystem behaviour, in particular, for microbial ecosystems. Moreover, the hypotheses and findings obtained from the model can be taken advantage of when designing further experimental and modelling studies to examine opportunities and key factors for biodegradation improvement (cf. Sec. 8.3.1).

8.2 Main results

8.2.1 Summary of results

The first main result of this doctoral thesis (derived in Ch. 4) relates to the research objective of selecting relevant processes for an appropriate simulation model and achieving high accordance with observation data (cf. Sec. 1.2):

- *Relevance of conditional dispersal* – It was shown that the ecological concept of dispersal depending on resource uptake is likely to be of high relevance for certain microbial consumer-resource systems. In particular, the cessation of bacterial dispersal at high resource levels proved to be important. Moreover,

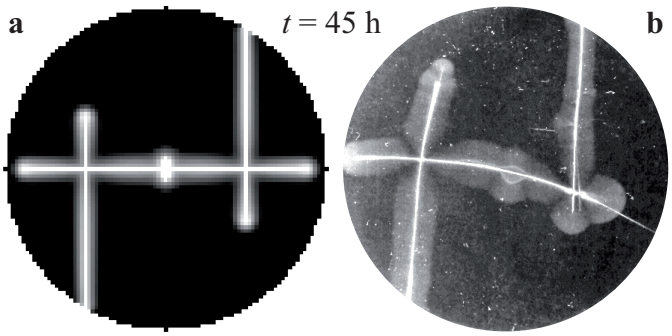

Figure 8.2 Spatial patterns of bacteria after 45 h under 0.1 g/l initial glucose concentration and 5 g/l agar concentration, with a dispersal network of three glass fibres (white grid). Bacterial concentrations are indicated by grey shading, increasing from black (no bacteria) to white. **a** Simulation model result (unmodified model version as described in Ch. 3). **b** Experimental result (experiments performed by Helen Brzezinski during her diploma thesis).

simulations have shown that conditional dispersal may significantly alter biodegradation performance compared to unconditional dispersal. The necessity to incorporate conditional bacterial dispersal, and also the relation to the concept of resource allocation, are discussed in more detail in section 4.4.

The following results (derived in Ch. 5; 6; 7) relate to the research objectives of finding out if, and depending on which factors, bacterial dispersal networks lead to biodegradation improvements (cf. Sec. 1.2):

- *Biodegradation benefits from dispersal networks* – It was shown that bacterial dispersal networks have the potential for significantly improving contaminant bioavailability and, thus, biodegradation performance. This finding proved to be valid both under homogeneous (i.e. as in the laboratory case study; cf. Ch. 2) and heterogeneous (i.e. more realistic with regard to the heterogeneity of contaminated soils; cf. Ch. 6) environmental conditions. Therefore, our results strongly support the idea of deliberately using soil fungi for enhanced natural attenuation.

- *Three key factors determine the degree of improvement* – Biodegradation benefits from bacterial dispersal networks depend sensitively on the abiotic conditions, the time horizon over which biodegradation performance is assessed and the spatial configuration of dispersal networks.

  Abiotic conditions – Highest biodegradation improvement by dispersal networks is observable under adverse abiotic conditions, for instance, when bacterial dispersal is initially restricted due to low humidity (high agar concentration). This finding was obtained under homogeneous, but also under a wide range of spatially heterogeneous abiotic conditions typical for contaminated soils. In the heterogeneous case, we found that the abundance of unfavourable abiotic conditions is of much higher importance than their explicit spatial distribution. We conclude that fungal networks may

compensate for negative effects of unfavourable abiotic conditions on biodegradation performance in soils (cf. detailed discussions in Sec. 5.4; 6.4).

Time horizon – Biodegradation improvements may be substantial only for certain time horizons considered, either because positive dispersal network effects are temporally delayed (e.g. when bacteria need to overcome an initial distance to the dispersal network) or because after a certain time biodegradation would be equally efficient also without dispersal networks. Ideally, the success of enhanced bioremediation by fungi should be assessed for several time horizons and/or one should be aware that expected effects might be small for a particular time horizon considered.

Dispersal network's spatial configuration – The dependence of biodegradation improvements on the spatial structure of bacterial dispersal networks can be characterised appropriately with a combination of two aggregated network metrics: network coverage and inoculum distance to the network (cf. detailed discussion in Sec. 7.4). High network coverage, that is, dense and widespread networks, together with low distance to inoculation point(s), that is, networks easily accessible to bacteria, lead to highest degradation benefits. Therefore, these two criteria need to be considered for the development of bioremediation strategies that include inoculation of bacteria and/or stimulation of fungal growth.

In many cases, the effects of these three key factors on biodegradation performance complexly depend on each other and can not be completely disentangled. For instance, a certain network configuration may improve biodegradation much more than another one for a certain time horizon considered, but the opposite is the case for a different time horizon.

8.2.2 Potential of fungal networks for enhancing biodegradation in soil

Successful bioremediation of soil-bound contaminants relies on the presence of degrading bacteria, optimal physical and chemical conditions for their activity, and the bioavailability of contaminants (cf. Sec. 1.1.2). Particularly the latter is often achieved by homogenisation of the contaminated matrix by mechanical treatment of soil. Our results, by contrast, suggest that fungal networks have the potential for greatly improving the bioavailability of contaminants to degrading bacteria in soil, without excavation and mechanical treatment. This is especially valid for otherwise adverse abiotic conditions for bacterial degradation. Thorough analyses, also under heterogeneously distributed abiotic conditions, which are known to be prevalent in contaminated soil sites (cf. Ch. 6), elevate these findings to a high level of reliability and generalisability.

We are convinced that in many cases stimulating the establishment of fungal networks (e.g. by planting trees associated with mycorrhizal fungi) will be more accomplishable for bioremediation *in situ* than improving the abiotic conditions (e.g. by increasing the humidity). In particular, this is very promising for the development of novel energy-efficient and environmentally sound bioremediation strategies for many contaminated soil sites. However, for assessing the prospective degradation benefits from fungal networks, it will also be important to consider their spatial structure and accessibility, and the time horizon over which biodegradation is expected to occur.

Additionally, our results are of high relevance for the performance of natural attenuation, that is, bioremediation without human intervention. In some cases, the given environmental conditions allow natural attenuation of contaminated soil sites (cf. Sec. 1.1.2). Considering the fact that fungi on average constitute about 75 % of the soil microbial biomass corresponding to up to 1000 m of fungal hyphae per gram of dried soil (Ritz and Young 2004), it is likely that favourable environmental conditions for bacterial degradation often already involve the presence of fungal networks that enhance bacterial dispersal. When assessing the feasibility and robustness of natural attenuation, it may therefore be important not only to consider the risk of impaired abiotic conditions (e.g. caused by climate change), but also the risk of fungal infrastructure losses (e.g. caused by fungicides).

8.3 Outlook on future research

8.3.1 Possible studies relating to research objectives of this thesis

An important element of the methodological approach developed in this doctoral thesis is the interplay between laboratory experiments and simulation model (cf. Fig. 8.1). We have extensively used experimental results to parameterise the simulation model (cf. Sec. 8.1.3) and to identify key processes and factors influencing bacterial degradation performance (cf. Sec. 8.1.4). However, another potential of the approach lies in the feedback from model to experiments. Commencing from the results summarised in section 8.2.1, it is now possible:

- To select appropriate scenarios for more complex field experiments (e.g. abiotic conditions with a high potential for improvement).
- To focus on particular factors when performing such experiments (e.g. the time horizon for biodegradation improvements to occur or the direct accessibility of fungal networks to bacteria).
- To create new laboratory setups to further examine certain hypotheses (e.g. the cessation of bacterial dispersal at high resource levels).

Hence, our studies provide a comprehensive basis for designing future experiments that will be necessary to promote the development of novel bioremediation strategies.

Moreover, the following extensions of the simulation model developed in this doctoral thesis are eligible:

- *Temporal heterogeneities* – So far, we have analysed various instances of spatial heterogeneities (particularly, in Ch. 6). In many contaminated soils, however, another dimension of environmental variability is added by temporal heterogeneities. For instance, changes in temperature and weather conditions may lead to alternating periods of favourable and unfavourable abiotic conditions. Then, bacterial dispersal networks might act as a resilience mechanism and support bacterial recovery from ‘stressful’ periods, comparable to how they enable bacteria to bridge areas of unfavourable

conditions in space (cf. Sec. 6.4). Therefore, we see potential in investigating also temporal variations and, consequently, spatiotemporal interactions in order to improve our ecological understanding of bacteria-fungi associations as a basis for the development of innovative bioremediation strategies (cf. Wick et al. 2010).

- *Spatial configuration of fungal networks* – By studying various random configurations of dispersal networks (Ch. 7), we have gained both a good understanding of the role of the spatial structure of fungal networks and confidence about their applicability for enhanced bioremediation. However, we are looking forward to experiments with natural fungi that let us observe sophisticated spatial configurations of real mycelia, possibly including also temporal dynamics (cf. above). After implementing such configurations in the model, which may necessitate certain modifications (e.g. regarding the spatial resolution), their impact on biodegradation performance could be tested, too. This would particularly allow further studies of (a) the suitability of approximations with artificial dispersal corridors to model the dispersal facilitating effects of fungi and (b) the two network characteristics coverage and accessibility, which were found to be crucial for assessing potential biodegradation benefits (cf. Sec. 8.2.1).

- *Transport networks for contaminants* – Recent studies revealed that fungal networks may not only facilitate the dispersal of bacteria, but also translocate contaminants (Furuno et al. 2010; Wick et al. 2010; Harms et al. 2011). This effect may lead to additional improvements of contaminant bioavailability to degrading bacteria and is, therefore, another option for further investigations with the simulation model.

During the analysis of spatially heterogeneous environments (Ch. 6), we referred to the issue of subsuming the effects of explicit heterogeneities in corresponding homogeneous scenarios with appropriate parameters. The advantage of such approximations is a reduction of complexity, leading to simplified, handier, easier comparable and computationally less expensive models (cf. Frank and Wissel 2002; Drechsler 2009). Not explicitly taking into account heterogeneities may, however, also lead to losses of important information (cf. Sec. 6.4.5). For future studies, we hence see high potential in analysing in detail if, under which conditions, and with regard to which system properties, judiciously parameterised homogeneous scenarios are applicable for reliable approximations of spatial, and potentially also temporal (cf. above), heterogeneities in the framework of modelling microbial ecosystems. Of particular interest would be the question, which aggregated parameters can adequately preserve the heterogeneities' characteristics concerning the specific research objectives addressed.

The performance of bacterial degradation of organic contaminants was fundamental to the studies of this thesis. This performance is directly observable in the simulation model via the quantity and spatial distribution of substrate, at any given point in time (e.g. Fig. 8.3a, c; cf. Sec. 3.3). However, to measure substrate consumption directly in laboratory experiments, and, particularly, to quantify its spatial distribution during

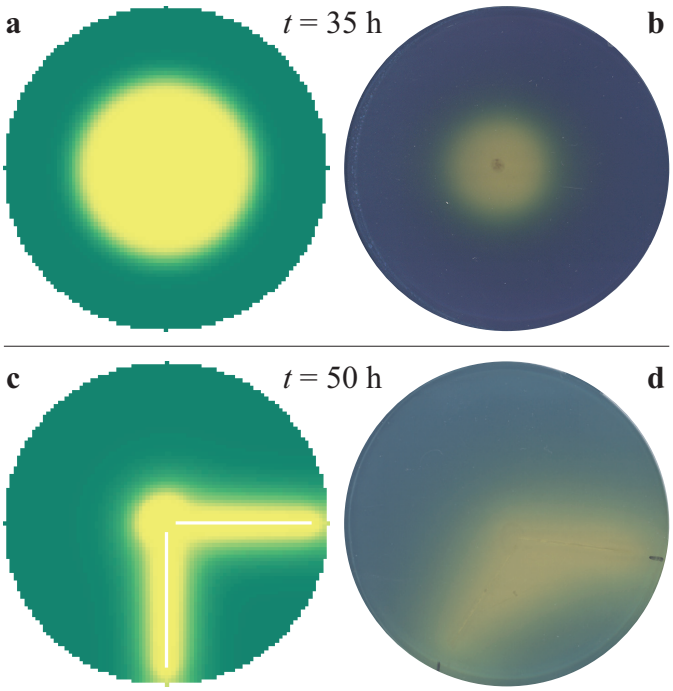

Figure 8.3 Spatial patterns of substrate (glucose) on agar plates. **a, c** Simulation model results. Substrate concentrations are indicated by colour shading, decreasing from green (1 g/l) to yellow (0 g/l). **b, d** Experimental results (experiments performed by Susann Pleger during her diploma thesis). pH values are indicated by colour shading, decreasing from blue (7.6) to yellow (6). **a, b** After 35 h under 1 g/l initial substrate concentration and 3 g/l agar concentration. **c, d** After 50 h under 1 g/l initial substrate concentration and 5 g/l agar concentration, with a dispersal network of two glass fibres.

bacterial colony growth, is very difficult, as added indicator compounds may modify the microbial systems dynamics. In relation to this thesis, it was tried to assess bacterial glucose consumption based on a pH indicator (bromothymol blue) that undergoes a change in colour when the pH value changes. Thus, a decreasing pH value, which is expected during glucose metabolism due to several acids released by bacteria, could be visualised (Fig. 8.3). The simulation model may be applied in this context for verification of experimentally observed spatiotemporal substrate patterns.

8.3.2 Further studies relating to research objectives beyond the scope of this thesis

Alongside with the studies for this doctoral thesis, additional collaborative projects have been initiated to apply the developed bacterial simulation model in different contexts. One example for potential applications is the investigation of bacterial chemotaxis, denoting directed bacterial movement either towards (positive chemotaxis) or away from (negative chemotaxis) a chemical gradient (Pandey and Jain 2002). Particularly in soils, bacterial chemotaxis towards contaminants is considered an essential process, which might increase the bioavailability and, thus, enhance the bioremediation of contaminants (Lanfranconi et al. 2003; Harms and Wick 2006; Ford and Harvey 2007).

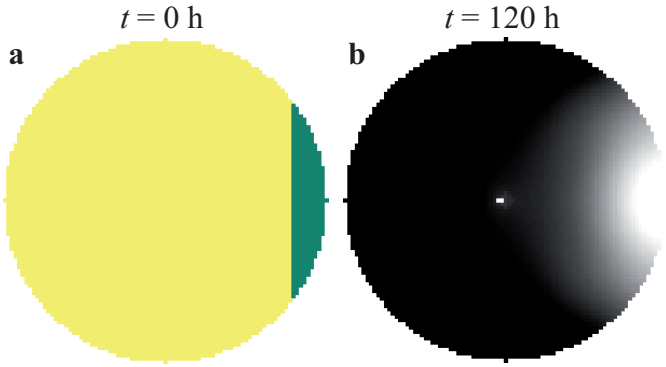

Figure 8.4 Simulation of positive chemotactic behaviour of *P. putida* towards a glucose gradient (unmodified model version as described in Ch. 3) under 3 g/l agar concentration. **a** Pattern of initial substrate concentrations, green grid cells – high initial substrate concentration (1 g/l), yellow grid cells – no initial substrate concentration (0 g/l). **b** Spatial pattern of bacteria after 120 h. Bacterial concentrations are indicated by grey shading, increasing from black (no bacteria) to white.

However, bacterial chemotaxis in typical heterogeneous soil environments with many air-water interfaces is still poorly understood.

The response of *Pseudomonas putida* PpG7 bacteria to both water-borne and air-borne contaminants (naphthalene) was tested experimentally and positive as well as negative chemotactic bacterial behaviour was observed (Hanzel et al. 2010). In the simulation model developed for this thesis, classical bacterial chemotaxis *sensu* Keller and Segel (1971a; 1971b; cf. also Lega and Passot 2003) was not implemented. However, due to the dependence of bacterial growth on substrate uptake (cf. Sec. 3.2.4) the model already allows for qualitatively reproducing positive chemotactic behaviour. Simulation results in figure 8.4 show directed dispersal and colony growth towards the area where substrate was initially distributed. We hope that only minor modifications will be necessary before the model can be used to confirm or reject hypotheses that were derived from observations of chemotaxis experiments.

Another potential model application is the simulation of two or more competing bacterial strains. The phenomenon of *surfing mutations*, denoting propagation of rare mutations at the front of expanding populations, has recently become prominent in ecology (Eswaran 2002; Edmonds et al. 2004; Klopfstein et al. 2006), for instance, to explain dynamic spatial patterns during range expansions (Münkemüller et al. 2011). It has also been investigated in microbial systems (Hallatschek et al. 2007). Particularly with regard to rapid global change and resulting habitat shifts, it is important to assess the chances of deleterious mutations (i.e. having fitness disadvantages) to surf and reach high densities at the wave front of expanding populations (cf. Travis et al. 2007).

To test, whether the phenomenon of surfing deleterious mutations may occur in reality, microbial laboratory experiments were performed. Two different strains of *Escherichia coli* JM109 bacteria, one wild type and one deleterious mutation with a growth rate reduced by half, were grown on glycerine agar (Fig. 8.5). The simulation model will be used to gain a mechanistic understanding of these experimental observations and to make further predictions. First tests to adjust a modified model version to experiments showed a qualitative agreement (cf. Fig. 8.5). However,

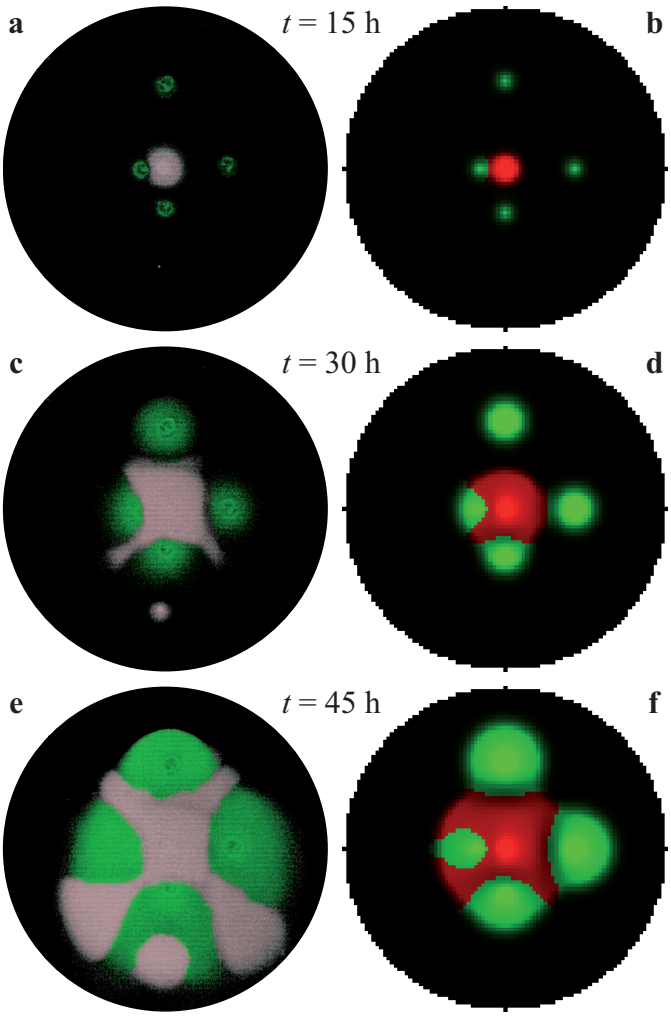

Figure 8.5 Spatial patterns of bacteria from two different *E. coli* strains on agar plates under 1 g/l initial glycerine concentration and 4 g/l agar concentration. Red – fast growing wildtypes, green – slow growing mutants. Bacterial concentrations are indicated by colour shading. **a, b** After 15 h. **c, d** After 30 h. **e, f** After 45 h. **a, c, e** Experimental results. **b, d, f** Simulation model results (modified model version).

additional simulations and calibration are needed and will be executed in the near future.

Symbols

Symbol	Description	Units[a]
α	bacterial dispersal reduction factor	-
∂	partial derivative symbol	-
Δt	time step	h, s
∇	gradient in space	mm^{-1}
∇^2	Laplace operator in space	mm^{-2}
χ	Euler characteristic	-
$\lambda_{\min}$	minimum dispersal fraction	-
$\mu_{eff}^{i,j,t}$	effective bacterial growth rate in cell (i, j) at time t	h^{-1}
$\mu_{\max}^{eff}$	maximum effective bacterial growth rate	h^{-1}
ρ	Spearman's rank correlation coefficient	-
$\overline{\rho}$	mean Spearman's rank correlation coefficient	-
a	maintenance biomass loss rate	h^{-1}
$\tilde{a}$	maintenance rate	$g_s\ g_x^{-1}\ h^{-1}$
C_a	agar concentration	$g_x\ l^{-1}$, $g_x\ mm^{-2}$ [b]
c_h	bacterial dispersal strategy threshold, $h = 1, 2 .. 4$	$g_s\ g_x^{-1}\ h^{-1}$
C_s	substrate concentration	$g_s\ l^{-1}$, $g_s\ mm^{-2}$ [b]
C_s^0	initial substrate concentration at $t = 0$	$g_s\ l^{-1}$, $g_s\ mm^{-2}$ [b]
$C_s^{i,j,t}$	substrate concentration in cell (i, j) at time t	$g_s\ l^{-1}$, $g_s\ mm^{-2}$ [b]
C_x	bacterial concentration (dry mass)	$g_x\ l^{-1}$, $g_x\ mm^{-2}$ [b]
$C_x^{i,j,t}$	bacterial concentration in cell (i, j) at time t	$g_x\ l^{-1}$, $g_x\ mm^{-2}$ [b]
$\overline{C}_x^{i,j,t}$	weighted average of bacterial concentrations in $NBH_{i,j}$	$g_x\ l^{-1}$, $g_x\ mm^{-2}$ [b]
$C_{x,\lambda}$	dispersal reduction limit	$g_x\ l^{-1}$, $g_x\ mm^{-2}$ [b]
$C_{x,\max}$	maximum dispersal concentration	$g_x\ l^{-1}$, $g_x\ mm^{-2}$ [b]
C_y	inactive bacterial concentration (dry mass)	$g_y\ l^{-1}$, $g_y\ mm^{-2}$ [b]
$C_y^{i,j,t}$	inactive bacterial concentration in cell (i, j) at time t	$g_y\ l^{-1}$, $g_y\ mm^{-2}$ [b]

Symbol	Description	Units[a]
cl	grid cell side length	mm
d	dispersal biomass loss rate	h^{-1}
d_{SA}	diameter of the simulation area	mm
$\widetilde{d}^{\,i,j,t}$	dispersal consumption rate in cell (i,j) at time t	$g_s\ g_x^{-1}\ h^{-1}$
$\widetilde{d}_{eff}^{\,i,j,t}$	effective dispersal consumption rate in cell (i,j) at time t	$g_s\ g_x^{-1}\ h^{-1}$
$\widetilde{d}_{\max}$	maximum dispersal consumption rate	$g_s\ g_x^{-1}\ h^{-1}$
D_s	substrate diffusion coefficient	$mm^2\ h^{-1}$
D_x	bacterial diffusion coefficient	$mm^2\ h^{-1}$
$D_x^{i,j,t}$	bacterial diffusion coefficient in cell (i,j) at time t	$mm^2\ h^{-1}$
$D_{x,eff}^{i,j,t,C_a}$	effective bacterial diffusion coefficient in cell (i,j) at time t for agar concentration C_a	$mm^2\ h^{-1}$
$D_{x,\max}^{C_a}$	maximum bacterial diffusion coefficient for agar concentration C_a	$mm^2\ h^{-1}$
$D_{x,\max}^{dn}$	maximum bacterial diffusion coefficient along dispersal networks	$mm^2\ h^{-1}$
DN	bacterial dispersal network (set of grid cells)	-
$\overline{h}$	harmonic mean	-
H	spatial autocorrelation (of fractal pattern)	-
i	spatial coordinate (in x-direction)	mm
idn	inoculum distance to dispersal network	-
j	spatial coordinate (in y-direction)	mm
k	spatial coordinate (in x-direction)	mm
K_s	Monod half-saturation constant	$g_s\ l^{-1}$, $g_s\ mm^{-2}$ [b]
l	spatial coordinate (in y-direction)	mm
m	index of replicate measurements	-
mdn	mean distance to dispersal network	-
n_l	number of closed loops in dispersal networks	-
n_o	number of dispersal network objects	-
n_r	number of simulation runs	-

Symbol	Description	Units[a]
na	dispersal network area	-
$NBH_{i,j}$	9 point neighbourhood of cell (i, j) (set of grid cells)	-
nc	dispersal network coverage	-
NC	set of grid cells covered by the dispersal network	-
p	relative abundance (of fractal pattern)	-
q	substrate uptake rate	$g_s\ g_x^{-1}\ h^{-1}$
$q^{i,j,t}$	substrate uptake rate in cell (i, j) at time t	$g_s\ g_x^{-1}\ h^{-1}$
$q_{eff}^{i,j,t}$	effective uptake rate for growth in cell (i, j) at time t	$g_s\ g_x^{-1}\ h^{-1}$
$q_{\max}$	maximum substrate uptake rate	$g_s\ g_x^{-1}\ h^{-1}$
r	index of simulation run	-
R	measure of agreement between simulated and measured bacterial colony area data	-
R^2	coefficient of determination	-
SA	simulation area (set of grid cells)	-
t	time	h, s
$TA_{mdl}^{C_a,C_s^0}$	modelled total area of bacterial colony	mm^2
$TA_{msr}^{C_a,C_s^0}$	measured total area of bacterial colony	mm^2
$VAR_{smth}^{C_a,C_s^0}$	smoothed variance of measurement data for agar concentration C_a and initial substrate concentration C_s^0	mm^4
$w_{k,l}$	weight for diffusion between cell (i, j) and cell (k, l)	-
$\bar{y}$	mean substrate consumption over n_r simulation runs	-
y_r	substrate consumption of simulation run r	-
$\bar{y}_r$	mean substrate consumption over all simulation runs belonging to the same class of network metric values as simulation run r	-
Y_g	bacterial growth yield coefficient	$g_x\ g_s^{-1}$

[a] g_s – grams of substrate, g_x – grams of dry active biomass, g_y – grams of dry inactive biomass

[b] All concentrations can be given in both units as the simulation model translates a three-dimensional agar plate into a plane two-dimensional grid. The agar plate's volume (0.03 l) and surface (6082.12 mm^2) are fixed. Hence, the relation between $g\ l^{-1}$ and $g\ mm^{-2}$ is constant for the simulated system ($1\ g\ l^{-1} = 4.9325 \times 10^{-6}\ g\ mm^{-2}$).

Figures

Tables

Bibliography

Alvarez PJJ, Illman WA (2006) Bioremediation and natural attenuation. Wiley, Hoboken, NJ.

Armsworth PR (2009) Conditional dispersal, clines, and the evolution of dispersiveness. Theor Ecol 2:105-117.

Auger J, Kunstmann JM, Czyglik F, Jouannet P (1995) Decline in semen quality among fertile men in Paris during the past 20 years. New Engl J Med 332:281-285.

Banitz T, Fetzer I, Johst K, Wick LY, Harms H, Frank K (2011a) Assessing biodegradation benefits from dispersal networks. Ecol Modell 222:2552-2560.

Banitz T, Huth A, Grimm V, Johst K (2008) Clumped versus scattered: how does the spatial correlation of disturbance events affect biodiversity? Theor Ecol 1:231-240.

Banitz T, Wick LY, Fetzer I, Frank K, Harms H, Johst K (2011b) Dispersal networks for enhancing bacterial degradation in heterogeneous environments. Environ Pollut (in press).

Bardos RP, Bakker LMM, Slenders HLA, Nathanail CP (2011) Sustainability and remediation. In: Swartjes FA, Ed. Dealing with contaminated sites. From theory towards practical application. Springer, Dordrecht, pp 889-948.

Battin TJ, Sloan WT, Kjelleberg S, Daims H, Head IM, Curtis TP, Eberl L (2007) Microbial landscapes: new paths to biofilm research. Nat Rev Microbiol 5:76-81.

Bees MA, Andresen P, Mosekilde E, Givskov M (2000) The interaction of thin-film flow, bacterial swarming and cell differentiation in colonies of *Serratia liquefaciens*. J Math Biol 40:27-63.

Ben-Jacob E, Schochet O, Tenenbaum A, Cohen I, Czirok A, Vicsek T (1994) Generic modelling of cooperative growth patterns in bacterial colonies. Nature 368:46-49.

Benton TG, Solan M, Travis JMJ, Sait SM (2007) Microcosm experiments can inform global ecological problems. Trends Ecol Evol 22:516-521.

Berryman A, Lima M (2006) Deciphering the effects of climate on animal populations: diagnostic analysis provides new interpretation of soay sheep dynamics. Am Nat 168:784-795.

Borland (1999) Borland Delphi Professional 5.0. Borland Software Corporation, Cupertino, CA.

Boswell GP, Jacobs H, Davidson FA, Gadd GM, Ritz K (2003) Growth and function of fungal mycelia in heterogeneous environments. Bull Math Biol 65:447-477.

Boswell GP, Jacobs H, Davidson FA, Gadd GM, Ritz K (2002) Functional consequences of nutrient translocation in mycelial fungi. J Theor Biol 217:459-477.

Boswell GP, Jacobs H, Ritz K, Gadd GM, Davidson FA (2007) The development of fungal networks in complex environments. Bull Math Biol 69:605-634.

Bowler DE, Benton TG (2005) Causes and consequences of animal dispersal strategies: relating individual behaviour to spatial dynamics. Biol Rev 80:205-225.

Brown JH, Gillooly JF, Allen AP, Savage VM, West GB (2004) Toward a metabolic theory of ecology. Ecology 85:1771-1789.

Cadotte MW, Drake JA, Fukami T (2005) Constructing nature: laboratory models as necessary tools for investigating complex ecological communities. In: Desharnais RA, Ed. Population dynamics and laboratory ecology. Advances in ecological research 37. Elsevier, Amsterdam, pp 333-353.

Carlsen E, Giwercman A, Keiding N, Skakkebaek NE (1992) Evidence for decreasing quality of semen during past 50 years. Brit Med J 305:609-613.

Clobert J, Danchin E, Dhondt AA, Nichols JD, Eds. (2001) Dispersal. Oxford University Press, Oxford.

Cohen I, Golding I, Kozlovsky Y, Ben-Jacob E, Ron IG (1999) Continuous and discrete models of cooperation in complex bacterial colonies. Fractals 7:235-247.

Cosner C (2009) Beyond diffusion: conditional dispersal in ecological models. Ulam Centennial Conference, March 10-11, 2009, pp. 1-15. University of Florida, Gainesville, FL.

Costanza R, d'Arge R, de Groot R, Farber S, Grasso M, Hannon B, Limburg K et al (1997) The value of the world's ecosystem services and natural capital. Nature 387:253-260.

DeAngelis DL, Mooij WM (2005) Individual-based modeling of ecological and evolutionary processes. Annu Rev Ecol Evol Syst 36:147-168.

Dellens AD (2007) Green remediation and the use of renewable energy sources for remediation projects. Report prepared for U.S. Environmental Protection Agency, Office of Solid Waste and Emergency Response, Office of Superfund Remediation and Technology Innovation, Washington, D.C.

Dewhirst S, Lutscher F (2009) Dispersal in heterogeneous habitats: thresholds, spatial scales, and approximate rates of spread. Ecology 90:1338-1345.

Díaz E (2004) Bacterial degradation of aromatic pollutants: a paradigm of metabolic versatility. Int Microbiol 7:173-180.

Drechsler M (2009) Predicting metapopulation lifetime from macroscopic network properties. Math Biosci 218:59-71.

Dunn NW, Gunsalus IC (1973) Transmissible plasmid coding early enzymes of naphthalene oxidation in *Pseudomonas putida*. J Bacteriol 114:974-979.

Edmonds CA, Lillie AS, Cavalli-Sforza LL (2004) Mutations arising in the wave front of an expanding population. PNAS 101:975-979.

Ehlers LJ, Luthy RG (2003) Contaminant bioavailability in soil and sediment. Environ Sci Technol 37:295A-302A.

Ernest SK, Brown JH, Parmenter RR (2000) Rodents, plants, and precipitation: spatial and temporal dynamics of consumers and resources. Oikos 88:470-482.

Ernest SKM, Enquist BJ, Brown JH, Charnov EL, Gillooly JE, Savage V, White EP et al (2003) Thermodynamic and metabolic effects on the scaling of production and population energy use. Ecol Lett 6:990-995.

Eswaran V (2002) A diffusion wave out of Africa - the mechanism of the modern human revolution? Current Anthropology 43:749-774.

Ferrer J, Prats C, Lopez D (2008) Individual-based modelling: an essential tool for microbiology. Journal of Biological Physics 34:19-37.

Ferrer J, Prats C, Lopez D, Vives-Rego J (2009) Mathematical modelling methodologies in predictive food microbiology: a SWOT analysis. Int J Food Microbiol 134:2-8.

Ford RM, Harvey RW (2007) Role of chemotaxis in the transport of bacteria through saturated porous media. Adv Water Resour 30:1608-1617.

Frank K, Wissel C (2002) A formula for the mean lifetime of metapopulations in heterogeneous landscapes. Am Nat 159:530-552.

Fredslund L, Sniegowski K, Wick LY, Jacobsen CS, De Mot R, Springael D (2008) Surface motility of polycyclic aromatic hydrocarbon (PAH)-degrading mycobacteria. Res Microbiol 159:255-262.

Friedenberg NA (2003) Experimental evolution of dispersal in spatiotemporally variable microcosms. Ecol Lett 6:953-959.

Furuno S, Pazolt K, Rabe C, Neu TR, Harms H, Wick LY (2010) Fungal mycelia allow chemotactic dispersal of polycyclic aromatic hydrocarbon-degrading bacteria in water-unsaturated systems. Environ Microbiol 12:1391-1398.

Gibbons JD, Chakraborti S (2010) Nonparametric statistical inference. CRC Press, Boca Raton, FL.

Ginovart M, Lopez D, Valls J (2002a) INDISIM, an individual-based discrete simulation model to study bacterial cultures. J Theor Biol 214:305-319.

Ginovart M, Lopez D, Valls J, Silbert M (2002b) Individual based simulations of bacterial growth on agar plates. Physica A 305:604-618.

Golding I, Cohen I, Ben-Jacob E (1999) Studies of sector formation in expanding bacterial colonies. Europhys Lett 48:587-593.

Golding I, Kozlovsky Y, Cohen I, Ben-Jacob E (1998) Studies of bacterial branching growth using reaction-diffusion models for colonial development. Physica A 260:510-554.

Gregory R, Saunders JR, Saunders VA (2006) The Paton individual-based model legacy. BioSystems 85:46-54.

Grijspeerdt K, Kreft JU, Messens W (2005) Individual-based modelling of growth and migration of *Salmonella enteritidis* in hens' eggs. Int J Food Microbiol 100:323-333.

Grimm V, Railsback SF (2005) Individual-based modeling and ecology. Princeton University Press, Princeton, NJ.

Grimm V, Revilla E, Berger U, Jeltsch F, Mooij WM, Railsback SF, Thulke H-H et al (2005) Pattern-oriented modeling of agent-based complex systems: lessons from ecology. Science 310:987-991.

Hallatschek O, Hersen P, Ramanathan S, Nelson DR (2007) Genetic drift at expanding frontiers promotes gene segregation. PNAS 104:19926-19930.

Hanski I, Ovaskainen O (2000) The metapopulation capacity of a fragmented landscape. Nature 404:755-758.

Hanzel J, Harms H, Wick LY (2010) Bacterial chemotaxis along vapor-phase gradients of naphthalene. Environ Sci Technol 44:9304-9310.

Hardy GPMA, Demattos MJT, Neijssel OM (1993) Energy conservation by pyrroloquinoline quinol-linked xylose oxidation in *Pseudomonas putida* NCTC 10936 during carbon-limited growth in chemostat culture. FEMS Microbiol Lett 107:107-110.

Harms H, Bosma TNP (1997) Mass transfer limitation of microbial growth and pollutant degradation. J Ind Microbiol Biot 18:97-105.

Harms H, Schlosser D, Wick LY (2011) Untapped potential: exploiting fungi in bioremediation of hazardous chemicals. Nat Rev Microbiol 9:177-192.

Harms H, Wick LY (2006) Dispersing pollutant-degrading bacteria in contaminated soil without touching it. Eng Life Sci 6:252-260.

Harms H, Zehnder AJB (1994) Influence of substrate diffusion on degradation of dibenzofuran and 3-chlorodibenzofuran by attached and suspended bacteria. Appl Environ Microb 60:2736-2745.

Harshey RM (2003) Bacterial motility on a surface: many ways to a common goal. Annu Rev Microbiol 57:249-273.

Hastings A (1993) Complex interactions between dispersal and dynamics: lessons from coupled logistic equations. Ecology 74:1362-1372.

Hellweger FL, Bucci V (2009) A bunch of tiny individuals - individual-based modeling for microbes. Ecol Modell 220:8-22.

Hilborn R, Mangel M (1997) The ecological detective: confronting models with data. Monographs in population biology 28. Princeton University Press, Princeton, NJ.

Hill CJ (1995) Linear strips of rain forest vegetation as potential dispersal corridors for rain forest insects. Conserv Biol 9:1559-1566.

Hollander M, Wolfe DA (1999) Nonparametric statistical methods. Wiley, Hoboken, NJ.

Hovestadt T, Kubisch A, Poethke HJ (2010) Information processing in models for density-dependent emigration: a comparison. Ecol Modell 221:405-410.

Hovestadt T, Poethke HJ (2006) The control of emigration and its consequences for the survival of populations. Ecol Modell 190:443-453.

Huston MD, DeAngelis D, Post W (1988) New computer models unify ecological theory. BioScience 38:682-691.

Ims RA, Andreassen HP (2005) Density-dependent dispersal and spatial population dynamics. Proc R Soc Lond B 272:913-918.

Ims RA, Hjermann DØ (2001) Condition-dependent dispersal. In: Clobert J, Danchin E, Dhondt AA and Nichols JD, Eds. Dispersal. Oxford University Press, Oxford, pp 203-216.

Isken S, Derks A, Wolffs PFG, de Bont JAM (1999) Effect of organic solvents on the yield of solvent-tolerant *Pseudomonas putida* S12. Appl Environ Microb 65:2631-2635.

Jessup CM, Forde SE, Bohannan BJM (2005) Microbial experimental systems in ecology. In: Desharnais RA, Ed. Population dynamics and laboratory ecology. Advances in ecological research 37. Elsevier, Amsterdam, pp 273-307.

Jessup CM, Kassen R, Forde SE, Kerr B, Buckling A, Rainey PB, Bohannan BJM (2004) Big questions, small worlds: microbial model systems in ecology. Trends Ecol Evol 19:189-197.

Johst K, Berryman A, Lima M (2008) From individual interactions to population dynamics: individual resource partitioning simulation exposes the causes of nonlinear intra-specific competition. Popul Ecol 50:79-90.

Johst K, Brandl R (1997a) Evolution of dispersal: the importance of the temporal order of reproduction and dispersal. Proc R Soc Lond B 264:23-30.

Johst K, Brandl R (1997b) The effect of dispersal on local population dynamics. Ecol Modell 104:87-101.

Johst K, Schöps K (2003) Persistence and conservation of a consumer-resource metapopulation with local overexploitation of resources. Biol Conserv 109:57-65.

Kawasaki K, Mochizuki A, Matsushita M, Umeda T, Shigesada N (1997) Modeling spatio-temporal patterns generated by *Bacillus subtilis*. J Theor Biol 188:177-185.

Keller EF, Segel LA (1971a) Model for chemotaxis. J Theor Biol 30:225-234.

Keller EF, Segel LA (1971b) Traveling bands of chemotactic bacteria - theoretical analysis. J Theor Biol 30:235-248.

Kerr B, Riley MA, Feldman MW, Bohannan BJM (2002) Local dispersal promotes biodiversity in a real-life game of rock-paper-scissors. Nature 418:171-174.

Kessler DA, Levine H (1998) Fluctuation-induced diffusive instabilities. Nature 394:556-558.

Kim SH, Han HY, Lee YJ, Kim CW, Yang JW (2010) Effect of electrokinetic remediation on indigenous microbial activity and community within diesel contaminated soil. Sci Total Environ 408:3162-3168.

Kitsunezaki S (1997) Interface dynamics for bacterial colony formation. J Phys Soc Jpn 66:1544-1550.

Klopfstein S, Currat M, Excoffier L (2006) The fate of mutations surfing on the wave of a range expansion. Mol Biol Evol 23:482-490.

Köhler T, Curty LK, Barja F, van Delden C, Pechere JC (2000) Swarming of *Pseudomonas aeruginosa* is dependent on cell-to-cell signaling and requires flagella and pili. J Bacteriol 182:5990-5996.

Kohlmeier S, Smits THM, Ford RM, Keel C, Harms H, Wick LY (2005) Taking the fungal highway: mobilization of pollutant-degrading bacteria by fungi. Environ Sci Technol 39:4640-4646.

Kreft JU (2004) Biofilms promote altruism. Microbiology 150:2751-2760.

Kreft JU, Booth G, Wimpenny JWT (1998) BacSim, a simulator for individual-based modelling of bacterial colony growth. Microbiology 144:3275-3287.

Kreft JU, Picioreanu C, Wimpenny JWT, van Loosdrecht MCM (2001) Individual-based modelling of biofilms. Microbiology 147:2897-2912.

Krone SM, Lu R, Fox R, Suzuki H, Top EM (2007) Modelling the spatial dynamics of plasmid transfer and persistence. Microbiology 153:2803-2816.

Kuiper I, Bloemberg GV, Lugtenberg BJJ (2001) Selection of a plant-bacterium pair as a novel tool for rhizostimulation of polycyclic aromatic hydrocarbon-degrading bacteria. Mol Plant Microbe In 14:1197-1205.

Lanfranconi MP, Alvarex HM, Studdert CA (2003) A strain isolated from gas oil-contaminated soil displays chemotaxis towards gas oil and hexadecane. Environ Microbiol 5:1002-1008.

Lega J, Passot T (2003) Hydrodynamics of bacterial colonies: a model. Phys Rev E 67:031906-1-18.

Lega J, Passot T (2004) Hydrodynamics of bacterial colonies: phase diagrams. Chaos 14:562-570.

Lewis RM, Torczon V (1998) A globally convergent augmented Lagrangian pattern search algorithm for optimization with general constraints and simple bounds. ICASE Report No. 98-31. National Aeronautics and Space Administration - Langley Research Center, Hampton, VI.

Lewis RM, Torczon V (1999) Pattern search algorithms for bound constrained minimization. SIAM J Optimiz 9:1082-1099.

Lohner ST, Tiehm A (2009) Application of electrolysis to stimulate microbial reductive PCE dechlorination and oxidative VC biodegradation. Environ Sci Technol 43:7098-7104.

Madigan M, Martinko J, Dunlap P (2008) Brock biology of microorganisms. Pearson Benjamin Cummings, San Francisco, CA.

Matsushita M, Hiramatsu F, Kobayashi N, Ozawa T, Yamazaki Y, Matsuyama T (2004) Colony formation in bacteria: experiments and modeling. Biofilms 1:305-317.

Matsuyama T, Nakagawa Y (1996) Bacterial wetting agents working in colonization of bacteria on surface environments. Colloid Surface B 7:207-214.

Mayer P, Vaes WHJ, Wijnker F, Legierse KCHM, Kraaij RH, Tolls J, Hermens JLM (2000) Sensing dissolved sediment porewater concentrations of persistent and bioaccumulative pollutants using disposable solid-phase microextraction fibers. Environ Sci Technol 34:5177-5183.

Mimura M, Sakaguchi H, Matsushita M (2000) Reaction-diffusion modelling of bacterial colony patterns. Physica A 282:283-303.

Monod J (1949) The growth of bacterial cultures. Annu Rev Microbiol 3:371-394.

Münkemüller T, Johst K (2008) Spatial synchrony through density-independent versus density-dependent dispersal. J Biol Dynam 2:31-39.

Münkemüller T, Travis MJ, Burton OJ, Schiffers K, Johst K (2011) Density-regulated population dynamics and conditional dispersal alter the fate of mutations occurring at the front of an expanding population. Heredity 106:678-689.

Murdoch WM, Briggs CJ, Nisbet RM (2003) Consumer-resource dynamics. Princeton University Press, Princeton, NJ.

Murray JD (2002) Mathematical biology I. 17 Springer, Berlin, Heidelberg, New York.

Ohgiwari M, Matsushita M, Matsuyama T (1992) Morphological changes in growth phenomena of bacterial colony patterns. J Phys Soc Jpn 61:816-822.

Or D, Smets BF, Wraith JM, Dechesne A, Friedman SP (2007) Physical constraints affecting bacterial habitats and activity in unsaturated porous media - a review. Adv Water Resour 30:1505-1527.

Orfanidis SJ (1995) Introduction to signal processing. Prentice-Hall, Englewood Cliffs, NJ.

Pandey G, Jain RK (2002) Bacterial chemotaxis toward environmental pollutants: role in bioremediation. Appl Environ Microb 68:5789-5795.

Panikov NS (1996) Mechanistic mathematical models of microbial growth in bioreactors and in natural soils: explanation of complex phenomena. Maths Comput Simul 42:179-186.

Pena TS, Johst K, Grimm V, Arntz W, Tarazona J (2005) Population dynamics of a polychaete during three El Niño events: disentangeling biotic and abiotic factors. Oikos 111:253-258.

Piceno YM, Lovell CR (2000) Stability in natural bacterial communities: II. plant resource allocation effects on rhizosphere diazotroph assemblage composition. Microb Ecol 39:41-48.

Picioreanu C, Head IM, Katuri KP, van Loosdrecht MCM, Scott K (2007) A computational model for biofilm-based microbial fuel cells. Water Res 41:2921-2940.

Picioreanu C, Kreft JU, van Loosdrecht MCM (2004) Particle-based multidimensional multispecies biofilm model. Appl Environ Microb 70:3024-3040.

Pilon-Smits E (2005) Phytoremediation. Annu Rev Plant Biol 56:15-39.

Poethke HJ, Hovestadt T (2002) Evolution of density-and patch-size-dependent dispersal rates. Proc R Soc Lond B 269:637-645.

Press WH, Teukolsky SA, Vetterling WT, Flannery BP (2007) Numerical recipes. Cambridge University Press, Cambridge.

Prosser JI, Bohannan BJM, Curtis TP, Ellis RJ, Firestone MK, Freckleton RP, Green JL et al (2007) Essay - the role of ecological theory in microbial ecology. Nat Rev Microbiol 5:384-392.

Rasband WS (1997) ImageJ. US National Institutes of Health, Bethesda, MD.

Rashid MH, Kornberg A (2000) Inorganic polyphosphate is needed for swimming, swarming, and twitching motilities of *Pseudomonas aeruginosa*. PNAS 97:4885-4890.

Ritz K, Young IYI (2004) Interactions between soil structure and fungi. Mycologist 18:52-59.

Roth K, Boike J, Vogel HJ (2005) Quantifying permafrost patterns using Minkowski densities. Permafrost Periglac 16:277-290.

Roughgarden J, Gaines S, Possingham H (1988) Recruitment dynamics in complex life cycles. Science 241:1460-1466.

Salt DE, Smith RD, Raskin I (1998) Phytoremediation. Annu Rev Plant Physiol Plant Mol Biol 49:643-668.

Saupe D (1988) Algorithms for random fractals. In: Peitgen HO and Saupe D, Eds. The science of fractal images. Springer, New York, pp 71-136.

Schroll R, Becher HH, Dorfler U, Gayler S, Hartmann HP, Ruoss J (2006) Quantifying the effect of soil moisture on the aerobic microbial mineralization of selected pesticides in different soils. Environ Sci Technol 40:3305-3312.

Schuler AJ (2005) Diversity matters: dynamic simulation of distributed bacterial states in suspended growth biological wastewater treatment systems. Biotechnol Bioeng 91:62-74.

Schwarzenbach RP, Gschwend PM, Imboden DM (2002) Environmental organic chemistry. Wiley-Interscience, Hoboken, NJ.

Semple KT, Doick KJ, Jones KC, Burauel P, Craven A, Harms H (2004) Defining bioavailability and bioaccessibility of contaminated soil and sediment is complicated. Environ Sci Technol 38:228A-231A.

Semple KT, Doick KJ, Wick LY, Harms H (2007) Microbial interactions with organic contaminants in soil: definitions, processes and measurement. Environ Pollut 150:166-176.

Semple KT, Morriss AWJ, Paton GI (2003) Bioavailability of hydrophobic organic contaminants in soils: fundamental concepts and techniques for analysis. Eur J Soil Sci 54:809-818.

Singh H (2006) Mycoremediation. Wiley, Hoboken, NJ.

Sizmur T, Hodson ME (2009) Do earthworms impact metal mobility and availability in soil? - a review. Environ Pollut 157:1981-1989.

Taylor TB, Buckling A (2010) Competition and dispersal in *Pseudomonas aeruginosa*. Am Nat 176:83-89.

Tiehm A, Augenstein T, Ilieva D, Schell H, Weidlich C, Mangold KM (2010) Bio-electro-remediation: electrokinetic transport of nitrate in a flow-through system for enhanced toluene biodegradation. J Appl Electrochem 40:1263-1268.

Tischendorf L, Irmler U, Hingst R (1998) A simulation experiment on the potential of hedgerows as movement corridors for forest carabids. Ecol Modell 106:107-118.

Tischendorf L, Wissel C (1997) Corridors as conduits for small animals: attainable distances depending on movement pattern, boundary reaction and corridor width. Oikos 79:603-611.

Travis JM, Dytham C (1999) Habitat persistence, habitat availability and the evolution of dispersal. Proc R Soc Lond B 266:723-728.

Travis JMJ, Münkemüller T, Burton OJ, Best A, Dytham C, Johst K (2007) Deleterious mutations can surf to high densities on the wave front of an expanding population. Mol Biol Evol 24:2334-2343.

Travis JMJ, Mustin K, Benton TG, Dytham C (2009) Accelerating invasion rates result from the evolution of density-dependent dispersal. J Theor Biol 259:151-158.

van Bodegom P (2007) Microbial maintenance: a critical review on its quantification. Microb Ecol 53:513-523.

van Loosdrecht MCM, Heijnen JJ, Eberl H, Kreft J, Picioreanu C (2002) Mathematical modelling of biofilm structures. Anton Leeuw 81:245-256.

Vogel H-J (2002) Topological characterization of porous media. In: Mecke KR and Stoyan D, Eds. Morphology of condensed matter. Lecture notes on physics 600. Springer, Berlin Heidelberg, pp 75-92.

Vrugt JA, Gupta HV, Bouten W, Sorooshian S (2003) A Shuffled Complex Evolution Metropolis algorithm for optimization and uncertainty assessment of hydrologic model parameters. Water Resour Res 39:SWC 1-1-SWC 1-14.

Wackett LP (2003) *Pseudomonas putida* - a versatile biocatalyst. Nat Biotechnol 21:136-138.

Wackett LP, Bruce NC (2000) Environmental biotechnology towards sustainability - editorial overview. Curr Opin Biotech 11:229-231.

Wakita J, Komatsu K, Nakahara A, Matsuyama T, Matsushita M (1994) Experimental investigation on the validity of population-dynamics approach to bacterial colony formation. J Phys Soc Jpn 63:1205-1211.

Whitman WB, Coleman DC, Wiebe WJ (1998) Prokaryotes: the unseen majority. PNAS 95:6578-6583.

Wick LY, Colangelo T, Harms H (2001) Kinetics of mass transfer-limited bacterial growth on solid PAHs. Environ Sci Technol 35:354-361.

Wick LY, Furuno S, Harms H (2010) Fungi as transport vectors for contaminants and contaminant-degrading bacteria. In: Timmis KN, Ed. Handbook of hydrocarbon and lipid microbiology. Springer, Berlin Heidelberg, pp 1555-1561.

Wick LY, Remer R, Wurz B, Reichenbach J, Braun S, Schäfer F, Harms H (2007a) Effect of fungal hyphae on the access of bacteria to phenanthrene in soil. Environ Sci Technol 41:500-505.

Wick LY, Shi L, Harms H (2007b) Electro-bioremediation of hydrophobic organic soil-contaminants: a review of fundamental interactions. Electrochim Acta 52:3441-3448.

Wimpenny JWT, Colasanti R (1997) A unifying hypothesis for the structure of microbial biofilms based on cellular automaton models. FEMS Microb Ecol 22:1-16.

With KA (1997) The application of neutral landscape models in conservation biology. Conserv Biol 11:1069-1080.

With KA, King AW (1999) Extinction thresholds for species in fractal landscapes. Conserv Biol 13:314-326.

Wösten HB, van Wetter MA, Lugones LG, van der Mei HC, Busscher HJ, Wessels JGH (1999) How a fungus escapes the water to grow into the air. Curr Biol 9:85-88.

Wösten HAB, Willey JM (2000) Surface-active proteins enable microbial aerial hyphae to grow into the air. Microbiology 146:767-773.

Xavier JB, Foster KR (2007) Cooperation and conflict in microbial biofilms. PNAS 104:876-881.

Young IM, Crawford JW (2004) Interactions and self-organization in the soil-microbe complex. Science 304:1634-1637.

Zhang T, Fang HHP (2005) Effective diffusion coefficients of glucose in artificial biofilms. Environ Technol 26:155-160.

Zorzano MP, Hochberg D, Cuevas MT, Gomez-Gomez JM (2005) Reaction-diffusion model for pattern formation in *E.coli* swarming colonies with slime. Phys Rev E 71:031908.

Acknowledgements

First of all, I would like to thank my supervisors Dr. Karin Johst, Dr. Lukas Wick and Prof. Karin Frank. I am deeply grateful for their knowledgeable guidance during the last years. Karin Johst was always available for any kind of question or discussion, and continuously helped me to meet the challenges of scientific research and producing a PhD thesis. In all respects relating to this thesis, she gave me both great support and the freedom to follow my own ideas. Lukas Wick was a very inspiring and discerning supervisor, who particularly helped me a lot to gain insights into the fascinating field of microbiology. Karin Frank vitally encouraged my work with her profound scientific expertise and enthusiasm for interdisciplinary research.

I would also like to express my sincere gratitude to Dr. Ingo Fetzer and Prof. Hauke Harms, who substantially contributed to the ambitious and fruitful working atmosphere within the 'MaMiMa' project. For supporting the scientific progress of this project with essential laboratory experiments, I am indebted to Dr. Daniela Inkrot, Susann Pleger and Helen Brzezinski.

Additionally, I would like to thank Dr. Cristian Picioreanu and the TU Delft Biofilm Modelling group for facilitating a research visit and providing comprehensive support in model development.

The conditions and the people at the department of Ecological Modelling make it a fantastic place for work, education and personal development, which considerably contributed to the production of this thesis during the last years. In particular, I would like to express my appreciation to Dr. Florian Hartig, Kamila Franz, Oliver Jakoby, Claudia Dislich, Dr. Isabel Martínez Cano and Franziska Taubert for plenty of helpful scientific as well as non-scientific discussions and/or commenting on the manuscript. Furthermore, I thank Gabriele Nagel, Heike Reichelt, Andreas Thiele and Michael Müller for helping me to overcome any troubles concerning administrative issues, literature, hard- and software.

I acknowledge the Helmholtz Centre for Environmental Research – UFZ for financing my PhD thesis within the research programme 'Terrestrial Environment', and the Helmholtz Impulse and Networking Fund for providing financial support through the Helmholtz Interdisciplinary Graduate School for Environmental Research HIGRADE.

Finally, I thank my family and friends for always encouraging me, during this thesis and long before.